

Development of a plant carbon-nitrogen interface coupling framework in a coupled biophysical-ecosystem-biogeochemical model (SSiB5/Triffid/DayCent-SOM v1.0): ~~Its parameterization, implementation, and evaluation~~

5

Zheng Xiang^{1,2}, Yongkang Xue^{2*}, Weidong Guo^{1,4*}, Melannie D. Hartman³, Ye Liu^{2,5}, William J. Parton³

¹School of Atmospheric Sciences, Nanjing University, Nanjing, China

²Department of Geography, University of California, Los Angeles, CA 90095, USA

³Natural Resource Ecology Laboratory, Colorado State University, CO 80523, USA

10 ⁴Joint International Research Laboratory of Atmospheric and Earth System Sciences, Nanjing, China

⁵Pacific Northwest National Laboratory, Richland, WA 99352, USA.

Correspondence to: Yongkang Xue (yxue@geog.ucla.edu), Weidong Guo (guowd@nju.edu.cn)

15 **Abstract.** Plant and microbial nitrogen (N) dynamics and N availability regulate the photosynthetic capacity and capture, allocation, and turnover of carbon (C) in terrestrial ecosystems. Studies have shown that a wide divergence in representations of N dynamics in land surface models leads to large ~~uncertainty~~uncertainties in the biogeochemical cycle of the terrestrial ecosystems and then in climate simulations as well as the projections of future trajectories. In this study, a plant C-N interface coupling framework is developed and implemented in a coupled biophysical-ecosystem-biogeochemical model

20 (SSiB5/TRIFFID/DayCent-SOM v1.0). The main concept and structure of this plant C-N framework and its coupling strategy are presented. ~~in this study.~~ This framework takes more plant N-related ~~metabolism~~ processes into account. ~~For instance, plant resistance and self adjustment is represented by a~~ dynamic C/N ratio for each plant functional type (PFT) ~~is introduced to consider plant resistance and adaptation to N availability to better evaluate the plant response to N limitation.~~ Furthermore, when available N is less than plant N demand, plant growth is restricted by a lower maximum carboxylation capacity of

25 Rubisco (~~Vmax level~~), reducing gross primary productivity (GPP). In addition, a module for plant respiration rates is introduced by adjusting the respiration with different rates at different plant components ~~for~~ the same N concentration. Since insufficient N can potentially give rise to lags ~~on~~ plant phenology, ~~phenology~~the phenological scheme is also adjusted ~~with a lag factor related~~in response to N ~~processes~~availability. All these considerations ensure a more comprehensive incorporation of N regulations to plant growth and C cycling. This new approach has been tested systematically to assess the effects of this

30 coupling framework and N limitation on the terrestrial carbon cycle. Long-~~term~~ measurements from ~~both~~ flux tower sites with

different PFTs and global satellite-derived products are employed as references to assess these effects. The results show a general improvement with the new plant C-N coupling framework, with more consistent emergent properties, such as GPP and leaf area index (LAI), compared to the observations. The main improvements occur in tropical Africa and boreal regions, accompanied by a decrease ~~of~~ in the bias in global GPP and LAI by 16.3% and 27.1%, respectively.

35 1 Introduction

Land surface processes substantially affect climate (Foley et al., 1998; Ma et al., 2013; Sellers et al., 1986; Xue et al., 2004, 2010, 2022) and are influenced by climate in turn (Bonan, 2008; Liu et al., 2019, 2020; Zhang et al., 2015), forming complex feedback loops to climate change (Friedlingstein et al., 2006; Gregory et al., 2009). To study these processes, the land surface components of Earth System Models (ESMs) have evolved from those that represent only physical processes (i.e., hydrology and the energy cycle) to those that include the terrestrial carbon (C) cycle, vegetation dynamics, and nutrient processes (Cox, 2001; Dan et al., 2020; Foley et al., 1998; Oleson et al., 2013; Sellers et al., 1996; Sitch et al., 2003; Wang et al., 2010; Zhan et al., 2003).

Current land surface models have large uncertainties in predicting historical and recent C exchanges (Beer et al., 2010; Kou-Giesbrecht et al., 2023; Richardson et al., 2012) (~~Beer et al., 2010; Richardson et al., 2012; Zaehle et al., 2015~~). The parameterization of some processes has been criticized for being oversimplified from an ecological point of view (Ali et al., 2015; Lawrence et al., 2019; Reich et al., 2006). The inclusion or exclusion of nutrient limitations on productivity is one of the critical factors., and the dynamic vegetation models tend to overestimate terrestrial C sequestration (Anav et al., 2015; Heikkinen et al., 2021; Murray-Tortarolo et al., 2013; Oliveira et al., 2021). The uncertainty/errors in predictions using land models have been attributed to many factors. The parameterization of some processes has been criticized for being oversimplified from an ecological point of view (Ali et al., 2015; Lawrence et al., 2019; Reich et al., 2006). The inclusion or exclusion of nutrient limitations on productivity is one of the critical factors. ~~These~~ The C-only models ignore significant nitrogen (N) impacts and therefore overestimate C sequestration by terrestrial ecosystems under climate change (Peñuelas et al., 2013; Zaehle et al., 2015). Ecosystem N cycling processes are among the dominant drivers of terrestrial C-climate interactions through their impacts, mainly N limitation, on vegetation growth and productivity (Reich et al., 2006), especially in N-poor younger soils at high latitudes (LeBauer & Treseder, 2008; Vitousek and Howarth, 1991), and on microbial decomposition of organic matter (Hu et al., 2001)

In the latest Coupled Model Intercomparison Project Phase 6 (CMIP6, Eyring et al., 2016). As such, the N cycle and its effect on C uptake in the terrestrial biosphere have been incorporated into land surface models (LSMs) of ESMs (Davies-Barnard et al., 2020) (Davies-Barnard et al., 2020; Kou-Giesbrecht et al., 2023) with various representations of N processes (Ali et al., 2015; Asaadi et al., 2021; Best et al., 2011; Clark et al., 2011; Davies-Barnard et al., 2020; Ghimire et al., 2016; Goll et al., 2017; Krinner et al., 2005; Lawrence et al., 2019; Matson et al., 2002; Oleson et al., 2013; Smith et al., 2014; Thum et al., 2019; Wang et al., 2010; Wiltshire et al., 2020; Yu et al., 2020; Zhu et al., 2019). (Ali et al., 2015; Asaadi et al., 2021; Ghimire

et al., 2016; Goll et al., 2017; Lawrence et al., 2019; Oleson et al., 2013; Smith et al., 2014; Thum et al., 2019; Wiltshire et al., 2020).

65 Adequate C-N coupling in plant N processes, however, although there were 112 different coupled models with various land surface models from 33 research teams, only about 10 models incorporated an N cycle module (Arora et al., 2020). The coupling of N processes is still an area of model development. Among these models including N processes, most of them pay more attention to microbial N dynamics in soil. The adequate C-N coupling in plant N processes has been indicated as an area that still needs intensive investigation (Thum et al., 2019; Ghimire et al., 2016; Goll et al., 2017; Yu et al., 2020; Zaehle et al.,

70 2015; Zhu et al., 2019). Some key plant N processes, such as N limitation on GPP, The fundamental aspects of N cycling for terrestrial biosphere models, such as N limitation of vegetation growth, strategies in which vegetation invests C to increase the N supply under N-limited conditions, and N limitation of decomposition, have been identified as important challenges for representing N cycling in terrestrial biosphere models (Meyerholt et al., 2020; Peng et al., 2020; Zaehle et al., 2015). Some key plant N processes, such as N limitation on gross primary productivity (GPP), the effect of biomass N content on autotrophic

75 respiration, plant N uptake, ecosystem N loss, and biological N fixation, have been introduced into LSMs with various complexity to present the N limitation effects in current land models. They include, for instance, using N to scale down the photosynthesis parameter $V_{c,max}$ (Ghimire et al., 2016; Zaehle et al., 2015) complexities to determine the effects of N limitation in current land models. These methods include, for instance, using N to scale down the photosynthesis parameter $V(c, max)$ (Ghimire et al., 2016; Zaehle et al., 2015) or potential GPP to reflect N availability (Gerber et al., 2010; Oleson et al., 2013;

80 Wang et al., 2010); defining a (Gerber et al., 2010; Oleson et al., 2013; Wang et al., 2010), defining the C cost of N uptake (Fisher et al., 2010) (Fisher et al., 2010a) and optimizing N allocation for leaf processes (Ali et al., 2015). The wide variety of assumptions and formulations of N cycling processes and C-N coupling reflects knowledge gaps and divergent theories, and further investigation is imperative (Kou-Giesbrecht et al., 2023). The coupling of N processes is still an area of model development. In the latest Coupled Model Intercomparison Project Phase 6 (CMIP6, Eyring et al., 2016), although there were

85 112 different coupled models with various land surface models from 33 research teams, only about 10 models incorporated an N cycle module (Arora et al., 2020). (Ali et al., 2015). In many of these approaches, N limitation is represented as instantaneous down regulation of potential photosynthesis rates based on soil mineral N availability.

This paper presents a recently developed process-based approach, which mainly focuses on the N limitation effects and plant resistance on photosynthesis, plant respiration, and plant phenology. The dynamic plant C/N ratio is a key concept in

90 representing plant resistance, self-adjustment, and C/N interactions. Due to their relative immobility, plants often face significant challenges in obtaining an adequate supply of nutrients to meet the demands of basic cellular processes. A deficiency of any type of nutrient may result in decreased plant productivity and/or fertility. This paper presents a recently developed process-based plant C-N coupling framework with a consistent coupling strategy between biophysical and biogeochemical processes. The framework mainly focuses on the effects of N limitation on plant photosynthesis (Section

95 2.2.3), plant respiration (Section 2.2.4), and plant phenology (Section 2.2.5) with a dynamic C/N ratio (CNR, section 2.2.2). The dynamic plant CNR is a more realistic representation than the fixed plant CNR in assessing the effect of N limitation on

plant C processes and interactions between plant C and N processes. (~~McDowell et al., 2008; Morgan and Connolly, 2013; Stenberg and Muola, 2017~~). Evidence has shown that plant C/N ratios have to change over the plant's lifecycle with nutrient availability (Chen and Chen, 2021; McGroddy et al., 2004; Meyer-Grünefeldt et al., 2015; Sardans et al., 2012; Smith, 1991; Yang et al., 2021; Zhang et al., 2011) through plant self-adjustment. Plant cells C/N ratios are influenced by the accumulation of C polymers, such as carbohydrates and lipids, and are greater when cells are nutrient starved, or exposed to high light (~~Aber et al., 2003; MacDonald et al., 2002; Talmy et al., 2014~~). However, many land models specify fixed plant C/N ratios for each plant functional type (PFT) (e.g., Best et al., 2011; Clark et al., 2011; Krinner et al., 2005; Oleson et al., 2013; Wang et al., 2010). In this paper, we present a new plant C-N coupling framework with flexible C/N ratios (Section 2.2.2), in which N regulates photosynthesis (Section 2.2.3), respiration (Section 2.2.4), and plant phenology (Section 2.2.5), as well as produces a consistent coupling between biophysical and biogeochemical processes. Allometric relations and empirical data sets are used to constrain the range of possible C/N ratios. This dynamic C/N ratio depends on the degree to which the N demands of different plant organs (e.g., leaf, root, and wood) are satisfied over the past several days. This plant C-N framework takes some plant N metabolism processes into account and prevents unrealistic instantaneous down-regulation of potential photosynthesis rates.

We implement this plant C-N framework by coupling a soil organic matter and nutrient cycling model (DayCent-SOM; Del Grosso et al., 2000; Parton et al., 1998, 2010) with a biophysical/dynamic vegetation model (SSiB5/TRIFFID, the Simplified Simple Biosphere Model version 5/Top-down Representation of Interactive Foliage and Flora Including Dynamics Model, Cox, 2001; Harper et al., 2016; Liu et al., 2019; Xue et al., 1991; Zhan et al., 2003; Zhang et al., 2015). The SSiB and TRIFFID have been extensively used for the land-atmosphere interaction studies (Harper et al., 2016; Xue et al., 2004, 2010, 2022, 2023). DayCent-SOM, which includes only the soil organic matter (SOM) cycling and trace gas subroutines from the DayCent ecosystem model (Parton et al., 1998, 2010)-, represents SOM transformations, below-ground N cycling, soil N limitation to microbial processes and plant growth, and nitrification/denitrification processes. In the coupled model, the potential N uptake depends on plant N demand from a biophysical and dynamic vegetation model, SSiB5/TRIFFID. The actual plant N uptake is limited based on soil N availability, as predicted by DayCent-SOM (Del Grosso et al., 2000; Parton et al., 1998, 2010). Although this plant C-N coupling framework is developed based on SSiB5, TRIFFID, and DayCent-SOM, the methodology and approach in this study could be applied to other process-based land models with similar physical, biological, and ecological principles. The coupled model is verified at thirteen flux tower sites (Lund et al., 2012; Pastorello et al., 2020) with different plant functional types (PFTs) and is used to conduct several sets of global 2-D offline simulations from 1948 to 2007 to assess the effects of the coupling process. Model predictions of global GPP and LAI have been evaluated against satellite-derived observational data (Jung et al., 2009; Sheffield et al., 2006; Zhu et al., 2013). The results demonstrate the relative importance of different plant N processes in this C-N framework.

The model used in this paper is presented in section 2.1. The development and implementation of this plant C-N framework is/are presented in section 2.2. The model forcing and validation data used in this paper are presented in section 2.3. In section 3, the experimental design is described. In section 4, the measurements from the flux tower sites with different PFTs and the

global satellite-derived observations from ~~1948~~1982-2007 are used as references to assess the effect of the C-N coupling process on the long-term mean vegetation distribution ~~and terrestrial C cycling~~ using the offline SSiB5/TRIFFID/DayCent-SOM. Some issues and conclusions are presented in section 5.

2 Methods

135 2.1 Model description

2.1.1 SSiB4/TRIFFID model

The Simplified Simple Biosphere Model (SSiB, Xue et al., 1991; Sun and Xue, 2001; Zhan et al., 2003) is a biophysical model that simulates fluxes of surface radiation, momentum, sensible ~~heat~~ heat, and latent heat, as well as runoff, soil moisture ~~and temperature~~, surface temperatures, and vegetation GPP, based on energy and water balance and photosynthesis processes. The
140 SSiB was coupled with a dynamic vegetation model, the Top-down Representation of Interactive Foliage and Flora Including Dynamics Model (TRIFFID), to calculate ~~NPP, LAI,~~ net primary productivity (NPP), leaf area index (LAI), canopy height, and PFT fractional coverage according to the C balance (Cox, 2001; Harper et al., 2016; Liu et al., 2019; Zhang et al., 2015). Moreover, the surface albedo and aerodynamic resistances are also updated based on the vegetation ~~conditions~~ LAI, vegetation cover, vegetation height, and greenness. Previous work has improved the PFT competition strategy and plant physiology
145 processes to make the SSiB4/TRIFFID suitable for seasonal, interannual, and decadal studies (Zhang et al., 2015). SSiB4/TRIFFID includes seven PFTs: (1) broadleaf evergreen trees (BET), (2) needleleaf evergreen trees (NET), (3) broadleaf deciduous trees (BDT), (4) C3 grasses, (5) C4 plants, (6) shrubs, and (7) tundra. PFT coverage is determined by ~~net C availability~~ NPP, competition between species, and disturbance, which includes mortality due to fires, pests, and windthrow. A detailed description and validation of SSiB4/TRIFFID can be found in Zhang et al. (2015), Liu et al. (2019), and Huang et al. (2020). In this study, ~~The~~ DayCent-SOM (see the next section) is introduced and coupled with ~~the~~ SSiB5/TRIFFID using
150 the C-N interface coupling framework introduced in this study, which will be discussed in Section ~~section~~ 2.2.

2.1.2 DayCent-SOM model

DayCent-SOM, a subset of DayCent that excludes plant growth, soil hydrology, and soil temperature subroutines, consists of soil mineral N pools (ammonium and nitrate) and six types of organic C and N pools consisting of two non-woody plant litter
155 pools (metabolic and structural), three coarse woody debris pools (from the death of large wood, fine branches, and coarse roots), and three kinetically defined organic matter pools: (active, slow, and passive); all types of organic pools except the passive pool have both ~~above-ground~~ aboveground and ~~below-ground~~ belowground counterparts: (Table 1). Non-woody plant litter is partitioned into structural (lignin + cellulose) and metabolic (labile) litter based on the lignin: N ratio of the plant material (Parton et al., 1994) ~~).~~. The coarse woody debris pools decay in the same way that the structural pool decomposes,
160 with lignin and cellulose going to the slow soil organic matter pool and the labile fraction going to the active soil organic

matter pool. Each type of organic pool has its own intrinsic rate of decomposition, which is modified by temperature and moisture ~~effects~~ (Parton et al., 1994). Additionally, the decomposition rates of the structural material and coarse woody debris pools are functions of their respective lignin fractions. DayCent's litter decay model has been validated using extensive data from ~~the~~ LIDET litter decay experiments from all over the world (Bonan et al., 2013).

165 **Table 1.** The Nitrogen Pools in DayCent-SOM

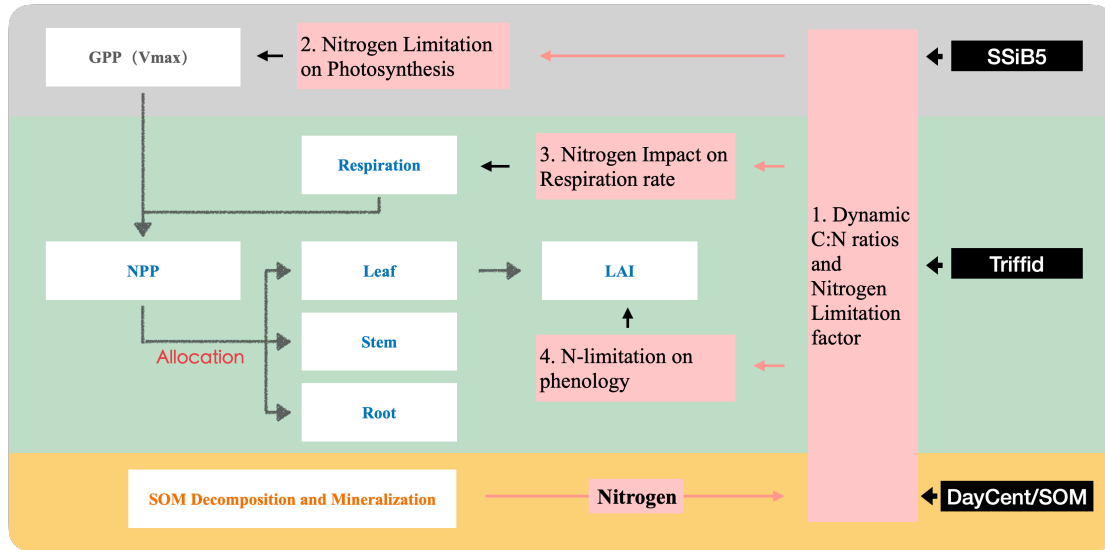
		<u>Aboveground</u>	<u>Belowground</u>
<u>Mineral N pool</u>	-	-	<u>Soil mineral N pools</u>
	<u>non-woody litter pools</u>	<u>Surface structural N</u> <u>Surface metabolic N</u>	<u>Soil structural N</u> <u>Soil metabolic N</u>
<u>Organic N pool</u>	<u>woody debris pool</u>	<u>Surface dead N</u>	
	<u>kinetically defined organic matter pools</u>	<u>Surface active N</u> <u>Surface slow organic N</u>	<u>Soil active organic N</u> <u>Soil slow organic N</u> <u>Soil passive organic N</u>

2.2 Development of a plant ~~Carbon-Nitrogen-carbon-nitrogen~~ (C-N) ~~Interface~~ interface coupling framework

175 2.2.1 Conceptual considerations and coupling strategy

To represent C and N interactions, we ~~have developed~~ develop a plant C-N interface framework to ~~take into account both~~ couple biophysical and ~~biochemical C/N biogeochemical~~ processes in ~~plant life activities~~ the terrestrial C and N cycles. In this study, we applied the coupling framework to SSiB5/TRIFFID/DayCent-SOM. ~~However, this approach could be applied to any other process-based models with similar physical/biological principles.~~ The conceptual considerations in developing this framework are presented in this section. For a process-based model, introducing a consistent coupling philosophy between biophysical and biogeochemical processes is necessary. ~~The surface water, radiation, carbon fluxes, and plant litter are calculated by SSiB5/TRIFFID.~~ The soil N dynamics model (DayCent-SOM) is directly driven by soil temperature, ~~soil moisture~~ as well as, net radiation and plant C and N litter inputs into soil. ~~Because the surface water, radiation, and carbon fluxes and plant litter are calculated by SSiB5, we force DayCent SOM with~~ soil organic pool, which are provided by the SSiB5-produced soil temperature, soil moisture, and SSiB5/TRIFFID-produced plant litter./TRIFFID. DayCent-SOM then computes daily changes ~~of~~ in all organic matter and mineral soil pools, estimates losses of N from nitrate leaching and N₂O, NO_x, and N₂ emissions, predicts the amount of inorganic N available to plants, and updates inorganic N pools after accounting for plant N uptake by SSiB5/TRIFFID. Following plant N uptake from DayCent-SOM, our plant C-N interface framework describes ~~the~~ the effects ~~on plant physiology from~~ of N on photosynthesis, plant autotrophic respiration, and plant phenology ~~plus~~ (Fig. 1). ~~All these effects are associated with~~ a dynamic C/N ratio (Fig. 1). ~~Following such~~ CNR. ~~In the original land surface model development philosophy, our framework not only considers N limitation on the general plant (SSiB4/TRIFFID), with assumed unlimited N availability and fixed CNR based on PFT, the assimilated C determined the N contents of leaves, stems, and roots, which~~

195 influenced photosynthesis process but also emphasizes the N limitation effect during the growth season, which can represent the physiological processes of C-N cycling and help us obtain, autotrophic respiration, NPP, and LAI. However, more information to understand evidence indicates that the attribution of N processes on CNR is not fixed in plant life, which will be further discussed in section 2.2.2. With the C-cycle, dynamic CNR, the effect of N limitation on Rubisco capacity and photosynthesis is assessed (section 2.2.3).



200 **Figure 1.** Schematic diagram of plant biogeochemistry and nitrogen impacts in SSiB5/TRIFFID/DayCent-SOM.

Notes: (1) Different background color represents colors represent three different modules: SSiB, TRIFFID, and DayCent/SOM; (2) White boxes indicate the main processes involved in C-N coupling in different modules; (3) Vermeil boxes indicate how nitrogen influences plant biogeochemistry through the C-N framework.

205 Moreover, nitrogen is not the only dominant regulator of photosynthesis and vegetation dynamics. Reich et al., (2008) demonstrated strong relationships between respiration and N limitation based on observational data from various species. In the common N concentration range, respiration rates are consistently lower on average in leaves than in stems or roots. Therefore, this framework introduces two parameters for stems and roots based on PFT and available N, respectively, to adjust the respiration rate (section 2.2.4). Furthermore, N also affects plant phenology and can be remobilized to supply spring bud
 210 break or vegetative shoot extension (Cox, 2001; Kolb and Evans, 2002; Marmann et al., 1997; Millard, 1994; Neilsen et al., 1997). The framework includes the impact of N on plant phenology by introducing an N limitation parameter, which will be discussed in section 2.2.5. With consideration of the effect on phenology, the N limitation effect during the growth season is emphasized. All these considerations in the framework should help to understand the effects of N processes to the C cycle more comprehensively

215 2.2.2 Dynamic C/N ratio based on plant growth and soil nitrogen storage

Plants often face significant challenges in obtaining an adequate supply of nutrients to meet the demands of basic cellular processes. Nutrient deficiency may result in decreased plant productivity and/or plant fertility (McDowell et al., 2008; Morgan and Connolly, 2013; Stenberg and Muola, 2017). Evidence has shown that plant CNR can change with nutrient availability (Chen and Chen, 2021; McGroddy et al., 2004; Meyer-Grünefeldt et al., 2015; Sardans et al., 2012; Smith, 1991). Plant cell CNRs are influenced by the accumulation of C polymers, such as carbohydrates, and are greater when cells are nutrient starved or exposed to high levels of photosynthetically active radiation (PAR) (Aber et al., 2003; MacDonald et al., 2002; Talmy et al., 2014). In the original land surface model (SSiB4/TRIFFID), with assumed unlimited N availability and fixed C/N ratios based on PFT, the assimilated C determined the N contents of leaf, stem, and root, which influenced autotrophic respiration, followed by GPP, LAI, and NPP. However, more evidence indicates the C/N ratio is not fixed in plant life. The studies of Ecological Stoichiometry—The studies of ecological stoichiometry (Sterner and Elser, 2002), which investigates how the availability of multiple elements, including carbon, nitrogen, and phosphorus, constrain ecological interactions, reveal that plants can adjust their resource requirements. Changes in response and adapt to lower N resource availability will result in changes to plant C allocation and partitioning. Studies show that plants resorb only about 50% of leaf N on average (Aerts, 1996) to conserve nutrients (Clarkson and Hanson, 1980) and to increase nutrient use efficiency (Herbert & Fownes, 1999; Vitousek, 1982). These processes cause a major internal nutrient flux and changes of C/N ratios (Herbert and Fownes, 1999; Vitousek, 1982). These processes cause changes in the CNR to reduce the impact of N limitation (Talhelm et al., 2011; Vicca et al., 2012). In addition, plant responses, such as plant resistance and self-adjustment, will be limited under fixed C/N ratios, which affect plant productivity and litter N content, thus driving changes in the underground biogeochemistry and ultimately C and N uptake and storage (Drewniak and Gonzalez-Meler, 2017). Some studies show that the increase in foliar N under increased soil N availability would improve plant responses because it allows adaptations in the stoichiometry of C and N (Bai et al., 2021; Chang et al., 2022; Ding et al., 2022; Kaiser et al., 2014; Lin et al., 2022; Zhang et al., 2022). The main impact will be to decrease C/N ratio in leaves when the available N increases, driving increases in productivity and changes in soil and litter N content (Drewniak and Gonzalez-Meler, 2017). A dynamic C/N ratio is employed in our framework to obtain N states more realistically and properly represent the effect of N processes (See section 2.2.2 for more details).

A commonly used parameterization of photosynthetic C assimilation by the terrestrial biosphere in ESMs For the response of vegetation to N limitation, i.e., the strategies in which vegetation invests C to increase N supply under N-limited conditions, some models represent flexible C/N stoichiometry, while others represent time-invariant C/N stoichiometry (Kou-Giesbrecht et al., 2023). Importantly, flexible vs. time-invariant C/N stoichiometry determines terrestrial C storage per unit N, followed by plant C allocation and partitioning. Plant responses are limited under a fixed CNR, which affects plant productivity and litter N content, thus affecting underground biogeochemistry and ultimately C and N uptake and storage. Comparing field measurements, it was found that allowing adaptations in the stoichiometry of C and N helped the land model improve the terrestrial surface C and N cycle simulation (Drewniak and Gonzalez-Meler, 2017; Medlyn et al., 2015).

In this study, dynamic CNRs are introduced into SSiB5/TRIFFID. This dynamic CNR can enable vegetation to increase N uptake under N-limited conditions, reduce N limitation, and sustain terrestrial C sequestration. Plant resistance and adaptation to N availability (N_{avail}) are represented by dynamic CNRs in SSiB5. The N availability (N_{avail}) for new growth limits the C assimilation rate through the CNRs, i.e., the model-simulated NPP should be no more than the N_{avail} is represented by the Farquhar, von Caemmerer, and Berry (FvCB) model of photosynthesis (Collatz et al., 1991; Farquhar et al., 1980). Plants require N as essential components of photosynthetic proteins involved in light capture, electron transport, and carboxylation (Evans, 1989). Nitrogen is an important constituent of the Rubisco enzyme and mitochondrial enzymes that regulate respiration and adenosine triphosphate (ATP) generation (Malkin and Osmond, 1991). One of the most important photosynthetic model parameters, the maximum carboxylation rate by the Rubisco enzyme ($V_{e,max}$) is a key parameter in the FvCB model (Farquhar et al., 1980) and has an extensive range across the models depending on the plant N content (Rogers, 2014). Since N is an important component of the Rubisco enzyme, leaf N content will affect $V_{e,max}$ and thus GPP. The original FvCB model did not explicitly consider the N effect on photosynthesis. In a number of LSMs, an empirical relationship is applied to relate $V_{e,max}$ to leaf N content N_{leaf} to generate the effect of N on photosynthesis, e.g., $V_{e,max} = i_p + s_p \times N_{leaf}$, where the intercept (i_p) and slope (s_p) are derived for each PFT based on observations (Kattge et al., 2009; Raddatz et al., 2007). Moreover, in some coupling approaches, only the relationship between the root N uptake and GPP/NPP is considered to represent the N limitation on C cycles (Ali et al., 2015; Fisher et al., 2010; Ghimire et al., 2016). However, because NPP is the difference between GPP and autotrophic respiration, adjusting NPP or GPP alone may cause the ratio between NPP and respiration to deviate from reality. Using the process-based N limitation factor produced from DayCent SOM to modify $V_{e,max}$ (See section 2.2.3) is a more realistic way to produce the N effect on the photosynthesis process. Moreover, when calculating the N limit to Rubisco capacity, an aforementioned dynamic C/N ratio is introduced in our approach to influence the N limit effect on photosynthesis.

Nitrogen is not only a dominant regulator of vegetation dynamics, GPP, NPP, and terrestrial C cycles; Reich et al., (2008) demonstrate strong relationships between respiration and N limitation based on observational data from various species. At any normal N concentration, respiration rates are consistently lower on average in leaves than in stems or roots. Therefore, we introduce two parameters for stems and roots, respectively, based on PFT to adjust the respiration rate in section 2.2.4.

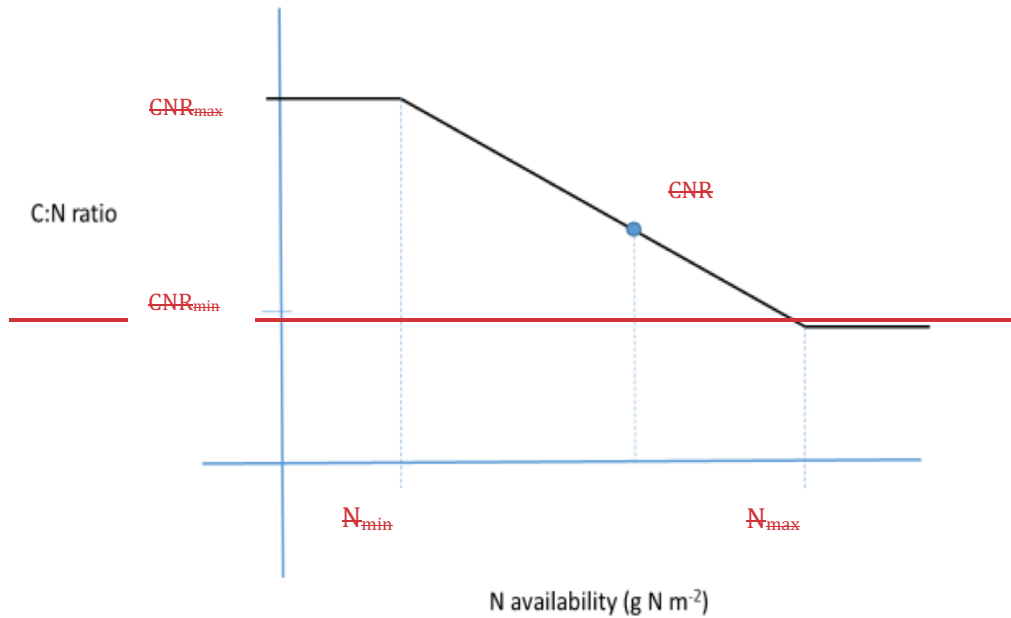
Nitrogen also affects plant phenology and can be remobilized to supply spring bud break or vegetative shoot extension (Kolb and Evans, 2002; Marmann et al., 1997; Millard, 1994; Nielsen et al., 1997). Nitrogen resorption is found during leaf senescence and growth in evergreens (May and Killingbeck, 1992). Because plants need time to turnover, the plant N processes also have a lag effect on plant phenology (Thomas et al., 2015). Phenology in SSiB4/TRIFFID modulates LAI evolution, including leaf mortality, but it is not directly linked to N. Since different N states and supplements will lead to different lags on phenology, we add N impact on plant phenology by introducing a N limitation parameter, which will be discussed in section 2.2.5.

280 **2.2.2 Dynamic C/N ratio based on plant growth and soil nitrogen storage**

Plant resistance and self-adjustment to N availability (N_{avail}) are represented by dynamic C/N ratios (CNRs) in SSiB5. The N availability for new growth limits the C assimilation rate through the CNRs, i.e., the model simulated NPP should be no more than $N_{avail} \times \text{CNR}$ of new plant material. In the original TRIFFID parameterization, the CNRs for different plant components (leaf, root, and ~~woodstem~~) are fixed based on plant functional types (Cox, 2001), and ~~changes the change~~ in CNR ~~occurred that~~ occurs over the ~~lifecycle of the plant, varied ecological process and varies~~ with nutrient availability, ~~and were was~~ not considered ~~in the original SSiB4/TRIFFID models.~~ A linear relationship between ~~the~~ CNR and N_{avail} , based on ~~the~~ DayCent's parameterization, is introduced to the SSiB5/TRIFFID/DayCent-SOM for each PFT's ~~components, component~~ (Fig. 2, Eq. 1).

$$\text{CNR} = \begin{cases} \text{CNR}_{max}, & N_{avail} \leq N_{min} \\ \frac{N_{avail} - N_{max}}{N_{min} - N_{max}} \times \text{CNR}_{min} + \frac{N_{avail} - N_{min}}{N_{max} - N_{min}} \times \text{CNR}_{max}, & N_{min} < N_{avail} < N_{max} \\ \text{CNR}_{min}, & N_{avail} \geq N_{max} \end{cases} \quad (1)$$

where N_{avail} is the amount of soil mineral nitrogen that was available at the end of the previous day (g N m^{-2}) calculated from DayCent-SOM.



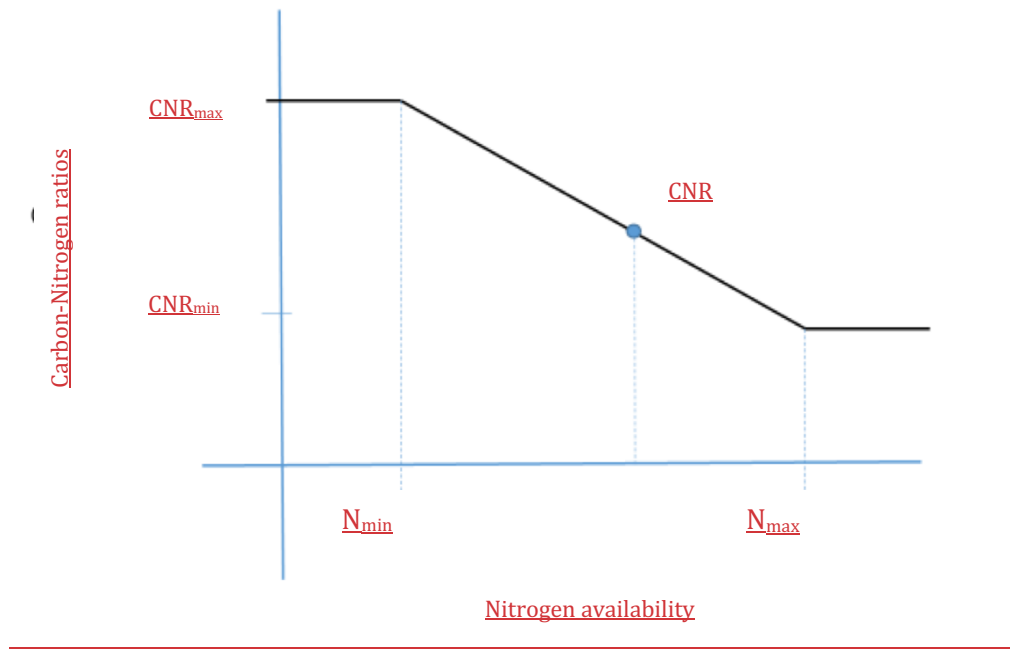


Figure 2. The relationship between soil nitrogen availability and plant carbon-nitrogen ratios.

295 The minimum and maximum amounts of nitrogen (N_{min} , N_{max}) necessary for the potential NPP_p ($\text{g C m}^{-2} \text{ day}^{-1}$), which is first calculated from the [SSiB4SSiB5/TRIFFID](#) with unlimited N, are:

$$N_{min} = \frac{NPP_p}{CNR_{max}} \quad (2)$$

$$N_{max} = \frac{NPP_p}{CNR_{min}} \quad (3)$$

where CNR_{min} and CNR_{max} are the minimum and the maximum C/N ratio CNRs, respectively, for each PFT's components component from the DayCent (Table 4-2). Allometric relations and empirical datasets are used to constrain the range of possible CNRs. The CNR ranges CNRs of leaves, fine roots, and stems/wood are were obtained from DayCent's user's manual and other published papers (Parton et al., 1993, 2007). Please note Note that Eq. (2) and Eq. (3) are calculated based on the potential NPP; the CNR that is calculated based on Eqs. 1-3 ensures that when N_{avail} varies between N_{min} and N_{max} ; the plant can adjust the CNR to support this potential NPP (as demonstrated in the schematic diagram in Figure 2). That said, the N limitation will have no effect on the C assimilation as long as N_{avail} is larger greater than N_{min} . However, the N content of plant litter falling to the soil was determined by this dynamic C/N ratio CNR. Compared with the constant CNR, the range of possible plant carbon variation with dynamic CNR is smaller, reducing the impact of N limitation. As reviewed in the introduction and previous beginning of this section, a number of recent studies have demonstrated that allowing adaptations in the stoichiometry of C and N would improve plant responses; for instance, an increase in available foliar N decreases the C/N ratio CNR in leaves, driving an increase in productivity.

Table 12. C:N ranges of leaves, fine roots, and stems/wood for each plant function type (PFT).

	Plant component	CNR_{min}	CNR_{max}
Broadleaf deciduous	leaves/Leaves	20	50
	roots/Roots	40	70
	wood/Stems	200	500
Broadleaf Evergreen	leaves/Leaves	20	40
	roots/Roots	40	70
	wood/Stems	150	300
Needleleaf Evergreen	leaves/Leaves	30	60
	roots/Roots	40	60
	wood/Stems	400	800
C3 grass	leaves/Leaves	20	40
	roots/Roots	40	50
	wood/Stems	40	80
C4 grass/plants	leaves/Leaves	20	60
	roots/Roots	60	100
	wood/Stem	60	100
shrub	leaves/Leaves	20	40
	roots/Roots	40	70
	wood/Stems	200	400
tundra-shrub	leaves/Leaves	20	40
	roots/Roots	40	80
	wood/Stems	300	700

Note: Data of The CNR_{min} and CNR_{max} data for each PFT's components component are from DayCent's user's manual and other publications (Parton et al., 1993, 2007)

The DayCent-SOM only provides the total available nitrogen (N_{avail}) for the plant within one grid box, (the soil is 3.2 m in depth), which consists of several PFTs. To apply equation 1, the nitrogen available for each PFT and its plant components in the grid box is calculated as

$$N_{avail}(i) = N_{avail} * frac_i \quad (4)$$

$$N_{avail}(i,j) = N_{avail}(i) * \Delta C_j / \sum_j \Delta C_j \quad (5)$$

where $frac_i$ is the fraction of PFT i in one grid, and ΔC_j is the fraction of carbon allocated to plant component j, which consists of leaf, root/leaves, roots, and wood/stems and is calculated in TRIFFID.

Furthermore, the dynamic CNR in this framework depends on the degree to which the N demands of different plant components (e.g., leaves, roots, and stems) have been satisfied over the past several days, and Eq. 1 prevents unrealistic instantaneous

downregulation of potential photosynthesis rates. “Instantaneous downregulation” refers to the fact that photosynthesis rates are limited as soon as N (either in leaves or soil) is not sufficient (Reich et al., 2006; Ghimire et al., 2016), which has been applied in some N-limited models (Davies-Barnard et al., 2020). In our framework, by adjusting C/N ratios, the N limitation effect under certain conditions does not instantaneously respond to available N. The N limitation will produce effects only when available N passes some critical value (see further discussions in section 2.2.3).

2.2.3 Effect of nitrogen limitation on photosynthesis based on soil available nitrogen and the plant C-/N ratio

The widely used parameterization of photosynthetic C assimilation by the terrestrial biosphere in ESMs, including our model, is represented by the Farquhar, von Caemmerer, and Berry (FvCB) model of photosynthesis (Collatz et al., 1991; Farquhar et al., 1980). At high levels of PAR, the photosynthetic rate is limited by the amount of Rubisco in the leaf and its cycling rate.

Nitrogen is an important constituent of the Rubisco enzyme and mitochondrial enzymes that regulate respiration and adenosine triphosphate (ATP) generation (Makino and Osmond, 1991). As one of the most important photosynthetic model parameters, the maximum carboxylation rate by the Rubisco enzyme ($V_{c,max}$) is a key parameter in the FvCB model (Farquhar et al., 1980) and has an extensive range across the models depending on the plant N content (Rogers, 2014). Therefore, leaf N content will affect $V_{c,max}$ and thus GPP. However, the original FvCB model did not explicitly consider the effect of N on photosynthesis.

While N limitation was introduced to terrestrial biosphere models, they differ in how N limitation in the plant C process is represented (Thomas et al., 2015; Fisher et al., 2010b). In a number of LSMs, an empirical relationship is applied to relate $V_{c,max}$ to leaf N content N_{leaf} to determine the effect of N on photosynthesis, e.g., $V_{c,max} = i_v + s_v \times N_{leaf}$, where the intercept (i_v) and slope (s_v) are derived for each PFT based on observations (Kattge et al., 2009; Raddatz et al., 2007). There are several different ways to represent N limitation effects in land models, including using N to scale down photosynthesis (Ghimire et al., 2016; Goll et al., 2017; Thum et al., 2019; Yu et al., 2020; Zaehle et al., 2015; Zhu et al., 2019), scaling down potential GPP based on N availability (Gerber et al., 2010; Oleson et al., 2013; Wang et al., 2010), or defining an NPP cost of nitrogen uptake (Fisher et al., 2010). We choose the most physiological way by adjusting maximum Rubisco carboxylation rate ($V_{c,max}$) during the photosynthesis process, rather than adjusting NPP at the end of the photosynthesis process. $V_{c,max}$ regulates both C assimilation and autotrophic respiration; and the photosynthesis assimilation product, GPP, is proportional to $V_{c,max}$, which is proportional to nitrogen content of the Rubisco leaf reserves.

We therefore introduce a downregulation of the canopy photosynthetic rate based on the available mineral N for new growth (N_{avail}) using a N availability factor, $f(N)$.

We therefore introduce a downregulation of the canopy photosynthetic rate based on the available mineral N for new growth (N_{avail}) using a N availability factor, $f(N)$.

We therefore introduce a downregulation of the canopy photosynthetic rate based on the available mineral N for new growth (N_{avail}) using a N availability factor, $f(N)$.

$$V_{c,max,Nlimit} = V_{c,max} * f(N) \tag{6}$$

The $f(N)$ is determined by nitrogen availability:

$$f(N) = \begin{cases} \frac{N_{avail}}{N_{min}} & N_{avail} \leq N_{min} \\ 1 & otherwise \end{cases} \tag{7}$$

360 ~~Because plants can adjust the relative allocations of C and N during N uptake via N remobilization and resorption to reduce the impact of N limitation, as discussed in the previous section for dynamic CNR, the N limit effect on photosynthesis only applies when nitrogen availability is lower than the minimum amounts of nitrogen (N_{min}) necessary for the potential NPP. We take into account that plants have resistance and self adjustment through this approach to make the N limit effect neither linearly nor instantaneously responsive to available N content. A linear relationship between $f(N)$ and N_{avail} is valid only when N availability is not sufficient for the minimum N demand for new growth.~~

~~Some studies applied the same N limitation factor to NPP or GPP (Ali et al., 2015; Fisher et al., 2010; Ghimire et al., 2016). If NPP is adjusted, the same N limitation for photosynthesis is applied for plant respiration, which is not reasonable based on plant physiology (Högberg et al., 2017). Such approaches may distort the ratio of NPP and respiration. On the other hand, if only the GPP is adjusted for N limitation, then the N limitation for respiration is ignored.~~

365 ~~We chose the most physiological method by adjusting the maximum Rubisco carboxylation rate ($V_{c,max}$), which is proportional to the nitrogen content of the Rubisco leaf reserve) during photosynthesis rather than adjusting the NPP at the end of photosynthesis. $V_{c,max}$ regulates both C assimilation and autotrophic respiration, and the photosynthesis assimilation product, GPP, is proportional to $V_{c,max}$. Empirical evidence has shown that $V_{c,max}$ decreases with decreasing leaf N (Walker et al., 2014). We therefore introduce a downregulation of the canopy photosynthetic rate based on the available mineral N for new growth (N_{avail}) using the N availability factor $f(N)$.~~

$$V_{c,max,Nlimit} = V_{c,max} * f(N) \tag{6}$$

~~The $f(N)$ is determined by nitrogen availability:~~

$$f(N) = \begin{cases} \frac{N_{avail}}{N_{min}} & N_{avail} \leq N_{min} \\ 1 & otherwise \end{cases} \tag{7}$$

375 ~~Because plants can adjust the relative allocations of C and N during N uptake via N remobilization and resorption to reduce the impact of N limitation, as discussed in the previous section for dynamic CNR, the N limitation effect on photosynthesis only applies when nitrogen availability is lower than the minimum amount of nitrogen (N_{min}) necessary for the potential NPP. We take into account the fact that plant responses include resistance and adaptation through this approach along with the dynamic CNR to make the N-limiting effect neither linear nor instantaneously downregulate the available N content, as discussed in the last section. A linear relationship between $f(N)$ and N_{avail} is valid only when N availability is not sufficient for the minimum N demand for new growth.~~

~~In fact, the factor, $f(N)$ can also be applied to NPP and GPP as shown in Equations 8a–b.~~

$$NPP_{Nlimit} = NPP * f(N) \tag{8a}$$

$$GPP_{Nlimit} = GPP * f(N) \tag{8b}$$

385 ~~If NPP is adjusted (Eq. 8a), this means the same N limitation for photosynthesis is applied for plant respiration, which is not reasonable based on plant physiology (Högberg et al., 2017). Such approach may distort the ratio of NPP and respiration. If~~

only GPP is adjusted for N-limitation, then the N limitation for respiration is ignored. Therefore, we choose an approach to adjust $V_{c,max}$, which is related to N during the photosynthesis process and affects both C uptake and autotrophic respiration.

2.2.4 Improvement in the impact of nitrogen ~~impact on~~ ~~Nitrogen affects plant~~ respiration rates based on field observations

Based on a database (Reich et al., 2008) of 2510 measurements from 287 species, the relationships between the mass-based dark respiration rate and nitrogen concentration of leaves, stems and roots were assessed. The results indicate strong respiration–nitrogen scaling relationships for all observations and for data averaged by species. At usual N concentrations, respiration rates are consistently lower on average in leaves than in stems or roots. In the original SSiB4/TRIFFID, the total maintenance respiration (R_{pm}) is given by Cox (2001):

$$R_{pm} = 0.012R_{dc} \frac{N_l + N_s + N_r}{N_l} \quad (9)$$

where R_{dc} is canopy dark respiration and is linearly dependent on $V_{c,max}$. ~~The introduced N limitation of $V_{c,max}$ in Section 2.2.3 also influences the N effect on maintenance respiration. N_l , N_s and N_r are the N contents of leaf, stem, and root, respectively, and the factor of 0.012 is from the unit conversion. Eq. (9) assumes the respiration rates in root and stem have the same dependence on N content as leaf. However, studies (Reich et al., 2008) have shown that the respiration rates at any common N concentration were consistently lower in leaves than in stems or roots on average. Thus, we introduce two PFT-specific parameters ($ResA_S$, $ResA_R$) from field observations (Wang et al., 2006; Yang et al., 1992) to adjust root and stem respirations. Their values are listed in Table 2. The introduced N limitation of $V_{c,max}$ in section 2.2.3 also influences the effect of N on maintenance respiration. N_l , N_s and N_r are the N contents of the leaf, stem, and root, respectively, and the factor of 0.012 is from the unit conversion. Eq. (9) assumes that the respiration rates in roots and stems have the same dependence on the N content as that in leaves.~~

Based on the information derived from field measurements for different PFTs (Reich et al., 2008; Wang et al., 2006; Yang et al., 1992), we introduce two PFT-specific parameters ($ResA_S$, $ResA_R$) to adjust root and stem respiration. Their values are listed in Table 3.

$$R_{pm,Nlimit} = 0.012R_{dc} \frac{N_l + ResA_S * N_s + ResA_R * N_r}{N_l} \quad (10)$$

Table 23. The values of $ResA_S$ and $ResA_R$ for each plant function type (PFT).

PFT	Broadleaf deciduous	Broadleaf Evergreen	Needleleaf Evergreen	C3 grass	C4 grassplants	shrub	tundra shrub
$ResA_S$	1.36	1.36	1.44	1.0	1.0	1.25	1.25
$ResA_R$	1.72	1.72	1.95	1.3	1.3	1.40	1.40

Since $ResA_S$ and $ResA_R$ are generally larger than 1, new R_{pm} is larger than the original one, and the increased respiration due to the nitrogen limitation will decrease the NPP.

2.2.5 Effect of N limitation on the LAI based on plant phenology

Studies (Aerts and Berendse, 1988; Thomas et al., 2015) show that leaf turnover and aboveground productivity are related to nutrient availability and that plant N processes can potentially give rise to lags on phenology. In TRIFFID, a leaf phenology parameter, p , (Cox, 2001) is introduced to represent the vegetation's phenological status, to calculate the leaf drop rate, and to adjust the model-simulated maximum possible LAI, which is based on carbon balance, ($LAI_{balance}$), to actual LAI and produce realistic phenology.

Nutrient availability affects vegetation activity and thus plant phenology (May and Killingbeck, 1992; Millard, 1994; Neilsen et al., 1997; Piao et al., 2019; Thomas et al., 2015; Vitasse et al., 2021; Zhou et al., 2022). Studies have demonstrated that variations in nitrogen availability could change the spring and fall phenology, such as spring bud break or vegetative shoot extension (Yang et al., 2016; Yin et al., 2017; Fu et al., 2019), as well as the length of the growing season (Wang and Tang, 2019; Zhou et al., 2022). Increased soil nitrogen availability could supplement nutrient deficiencies and thus stimulate plant growth under low temperatures in early fall (Luke McCormack et al., 2014; Delpierre et al., 2016; Yin et al., 2017) and delay the end of the growing season (Wingler et al., 2006).

In TRIFFID, the leaf mortality rate and a leaf phenology parameter, p , (Cox, 2001), are introduced to represent the vegetation's phenological status (Eqs. 11 and 12) and to adjust the model-simulated seasonal maximum possible leaf area index ($LAI_{balance}$), which is based on surface carbon balance (Cox, 2001; Enquist et al, 1998), to determine the actual LAI and produce realistic phenology.

$$LAI = p \times LAI_{balance} \quad (11)$$

and

$$\frac{dp}{dt} = \begin{cases} -\gamma_p & \gamma_{lm} > 2\gamma_0 \\ \gamma_p(1-p) & \gamma_{lm} \leq 2\gamma_0 \end{cases} \quad (12)$$

where the leaf constant absolute drop rate $\gamma_p = 20 \text{ yr}^{-1}$, the leaf mortality rate γ_{lm} is a function of temperature T (Cox, 2001), and the minimum leaf turnover rate $\gamma_0 = 0.25$ (Cox, 2001). ~~This phenology parameter, p ;~~ This phenology in SSiB4/TRIFFID modulates LAI seasonal evolution, which considers leaf mortality and the temperature threshold for leaf drop, but it is not directly linked to N. The phenology parameter p indicates that “full leaf” is approached asymptotically during the growing season, and p is reduced at a constant absolute rate when the mortality rate is ~~larger~~ greater than a certain threshold value. Otherwise, p increases, but the rate of increase ~~is reduced~~ decreases as the growing season ~~evolves. To reflect~~ progresses.

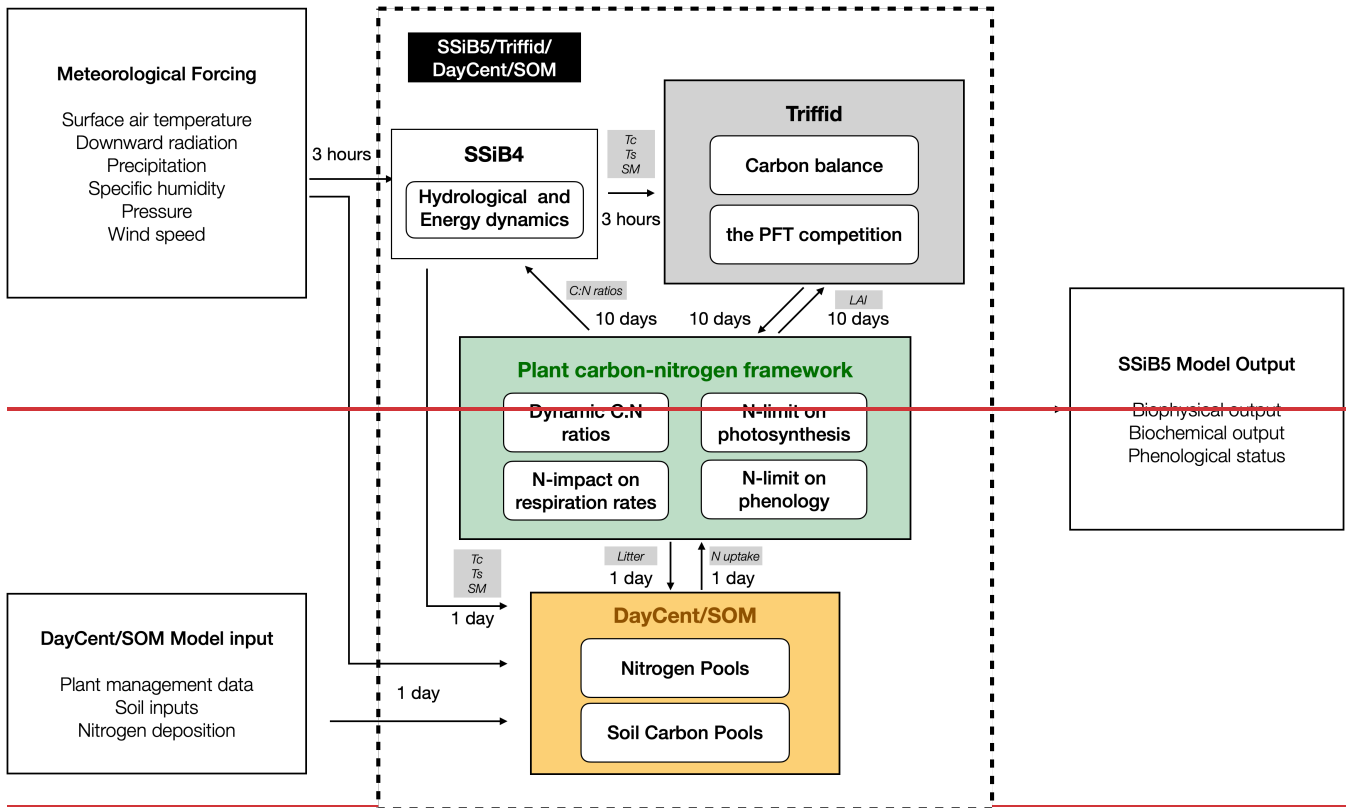
Since different N states and supplies affect phenology, as discussed above, this framework includes the impact of N on plant phenology by introducing N limitation in SSiB5/TRIFFID/DayCent-SOM, ~~we to take into account the effects of N on phenology.~~ We assume that p is limited by N availability, with the new nitrogen ~~limited~~ limitation $p_{N\ Limit}$ determined by

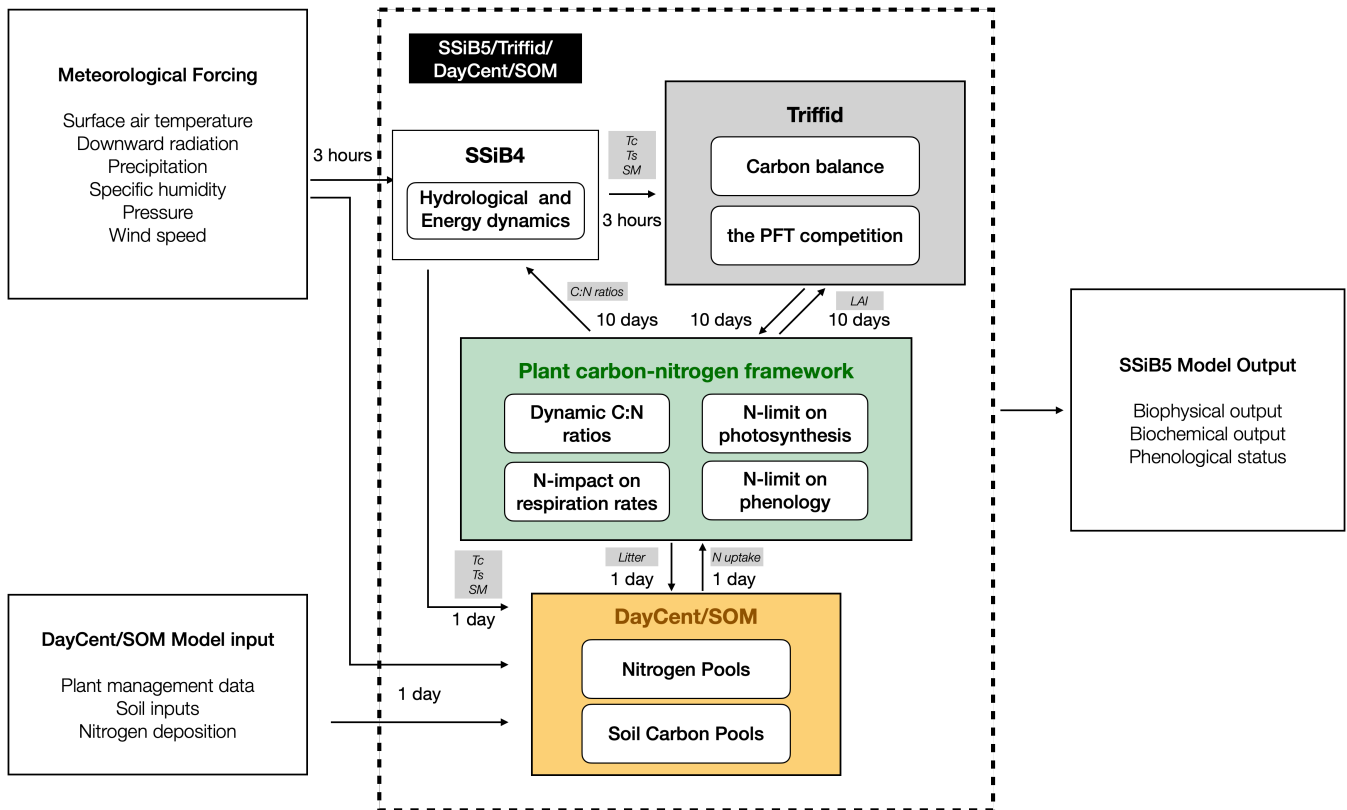
$$445 \quad p_{N\ Limit} = f(N) \times p \quad (13)$$

where $f(N)$ is calculated as described in section 2.2.3.

2.2.6 The computational flow of SSiB5/TRIFFID/DayCent-SOM

In SSiB5/TRIFFID/DayCent-SOM, SSiB5 provides GPP, autotrophic respiration, and other physical variables, such as canopy and soil temperatures and soil moisture, every 3 hours for TRIFFID (Fig. 3). The TRIFFID accumulates the GPP from SSiB5 and produces biotic C, PFT fractional coverage, vegetation height, and LAI every ten days, which are used to update surface properties in SSiB5, such as albedo, surface roughness length, and aerodynamic ~~and~~ canopy resistances. The plant C-N framework uses ~~the~~ meteorological forcings (i.e., air temperature, humidity, wind, radiation, and precipitation) and physical variables (i.e., soil moisture and soil temperature) provided by SSiB5 every 3 hours and ~~the~~ biophysical properties (vegetation fraction and biotic C) provided by TRIFFID, which ~~is~~ are updated every ten days. The plant C-N interface framework calculates the dynamic ~~C/N ratios~~ CNR, N-limited photosynthesis, and N-impacted respiration rate every 3 hours. ~~The~~ C loss and potential N uptake ~~are accumulated~~ accumulate within one day in the C-N ~~Interface Framework~~ interface framework, and plant C and N ~~litter fall~~ litterfall are transferred to DayCent-SOM at the end of the day. DayCent-SOM calculates the amount of inorganic N available for plant N uptake (N_{avail}) and the N losses from nitrate leaching and N-trace gas emissions each day. The TRIFFID updates the vegetation dynamics based on the C balance on day 10, including PFT competition. The updated vegetation dynamics are transferred to SSiB5 to calculate N-limited phenology to reflect ~~N~~ the impact of N on the C cycle, which is significant during the growth season.





465 **Figure 3.** Flowchart of plant carbon-nitrogen interactions in SSiB5/TRIFFID/DayCent-SOM; the main variables are listed between the two modules are listed.

Notes: Tc: canopy temperature; Ts: land surface temperature; SM: soil moisture; GPP: gross primary productivity; Res: autotrophic respiration.

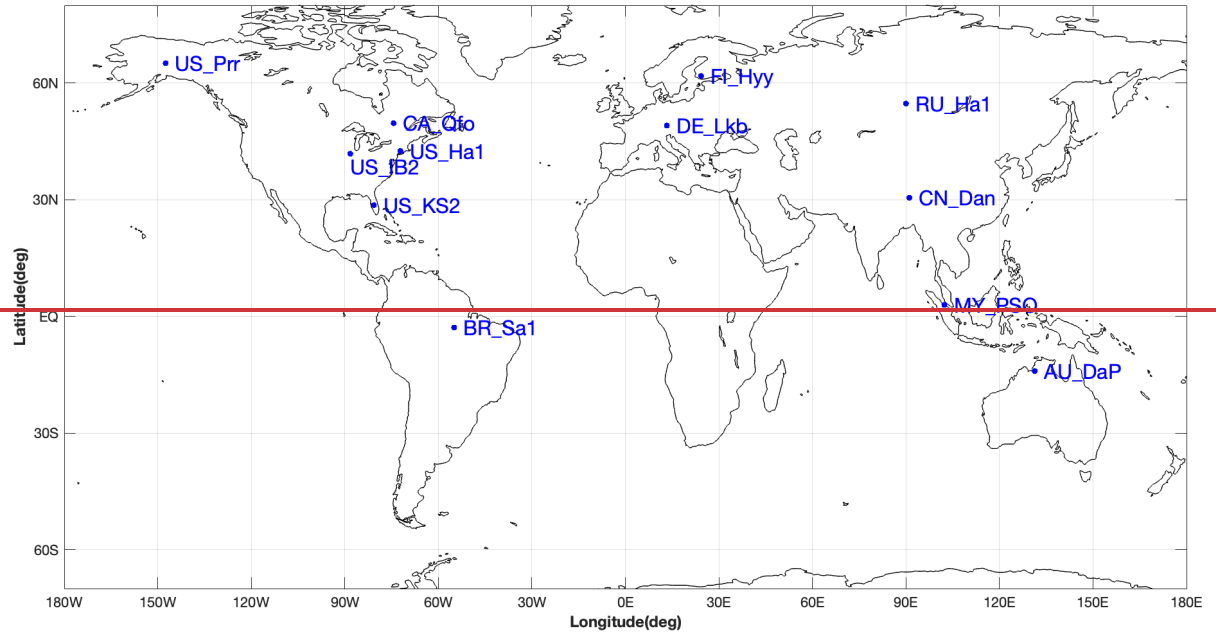
470 2.3 Model forcing and validation data

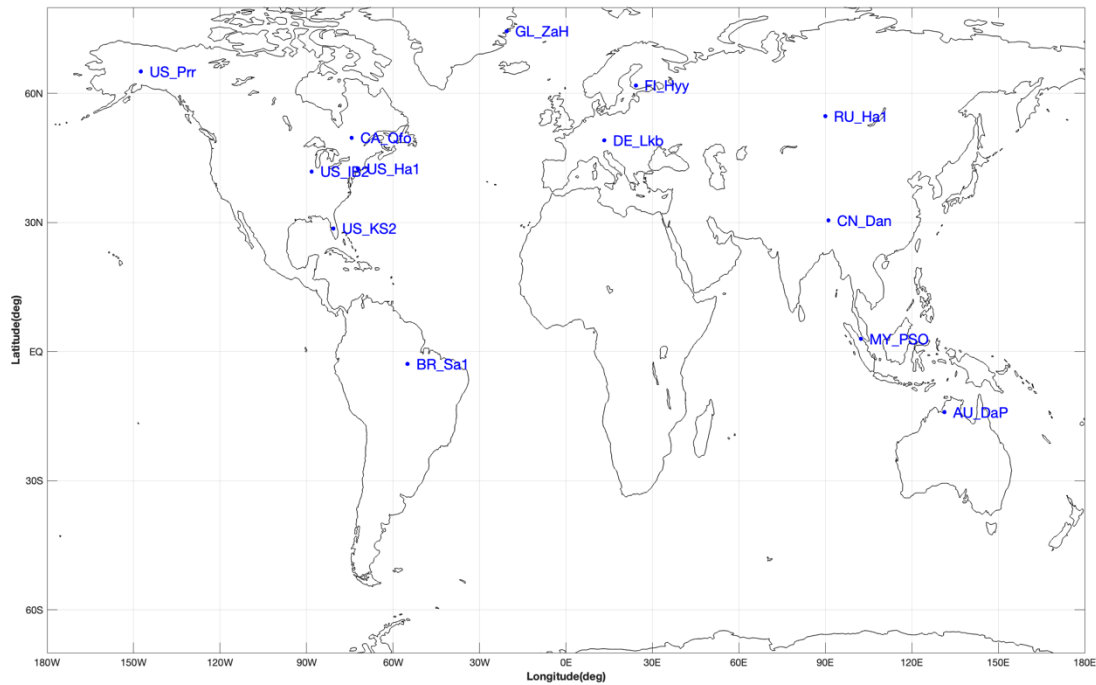
Long-term measurements from flux tower sites with different PFTs and global satellite-derived products are employed as references to systematically assess the effects of this coupling framework and N limitation on the terrestrial carbon cycle. Flux tower sitesite data are presented in section 2.3.1. The global meteorological forcing and validation data are listed in sections 2.3.2 and 2.3.3 separately, respectively.

475 2.3.1 Ground measurement data

To validate the coupled model, twelvethirteen sites with representative biome types and climate zones were selected to evaluate the simulations of the seasonal patterns of GPP, sensible heat flux, and latent heat flux. TheAll driving data were a half-hourly dataset, including air temperature, specific humidity, wind velocity, air pressure, precipitation, and short-shortwave and long-

480 wavelongwave radiation data from the FLUXNET 2015 dataset (Pastorello et al., 2020). The GL-ZaH data were obtained from a tundra heath site (Lund et al., 2012). The geographical distribution of the selected FLUXNET 2015 sites is displayed in Figure 4, and the detailed site information is listed in Table 3-4.





485 **Figure 4.** Geographical distribution of selected FLUXNET 2015 sites. The information [of](#) these FLUXNET sites is listed in [Table 44](#).

Table 3-4. [The](#) FLUXNET sites, latitude (LAT), longitude (LONG), plant function type (PFT), and time frame (Time) used for [the](#) SSiB5/TRIFFID/-DayCent-SOM model validation.

Site_ID	Site name	LAT	LONG	PFT	Time
AU_DaP	Daly River Savanna	-14.06	131.32	C4 grassplants	2007-2013
BR-Sa1	Santarem-Km67-Primary Forest	-2.86	-54.96	Broadleaf Evergreen	2002-2011
CA_Qfo	Quebec - Eastern Boreal, Mature Black Spruce	49.69	-74.34	Needleleaf Evergreen	2003-2010
CN-Dan	Dangxiong	30.50	91.07	C3 grass	2004-2005
DE_Lkb	Lackenberg	49.10	13.30	Needleleaf Evergreen	2009-2013
FI_Hyy	Hyytiala	61.85	24.29	Needleleaf Evergreen	1996-2014
MY_PSO	Pasoh Forest Reserve	2.97	102.31	Broadleaf Evergreen	2003-2009
RU_Ha1	Hakasia steppe	54.73	90.00	C3 grass	2002-2004
US_Ha1	Harvard Forest EMS Tower (HFR1)	42.54	-72.17	Broadleaf deciduous	1991-2012

US_IB2	Fermi National Accelerator Laboratory- Batavia (Prairie site)	41.84	-88.24	C3 grass	2004-2011
US-KS2	Kennedy Space Center (scrub oak)	28.61	-80.67	Shrub	2003-2006
US_Prr	Poker Flat Research Range Black Spruce Forest	65.12	-147.49	Needleleaf Evergreen	2010-2014
<u>GL_ZaH</u>	<u>Zackenbergh Heath</u>	<u>74.47</u>	<u>-20.55</u>	<u>Tundra</u>	<u>2000-2014</u>

490

2.3.2 Meteorological forcing data

The Princeton global meteorological dataset for land surface ~~modelling~~ modeling (Sheffield et al., 2006) was used to drive the SSiB4/TRIFFID global simulations from 1948 to 2007 at 1° x 1° spatial resolution and a 3-hour temporal interval. This dataset, ~~including which included~~ surface air temperature, pressure, specific humidity, wind speed, downward ~~short waves~~ shortwave radiation flux, downward ~~long wave~~ longwave radiation flux, and precipitation, was constructed by combining a suite of global observation-based datasets with the National Center for Environmental Prediction/National Center for Atmospheric Research reanalysis data.

495

2.3.3 Global remote-sensing data

To assess the climatological status, variation, and trends of the simulated LAI, two widely used global LAI products were used as references in this study: the Global Inventory Modeling and Mapping Studies (GIMMS) LAI and the Global LAnd Surface Satellite (GLASS) LAI. GIMMS-LAI is based on the third generation of ~~Normalized Difference Vegetation Index~~ the normalized difference vegetation index (NDVI3g) from the GIMMS group and an ~~Artificial Neural Network~~ artificial neural network model (Zhu et al., 2013). GIMMS-LAI provides a 1/12-degree resolution, 15-day composites, and spans from July 1981 to December 2011. GLASS-LAI is generated from Advanced Very High Resolution Radiometer (AVHRR) (from 1982 to 1999 with 0.05-degree resolution) and Moderate Resolution Imaging Spectroradiometer (MODIS, from 2000 to 2012 with 1 km resolution) reflectance data using general regression neural networks (Xiao et al., 2014). The GIMMS and GLASS ~~LAI~~ LAIs and the meteorological forcing data for the overlap period ~~o~~ from 1982 to 2007 were remapped to a 1-degree spatial resolution and a monthly temporal interval.

500

505

The Model Tree Ensemble (MTE) GPP product (Jung et al., 2009) was used as a reference to evaluate the simulated GPP. MTE is based on a machine learning technique in which the model is trained to predict the five C fluxes at FLUXNET sites driven by observed meteorological data, land cover data, and the remotely-sensed fraction of absorbed ~~photosynthetic~~ photosynthetically active radiation (Jung et al., 2009). The trained model was then applied at the grid scale driven by gridded forcing data. The MTE-GPP data were resampled to a 1-degree spatial resolution and a monthly temporal resolution. However, the MTE data do not include CO₂ fertilization. Liu et al. (2019) ~~discuss~~ discussed this issue and ~~indicate~~ indicated that the lack of CO₂ fertilization mainly affects the trend. Since this paper focuses on climatological

510

515

~~mean~~means as well as differences between different experiments in which the CO₂ fertilization effect ~~would be~~is largely cancelled, the ~~missing~~lack of CO₂ fertilization in ~~the~~ FLUXNET-MTE is not a factor in interpreting our results.

3 Experimental ~~design~~designs

520 To illustrate the reliability of the schemes ~~which~~that represent different processes of plant N in our framework, we first evaluated the model's short-term performance using in-situ measurements (section 3.2). Then, four sets of sensitivity experiments were designed to quantify the major effects of the plant N process and the relative contributions of different plant N processes on the terrestrial ecosystem carbon cycle (section 3.3).

3.1 Initial ~~condition~~conditions for the dynamic vegetation model

525 The initial condition of the dynamic vegetation SSiB4/TRIFFID needs to be obtained from a long-term equilibrium simulation (Zhang et al., 2015). There are different ways to initialize the surface conditions for quasi equilibrium simulations. Following previous SSiB4/TRIFFID studies (Huang et al., 2020; Liu et al., 2019; Zhang et al., 2015), we set up the initial ~~condition~~conditions for the run using the SSiB vegetation map and SSiB vegetation table, which are based on ground surveys and satellite-derived information (Dorman and Sellers, 1989; Sellers et al., 1986; Xue et al., 2004; Zhang et al., 2015) with 100% occupation at each grid point for the dominant PFT and zero occupation for other PFTs. We then ran the SSiB4/TRIFFID
530 model with ~~the~~ climate forcing and the atmospheric CO₂ concentration at the 1948 level for 100 years to reach equilibrium ~~conditions~~. The vegetation and soil conditions from the equilibrium results were used as the initial conditions for the subsequent model runs.

Determining the initial conditions for SSiB5/TRIFFIID/DayCent-SOM was carried out as described for SSiB4/TRIFFID with one additional step ~~in order~~ to initialize the global soil C and N levels. We saved 60 years of daily litter C/N inputs and soil
535 temperature and moisture conditions from the SSiB4/TRIFFID ~~that, which~~ were based on historical meteorological forcings (1948-2007). An offline version of DayCent-SOM was run for 2000 years for each grid cell using these 60 years of data, repeated ~~over and over~~repeatedly, to determine the quasi-equilibrium soil C & N levels; these soil C and N values were read in by SSiB5/TRIFFIID/DayCent-SOM at the start of the global simulation in 1948. This approach was applied for both measurement sites and global 2-D simulations.

540 3.2 Site-level validation

This paper focuses on the impact of N processes on the climatology of the global carbon cycle. Most current ~~Dynamic Global Vegetation Models~~dynamic global vegetation models (DGVMs) are mainly focused on long-term (decadal to thousands of years or even longer) simulations at the global scale; ~~the~~ diurnal and seasonal variations are not ~~at~~the subject ~~for~~of their ~~modelling~~modeling. Moreover, adequate long-term in-situ measurements are ~~also~~ not available for comparison. However,

545 since the SSiB5/TRIFFID is a process-based model, we can evaluate the model's short-term performance using in-situ measurements.

~~Twelve~~Thirteen sites with representative biome types and ~~elimatesclimate~~ zones (Table ~~34~~ and Fig. 4) were selected to evaluate the simulations of seasonal patterns of fluxes ~~over~~across these sites. ~~The-site~~Site-level simulations were conducted by SSiB4/TRIFFID (a C-only model) and SSiB5/TRIFFID/DayCent-SOM separately to validate the model's performance. The model results were compared against ~~the~~ observed daily data obtained by the flux tower, including ~~the~~ GPP, sensible heat flux, and latent heat flux.

3.3 Global ~~2-D2D~~ offline control ~~run~~runs and sensitivity runs

In this study, ~~the~~ SSiB4/TRIFFID and ~~the~~ SSiB5/TRIFFID/DayCent-SOM were applied to conduct a series of global ~~2-D2D~~ offline runs (Table ~~45~~). All these runs employed the quasi-equilibrium simulation results as the initial ~~condition,conditions~~ ~~and were~~ then ~~were~~ driven by the historical meteorological forcing from 1948 through 2007. The run using ~~the~~ SSiB4/TRIFFID is referred to as the control run (Exp. SSiB4 hereafter). Using the control simulation, we first evaluated the ability of the model to produce the climatology and variability of several biotic variables by comparing the results to multiple observation-based datasets. In addition to the control run, ~~six~~four sets of sensitivity experiments were conducted to quantify the major effects of the N process and C-N interface coupling methodology on the C cycle. These sensitivity experiments were designed as follows:

(1) Nitrogen limitation on photosynthesis (Exp. NIPSN): The same meteorological forcing used for the control (Exp. SSiB4) drives the model, but dynamic ~~C/N-ratio~~CNR and N limitation on $V_{c,max}$ (Eq. 6) are introduced. The difference between Exp. SSiB4 and Exp. NIPSN indicates the effect of N limitation on photosynthesis.

(2) Nitrogen impact on ~~Respiration~~respiration rate (Exp. NIResp): The model was driven by the same meteorological forcing used for Exp. SSiB4, but dynamic ~~C/N-ratio~~CNR and N impacts on autotrophic respiration (Eq. 10) are introduced. The difference between Exp. SSiB4 and Exp. NIResp indicates the effect of N ~~impact~~ on ~~the~~ respiration rate.

(3) Nitrogen limitation on Phenology (Exp. NIPhen): The model was driven by the same meteorological forcing used for Exp. SSiB4, but dynamic ~~C/N-ratio~~CNR and N impacts on phenology (Eq. 13) ~~are~~were introduced. The difference between Exp. SSiB4 and Exp. NIPhen indicates the effect of nitrogen limitation on phenology.

(4) SSiB5/TRIFFID/DayCent-SOM (Exp. SSiB5): The model was driven by the same meteorological forcing used for Exp. SSiB4, but all four C-N coupling processes in the framework, i.e., dynamic ~~C/N-ratio~~CNR, N impacts on photosynthesis, autotrophic respiration, and phenology, are introduced. The difference between Exp. SSiB4 and Exp. SSiB5 indicates the effect of N dynamics, especially the sensitivity of C cycle variability and ~~trend~~trends to N process coupling. Furthermore, the difference between Exp. NIPSN and Exp. SSiB5 indicates ~~the~~ uncertainty (or possible errors) due to missing N ~~effect~~effects on autotrophic respiration and phenology in the coupling framework.

Although the model runs were from 1948 to 2007, we only present the results from 1982-2007 to avoid spinning up for the SSiB5/TRIFFID/DayCent-SOM after SSiB4/TRIFFID and DayCent-SOM each reached their historical equilibrium conditions.

Since the results from Exps. SSiB5 and NIPSN showed statistically significant differences from Exp. SSiB4 over many parts of the world, in the following discussion, we will mainly focus on the differences between these two experiments' ~~differences~~ ~~with and~~ Exp. SSiB4.

Table 45. Experimental design

100-year equilibrium	<u><i>Initial condition</i></u>	Real-forcing simulation 1948-2007
<i>Fixed climatology forcing</i>		<i>Transient forcing</i>
Control experiment		SSiB4: Control experiment NIPSN: Nitrogen limitation on photosynthesis (Vmax), Eq.6 NIResp: Nitrogen impact on Respiration rate, Eq.10 NIPhen: Nitrogen limitation on Phenology, Eq. 13 SSiB5: <u>including</u> all four nitrogen processes

4. Results

585 To test this framework, measurements from flux tower sites with different PFTs and global satellite-derived products from 1982–2007 are employed as references. The results from site simulation and global 2-D simulations are presented in sections 4.1 and 4.2, respectively. As mentioned in section 2, the framework takes some plant N metabolism processes into account. To illustrate the relative contributions of different plant N processes ~~onto~~ the terrestrial ecosystem carbon cycle, four sets of sensitivity experiments were designed (Table 45). The analyses are presented in section 4.2.

590

4.1 Evaluations using ~~the~~ measurements from flux tower sites

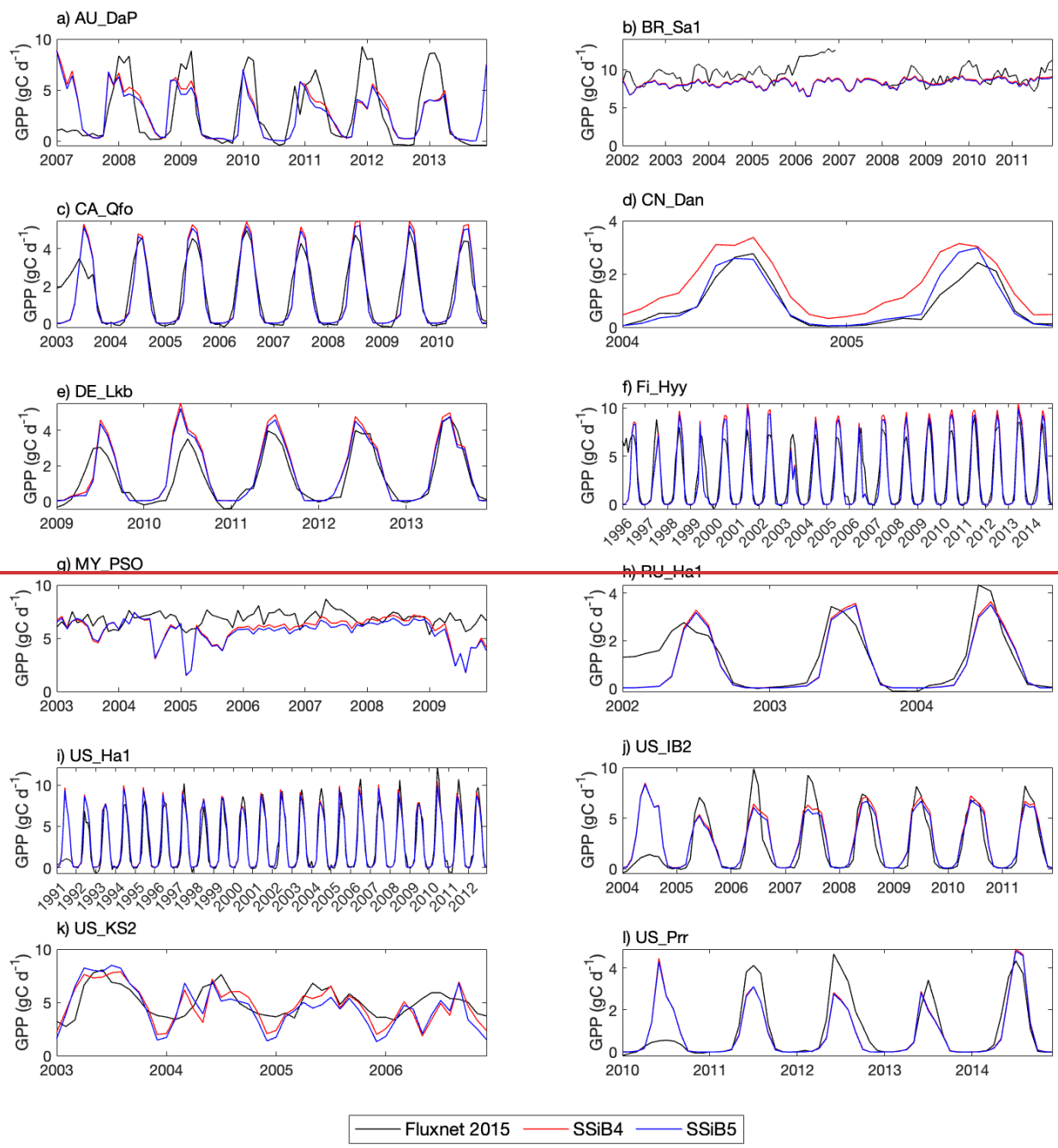
Land models with dynamic vegetation and nitrogen processes normally focus on ~~the~~ long-term climate ~~simulation with~~ ~~simulations at~~ large spatial scales. In this section, we validate the model performance for ~~twelvethirteen~~ sites with several years of simulation (Table 34) to ensure that, as a process-based model, the ~~short-term~~ SSiB5/TRIFFID ~~in the short-term~~ simulation is still able to properly represent the surface processes at seasonal scales after ~~introducing the~~ introduction of DayCent-SOM through the interface coupling framework. This evaluation also provides a glance at the model's performance at several sites with various ~~climateclimates~~ and PFTs (Table 34) with short-term data to gain preliminary confidence for further evaluation.

595

600 Figures 5, 6, and 7 show that both SSiB4 and SSiB5/TRIFFID/DayCent-SOM produce a reasonable seasonal cycle for GPP, sensible heat, and latent heat fluxes, respectively, and that the results are close to ~~observation~~the observations. Table ~~56~~ summarizes the major results. We use bias, root-mean-~~squared~~square error (RMSE), ~~as well as~~and standard deviation to assess model performance against ~~the~~in-situ site measurements. When we ~~evaluate~~evaluated the ~~12~~13-site average ~~of the 13 sites~~, the biases for GPP and sensible and latent heat fluxes ~~are~~ decreased by ~~about~~approximately 7%, ~~18~~17%, and 2-%, respectively. The average RMSEs over the ~~12~~13 sites for these three variables ~~are~~ also decreased by ~~about~~approximately 2%, consistent with the reduction in bias. Furthermore, ~~the~~ SSiB5/TRIFFID/DayCent-SOM ~~produces~~produced a closer standard deviation for GPP, sensible heat flux, and latent heat flux than ~~did~~ SSiB4/TRIFFID for the ~~12~~13-site averages. ~~By and large~~Overall, in these short-term simulations with specified initial vegetation conditions, both SSiB4 and SSiB5 produce reasonable GPP and surface heat fluxes compared with in-situ measurements, but adding N processes (SSiB5) ~~shows a slight improvement for~~slightly improved the ~~12~~13-site average. Although these improvements are rather marginal (except for the bias reduction for sensible heat), the results nevertheless demonstrate that, with short-term simulation, the improvement in the model simulations-~~improvement~~ is rather consistent.

615 With closer checking of the SSiB4 to SSiB5 results at each site, the results display various characteristics. For instance, while some sites ~~mainly show the improvement in both bias and RMSE, while others show improvement only in one or the other.~~ ~~Moreover, while some sites show improvements~~showed improvements in all three variables (GPP, and latent and sensible heat fluxes), others only ~~show improvement for~~showed improvements in one or two variables. It should be ~~pointed out~~noted that SSiB4 and SSiB5 are mainly used for global studies. For the validation of in-situ measurements, proper optimization of some site-specific soil and vegetation parameters is necessary (Xue et al., 1996, 1997). In this study, no model parameters were optimized during this validation exercise for a better fit between the simulated results and FLUXNET measurements. The discussions above ~~lead~~led us to conduct long-term experiments at a global scale to comprehensively investigate the ~~N-process~~ ~~effect~~effects of N processes and to help understand the mechanisms governing the global carbon cycle, which will be discussed in the following section.

620



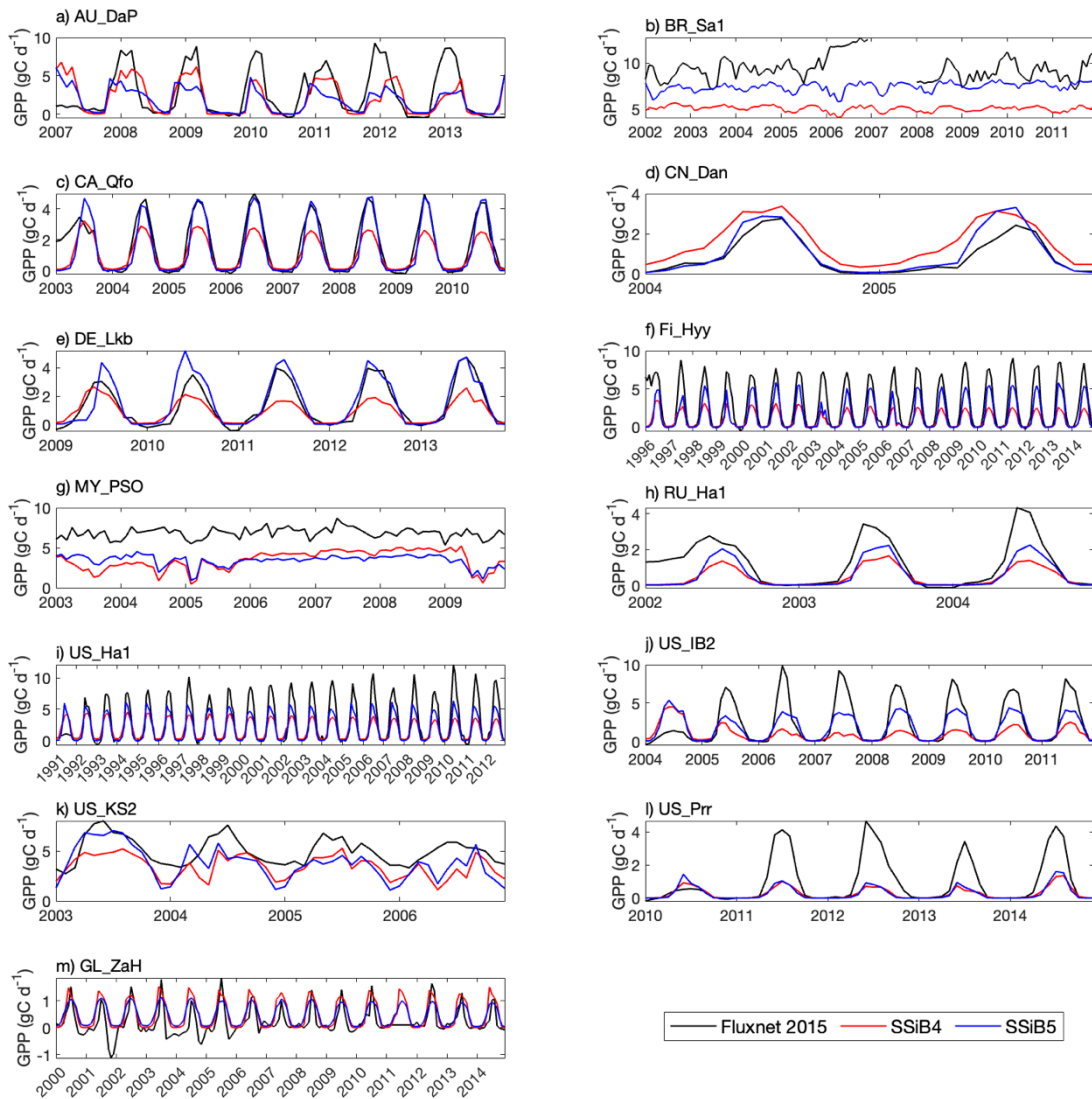
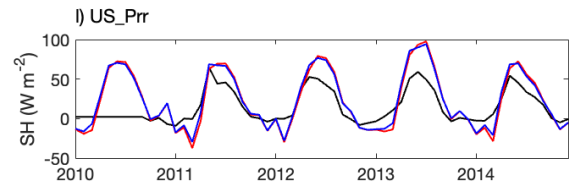
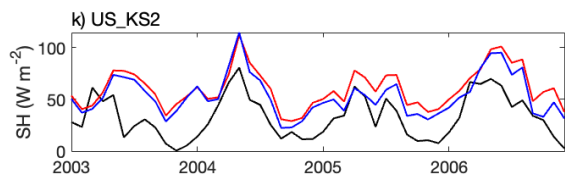
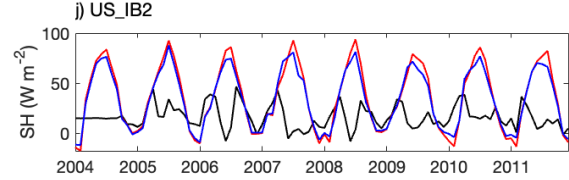
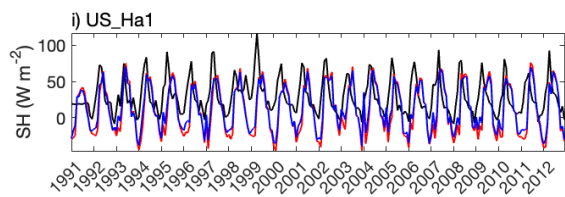
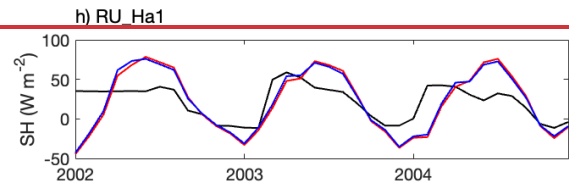
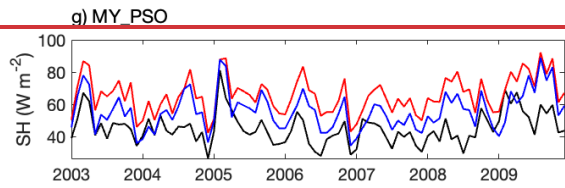
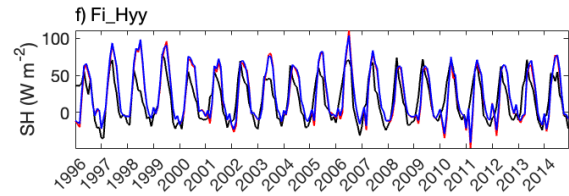
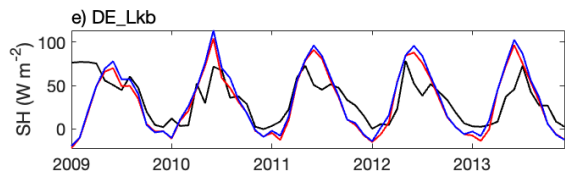
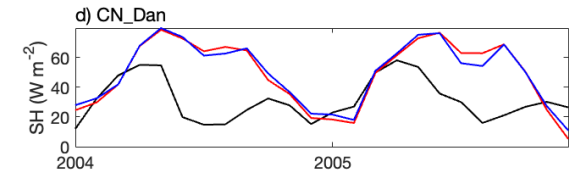
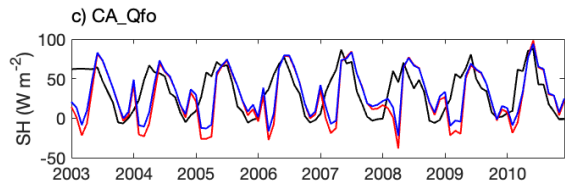
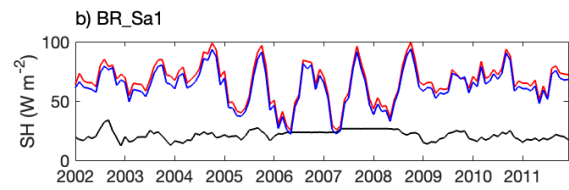
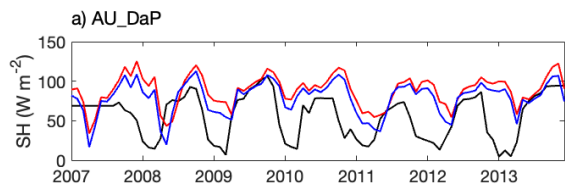
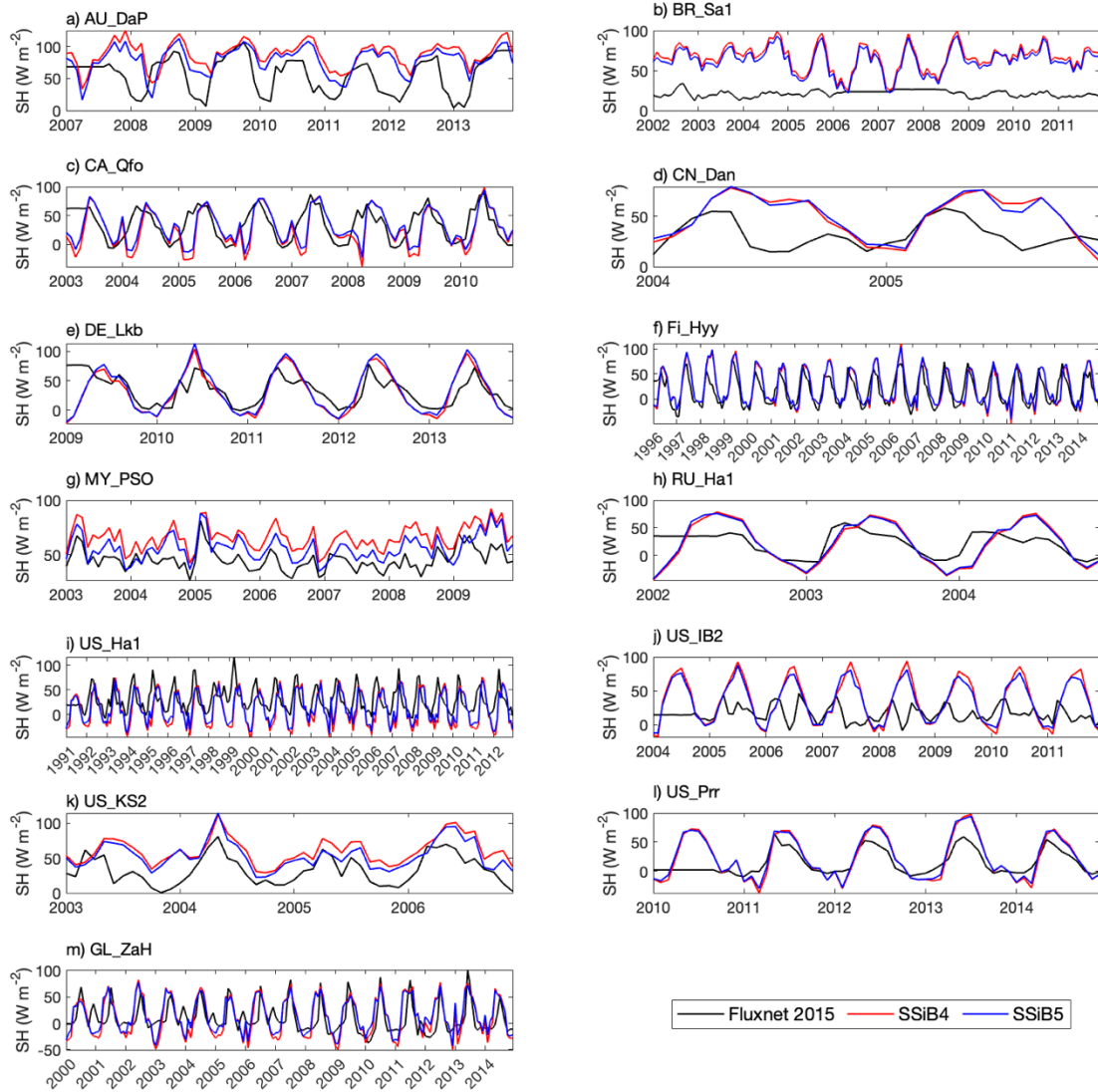


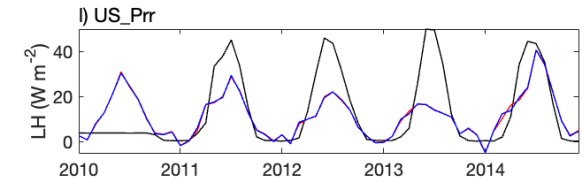
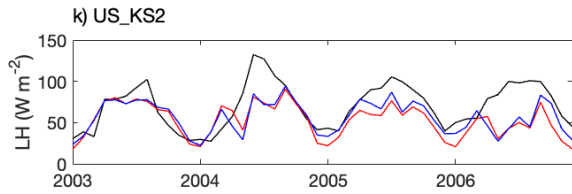
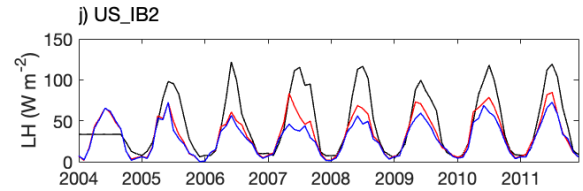
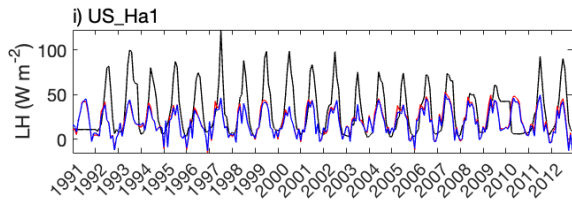
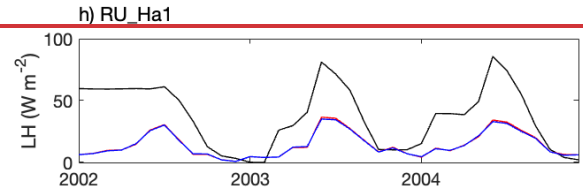
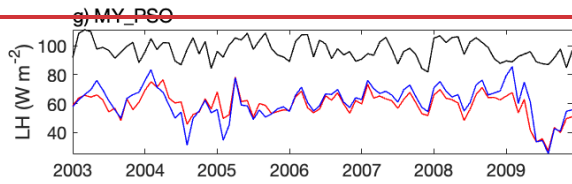
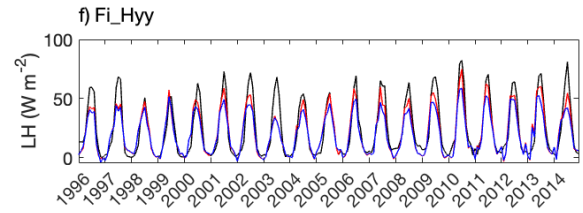
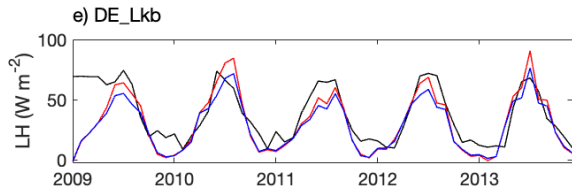
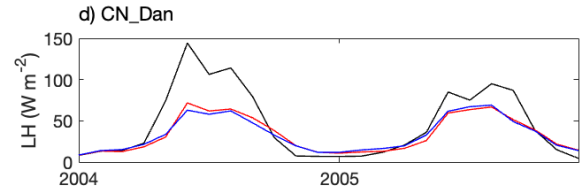
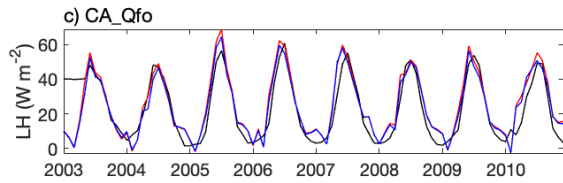
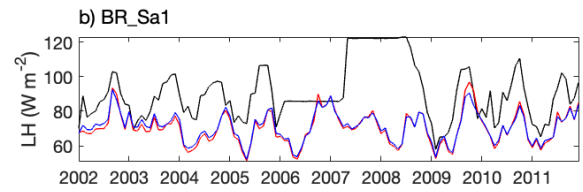
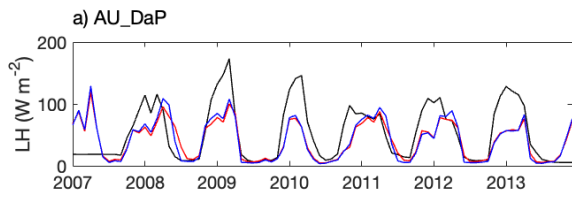
Figure 5. Simulated seasonal variations of GPP against observations at twelve FLUXNET sites representing different SSiB5 PFTs. Note: the information about these FLUXNET sites is listed in Table 34.



— Fluxnet 2015 — SSiB4 — SSiB5



630 **Figure 6.** Same as Figure 5, but for sensible heat flux.



— Fluxnet 2015 — SSiB4 — SSiB5

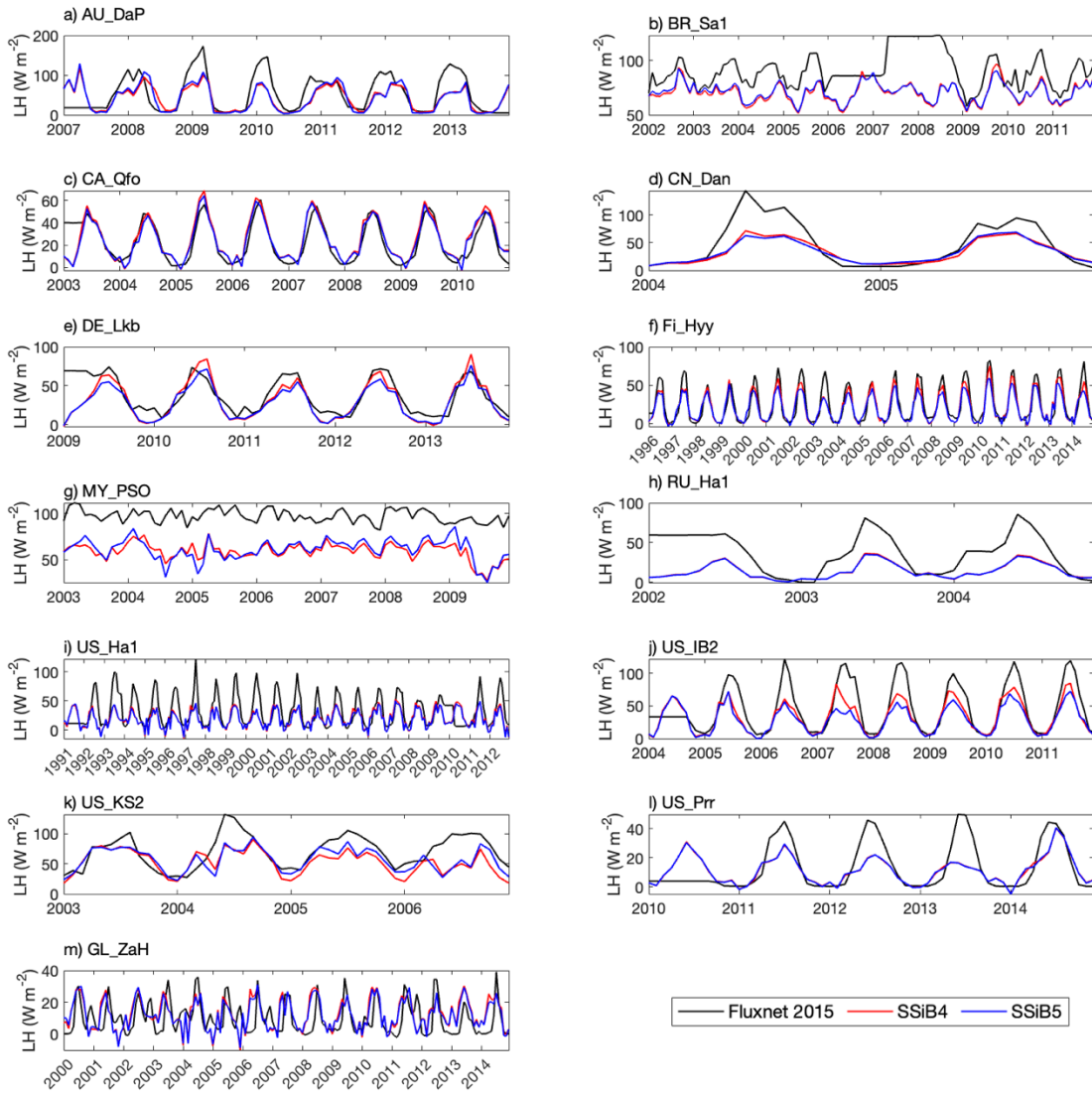


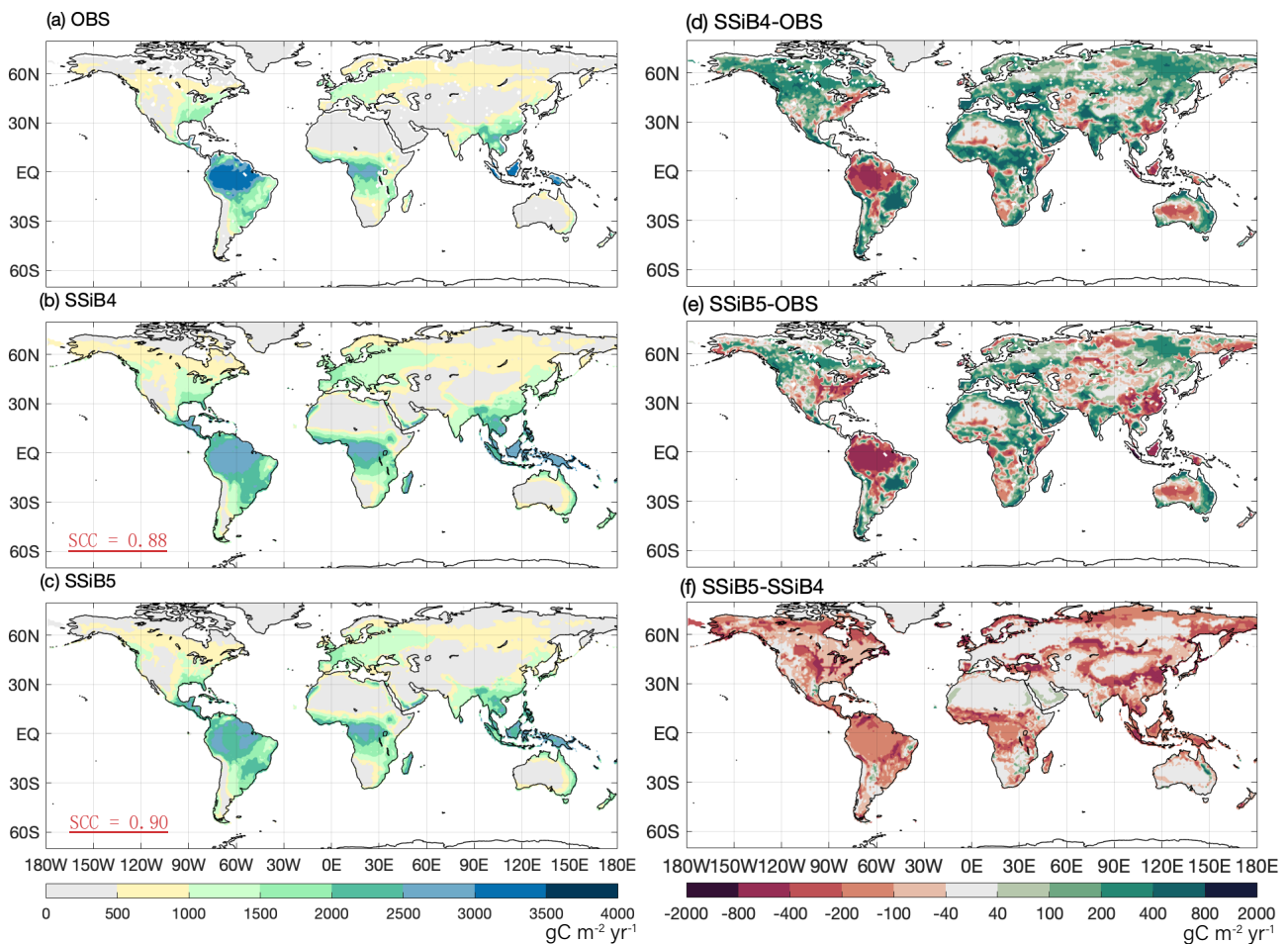
Figure 7. Same as Figure 5, but for the latent heat flux.

635 **Table 56.** The GPP, sensible heat flux, and latent heat flux ~~intercomparisons~~ comparisons of bias, standard deviation and RMSE between SSiB4 and SSiB5 ~~over twelve~~ at the thirteen sites.

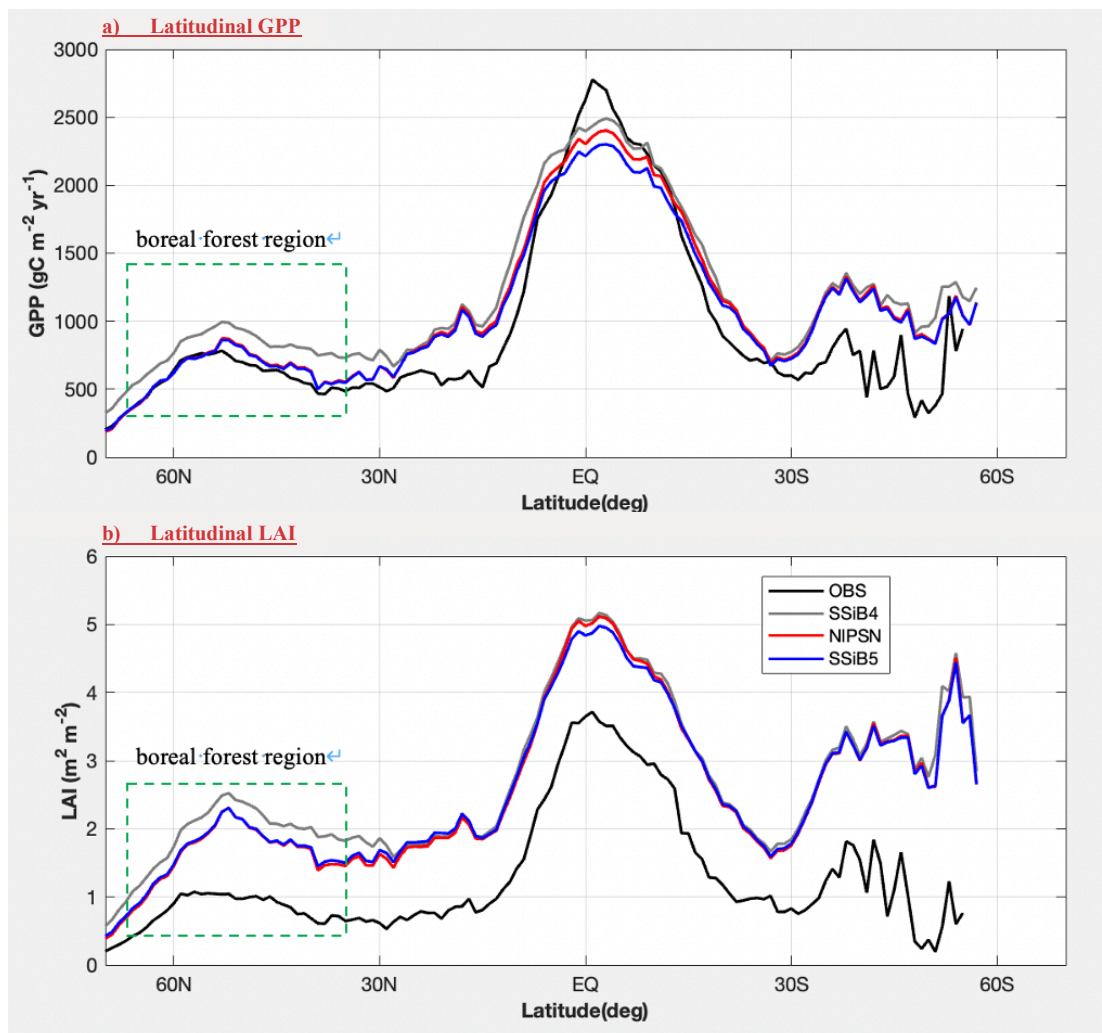
	Site_ID	Bias		Standard deviation			RMSE	
		SSiB4	SSiB5	Fluxnet	SSiB4	SSiB5	SSiB4	SSiB5
GPP (g C d ⁻¹)	AU_DaP	0.05	-0.05	3.11	2.46	2.33	2.60	2.61
	BR-Sa1	-1.07	-1.20	1.31	0.57	0.55	1.77	1.84
	CA_Qfo	-0.05	-0.11	1.71	1.99	1.92	0.78	0.75
	CN-Dan	0.70	0.08	0.92	1.08	1.03	0.80	0.33
	DE_Lkb	0.34	0.25	1.50	1.80	1.71	0.80	0.74
	FI_Hyy	-0.11	-0.22	2.93	3.47	3.32	1.51	1.44
	MY_PSO	-1.02	-1.20	0.65	1.28	1.21	1.63	1.72
	RU_Ha1	-0.24	-0.27	1.29	1.31	1.27	0.69	0.69
	US_Ha1	0.36	0.27	3.31	3.36	3.30	1.31	1.28
	US_IB2	0.56	0.42	2.91	2.70	2.57	1.80	1.79
	US-KS2	-0.28	-0.52	1.37	1.76	2.01	1.35	1.54
US_Prr	-0.08	-0.10	1.43	1.30	1.28	0.86	0.86	
	<u>GL_ZaH</u>	<u>0.28</u>	<u>0.25</u>	<u>0.50</u>	<u>0.53</u>	<u>0.37</u>	<u>0.48</u>	<u>0.43</u>
1213-site average		<u>0.4140</u>	<u>0.3837</u>	<u>1.8776</u>	<u>1.9282</u>	<u>1.8876</u>	<u>1.3326</u>	<u>1.3023</u>
Sensible Heat Flux (W m ⁻²)	AU_DaP	32.47	23.13	28.26	19.64	21.05	36.24	36.32
	BR-Sa1	45.29	40.94	4.04	16.32	15.98	25.61	25.07
	CA_Qfo	-7.04	-2.34	27.77	33.18	29.37	9.54	9.20
	CN-Dan	17.96	18.53	14.44	22.38	20.75	25.60	26.99
	DE_Lkb	-3.12	0.16	25.13	35.39	36.91	17.83	18.15
	FI_Hyy	5.53	7.20	28.17	33.57	33.63	8.99	10.91
	MY_PSO	20.49	10.86	10.03	11.30	11.98	39.22	37.99
	RU_Ha1	-0.14	0.84	21.71	39.19	38.02	29.42	29.67
	US_Ha1	-18.34	-15.80	24.40	33.71	29.42	24.33	24.66
	US_IB2	20.21	18.26	11.95	32.89	29.19	23.16	28.72
	US-KS2	27.74	20.81	21.01	19.17	20.14	27.31	24.73
US_Prr	8.10	9.35	20.93	36.84	35.45	12.02	12.01	
	<u>GL_ZaH</u>	<u>2.24</u>	<u>5.03</u>	<u>27.08</u>	<u>36.04</u>	<u>31.48</u>	<u>29.20</u>	<u>27.37</u>
1213-site average		<u>17.2016.05</u>	<u>14.0213.33</u>	<u>19.8220.38</u>	<u>27.8028.43</u>	<u>26.8227.18</u>	<u>23.2773</u>	<u>22.7023.98</u>
Latent Heat Flux (W m ⁻²)	AU_DaP	-11.02	-10.83	45.72	30.03	33.93	36.24	36.32
	BR-Sa1	-20.47	-19.82	16.15	9.44	8.47	25.61	25.07
	CA_Qfo	2.21	0.96	18.06	18.63	17.56	9.54	9.20
	CN-Dan	-12.63	-12.57	42.39	22.13	20.77	25.60	26.99
	DE_Lkb	-7.39	-10.00	22.81	24.57	20.79	17.83	18.15
	FI_Hyy	-3.06	-4.84	23.22	19.21	16.64	8.99	10.91
	MY_PSO	-38.18	-36.18	7.07	9.24	11.64	39.22	37.99
	RU_Ha1	-22.89	-23.10	25.68	10.43	10.08	29.42	29.67
	US_Ha1	-11.94	-13.14	27.06	15.53	14.71	24.33	24.66
	US_IB2	-12.90	-17.38	36.91	24.68	20.70	23.16	28.72
	US-KS2	-17.74	-13.41	27.63	20.28	19.65	27.31	24.73
US_Prr	-1.90	-1.87	16.44	9.62	9.68	12.02	12.01	
	<u>GL_ZaH</u>	<u>2.76</u>	<u>2.26</u>	<u>10.17</u>	<u>9.67</u>	<u>9.17</u>	<u>11.15</u>	<u>10.48</u>
1213-site average		<u>13.9312.80</u>	<u>13.6712.70</u>	<u>25.7624.56</u>	<u>17.8219</u>	<u>17.9516.45</u>	<u>24.2722.68</u>	<u>23.7022.34</u>

4.2 Evaluation of GPP and LAI at ~~global scale~~ the Global Scale

640 The SSiB model is mainly used for global study, in this section, we evaluate the model's performance using climate studies. It is important to adequately produce the observed global GPP and LAI data. The model's performance in these aspects is evaluated in this section. The SSiB4/TRIFFID-simulated global PFT distribution has been extensively discussed in Zhang et al. (2015) and Liu et al. (2019). The simulation results are generally consistent with observation. The spatial distribution from the SSiB5/TRIFFID/DayCent-SOM did not show substantial difference and will not be discussed here. The simulated GPP averaged over 1982-2007 ~~is~~ was compared to the FLUXNET-MTE GPP (Jung et al., 2011) to examine the impact of N processes and ~~itstheir~~ their coupling with C and ecosystem processes. Both SSiB4/TRIFFID (Exp. SSiB4) and SSiB5/TRIFFID/DayCent-SOM (Exp. SSiB5) capture the distribution of global GPP (Fig. 8) and its latitudinal distribution (Fig. 9a).



650 **Figure 8.** The 1982-2007 average gross primary production comparison for (a) FLUXNET-MTE GPP (OBS), (b) SSiB4/TRIFFID (SSiB4), and (c) SSiB5/TRIFFID/DayCent/SOM (SSiB5) and the difference between (d) SSiB4-OBS, (e) SSiB5-OBS, and (f) SSiB5-SSiB4. Note: SCC indicates the spatial correlation coefficient between the model simulation and satellite-derived datasets (OBS).



655 **Figure 9.** Intercomparisons of latitudinal LAI and GPP among OBS, SSiB4 (control), NIPSN (N limitation on photosynthesis only), and SSiB5 (all N processes) over the period of 1982-2007. Note: Observed LAI is the GIMMS LAI.

Table 7. Regional and global GPP for (a) FLUXNET-MTE GPP (observation), (b) SSiB4 (control), (c) NIPSN (N limitation on photosynthesis only) and (d) SSiB5 (N limitation on photosynthesis, autotrophic respiration, and phenology).

Regions	Sub-regions	GPP Mean ($\text{gC m}^{-2} \text{yr}^{-1}$)							
		MTE		SSiB4		NIPSN		SSiB5	
		mean	bias	mean	bias	mean	bias	mean	bias
Arid and Semi-Arid Areas	West Africa	893		1147	254(28.5%)	963	70(7.9%)	915	22(2.5%)
	West NA	438		549	111(25.4%)	454	16(3.5%)	431	-7(-1.6%)
	SA Savanna	1665		1860	195(11.7%)	1763	98(5.9%)	1675	10(0.6%)
	East Africa	1228		1533	306(24.9%)	1427	199(16.2%)	1356	128(10.4%)
	East Asian semi-arid	1440		1470	30(2.1%)	1199	-241(-16.7%)	1139	-301(-20.9%)
NH High-Mid Latitude Areas	NA High-Mid Latitude	552		814	262(47.6%)	700	149(27.0%)	665	114(20.6%)
	Eurasian High-Mid	844		966	122(14.5%)	871	27(3.2%)	827	16(-2.0%)
Equator	Amazon Basin	2993		2668	-326(-10.9%)	2631	-362(-12.1%)	2500	-494(-16.5%)
	Southeast Asia	2778		2540	-238(-8.6%)	2419	-359(-12.9%)	2298	-480(-17.3%)
	Equator Africa	2522		2645	123(4.9%)	2611	89(3.5%)	2481	-42(-1.7%)
Subarctic Areas and Tibet	NA Subarctic	234		364	130(55.7%)	240	6(2.4%)	228	-6(-2.7%)
	Eurasian Subarctic	331		484	153(46.2%)	328	-3(-1.0%)	311	-20(-6.0%)
	Tibet	409		561	153(37.3%)	298	-111(-27.2%)	283	126(-30.8%)
Global		863		1082	220(25.4%)	991	129(14.9%)	942	79(9.1%)

Note: the numbers in parentheses are relative biases: (bias/MTE mean)

The highest GPP occurs in ~~the~~ tropical evergreen ~~forest~~ forests and generally decreases with ~~the increase in latitudes~~ ~~in increasing latitude according to~~ both the observations and the model ~~simulations~~ simulations (Figs. 8 and 9a). Exp. SSiB4-simulated GPP has a positive bias over many parts of the world (Fig. 8d), including tropical Africa and the North American and eastern Siberian boreal regions, but a negative bias in some regions, mainly in the Amazon tropical forest. The simulated global GPP is $1082.36 \text{ g C m}^{-2} \text{ yr}^{-1}$ (Table ~~6~~;7), which is higher than the ~~estimate, estimated value of~~ $862.86 \text{ g C m}^{-2} \text{ yr}^{-1}$ in FLUXNET-MTE (Jung et al., 2011). After introducing ~~the~~ N limitation for ~~the~~ three processes, ~~the~~ SSiB5 reduced the positive bias in SSiB4 over many parts of the world (Figs. 8e, 8f, and 9a). Exp. SSiB5's global GPP prediction, $941.81 \text{ g C m}^{-2} \text{ yr}^{-1}$, is closer to ~~the~~ observations ~~compared to~~ than Exp. SSiB4, with a 16.3% reduction in the bias (Table ~~6~~7). Furthermore, the temporal correlation coefficients between ~~the~~ observed and simulated monthly/annual mean GPPs ~~are~~ increased from 0.46/0.98 (Exp. SSiB4) to 0.50/0.99 (Exp. SSiB5), respectively (Fig. 10), showing improvement in ~~the~~ simulation of the seasonal cycle in SSiB5. The correlation for interannual variability in SSiB4 is already very high (0.98). SSiB5 ~~shows no substantial improvement~~ ~~continues the high correlation of SSiB4~~.

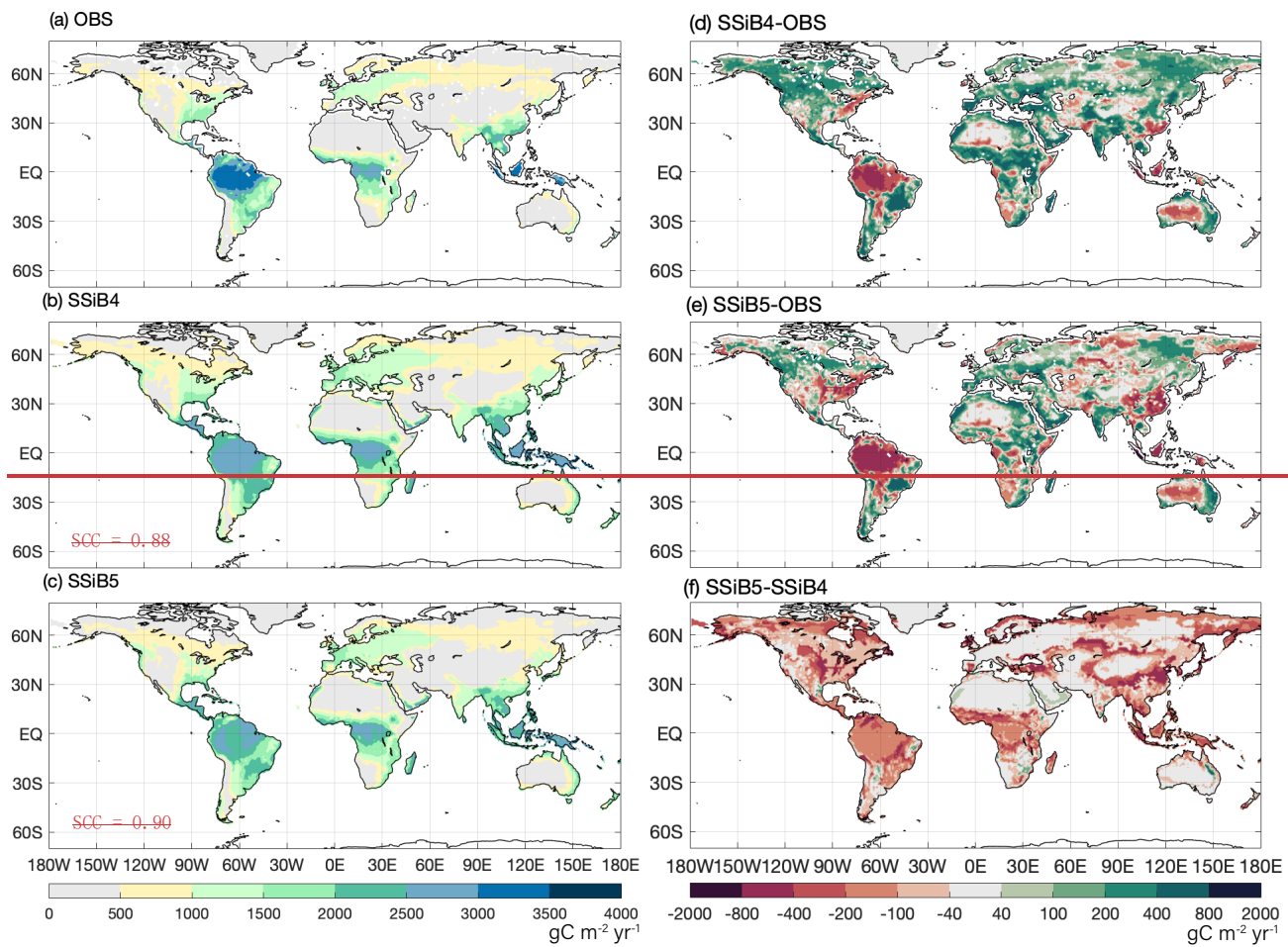


Figure 8. The 1982–2007 average gross primary production comparison for (a) FLUXNET MTE GPP (OBS), (b) SSiB4/TRIFFID (SSiB4), and (c) SSiB5/TRIFFID/DayCent/SOM (SSiB5), and difference between (d) SSiB4-OBS, and (e) SSiB5-OBS, (f) SSiB5-SSiB4. Note: SCC indicates the spatial correlation coefficient between model simulation and satellite derived datasets (OBS).

675

680

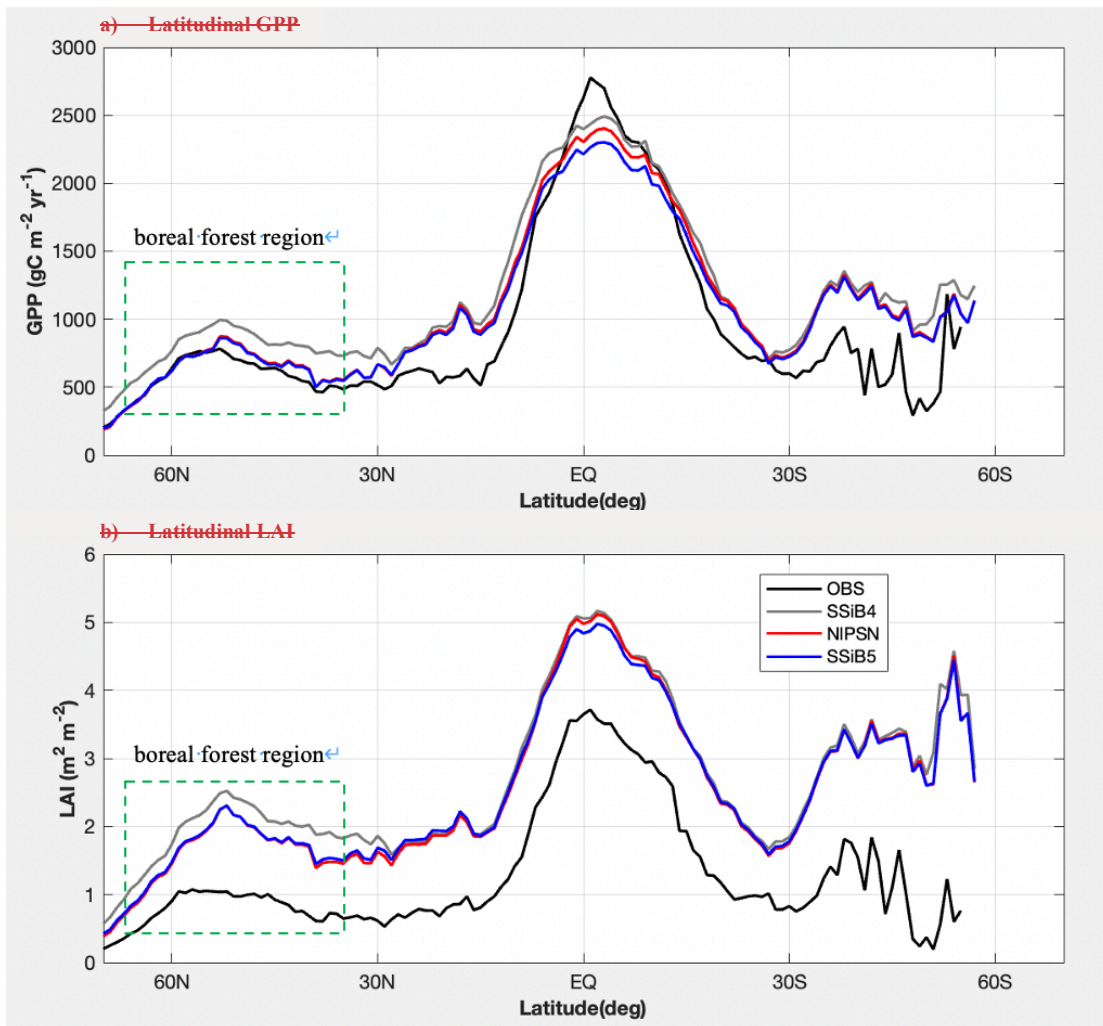


Figure 9. Intercomparisons of latitudinal LAI and GPP among OBS, SSiB4 (control), NIPSN (N limitation on photosynthesis only), and SSiB5 (all N processes) over the period 1982-2007.

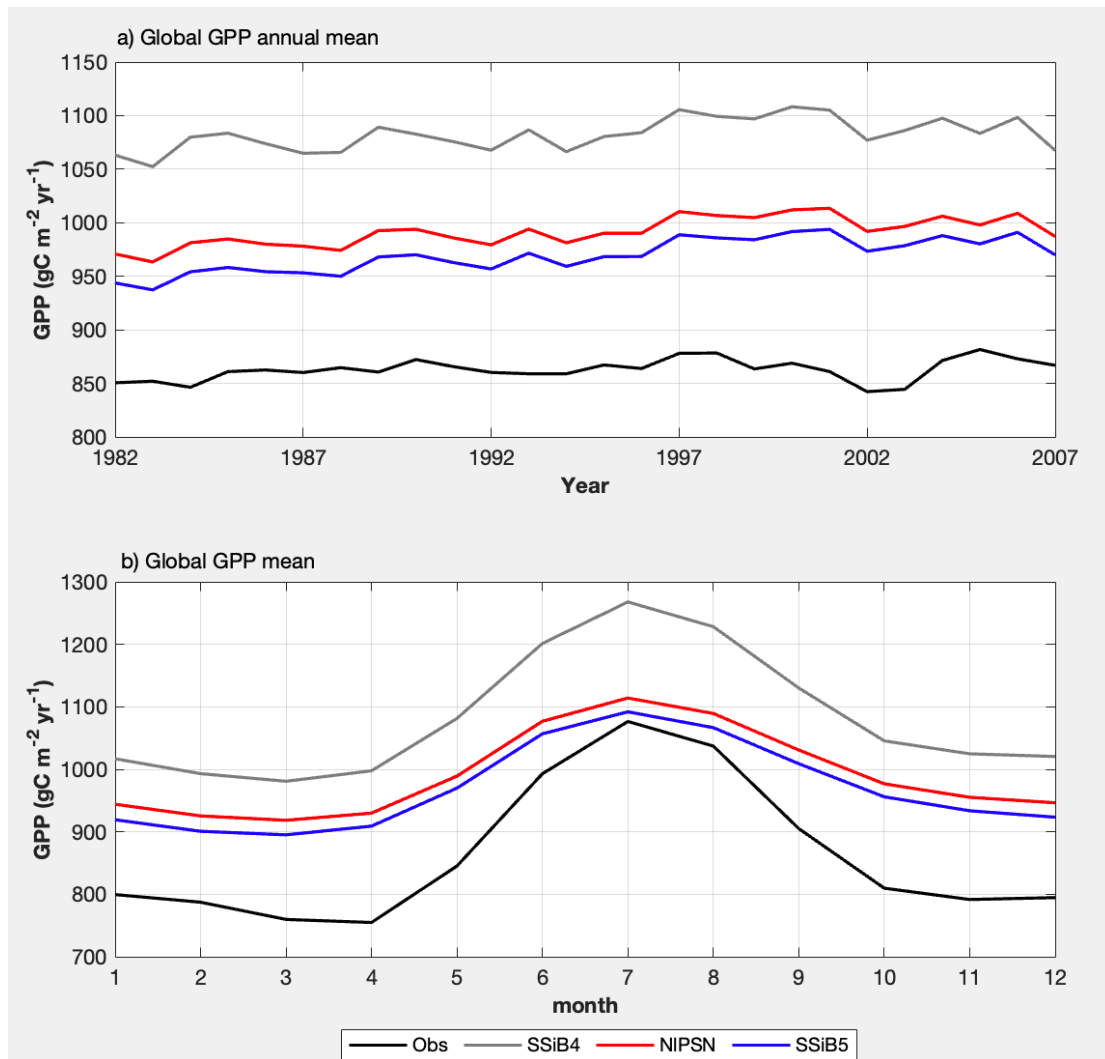
Table 6. Regional and Global GPP for (a) FLUXNET-MTE GPP (observation), (b) SSiB4 (control), (c) NIPSN (N limitation on photosynthesis only) and (d) SSiB5 (N limitation on photosynthesis, autotrophic respiration, and phenology).

Regions	Sub-regions	GPP Mean ($\text{gC m}^{-2} \text{yr}^{-1}$)							
		MTE		SSiB4		NIPSN		SSiB5	
		mean	bias	mean	bias	mean	bias	mean	bias
Arid and Semi-Arid Areas	West Africa	893		1147	254(28.5%)	963	70(7.9%)	915	22(2.5%)
	West NA	438		549	111(25.4%)	454	16(3.5%)	431	-7(-1.6%)
	SA Savanna	1665		1860	195(11.7%)	1763	98(5.9%)	1675	10(0.6%)
	East Africa	1228		1533	306(24.9%)	1427	199(16.2%)	1356	128(10.4%)
	East Asian semi-arid	1440		1470	30(2.1%)	1199	-241(-16.7%)	1139	-301(-20.9%)
NH High-Mid Latitude Areas	NA High-Mid Latitude	552		814	262(47.6%)	700	149(27.0%)	665	114(20.6%)
	Eurasian High-Mid	844		966	122(14.5%)	871	27(3.2%)	827	16(-2.0%)
Equator	Amazon Basin	2993		2668	-326(-10.9%)	2631	-362(-12.1%)	2500	-494(-16.5%)
	Southeast Asia	2778		2540	-238(-8.6%)	2419	-359(-12.9%)	2298	-480(-17.3%)
	Equator Africa	2522		2645	123(4.9%)	2611	89(3.5%)	2481	-42(-1.7%)
Subarctic Areas and Tibet	NA Subarctic	234		364	130(55.7%)	240	6(2.4%)	228	-6(-2.7%)
	Eurasian Subarctic	331		484	153(46.2%)	328	-3(-1.0%)	311	-20(-6.0%)
	Tibet	409		561	153(37.3%)	298	-111(-27.2%)	283	126(-30.8%)
Global		863		1082	220(25.4%)	991	129(14.9%)	942	79(9.1%)

~~Note: the numbers in parentheses are relative biases: (bias/MTE mean)~~

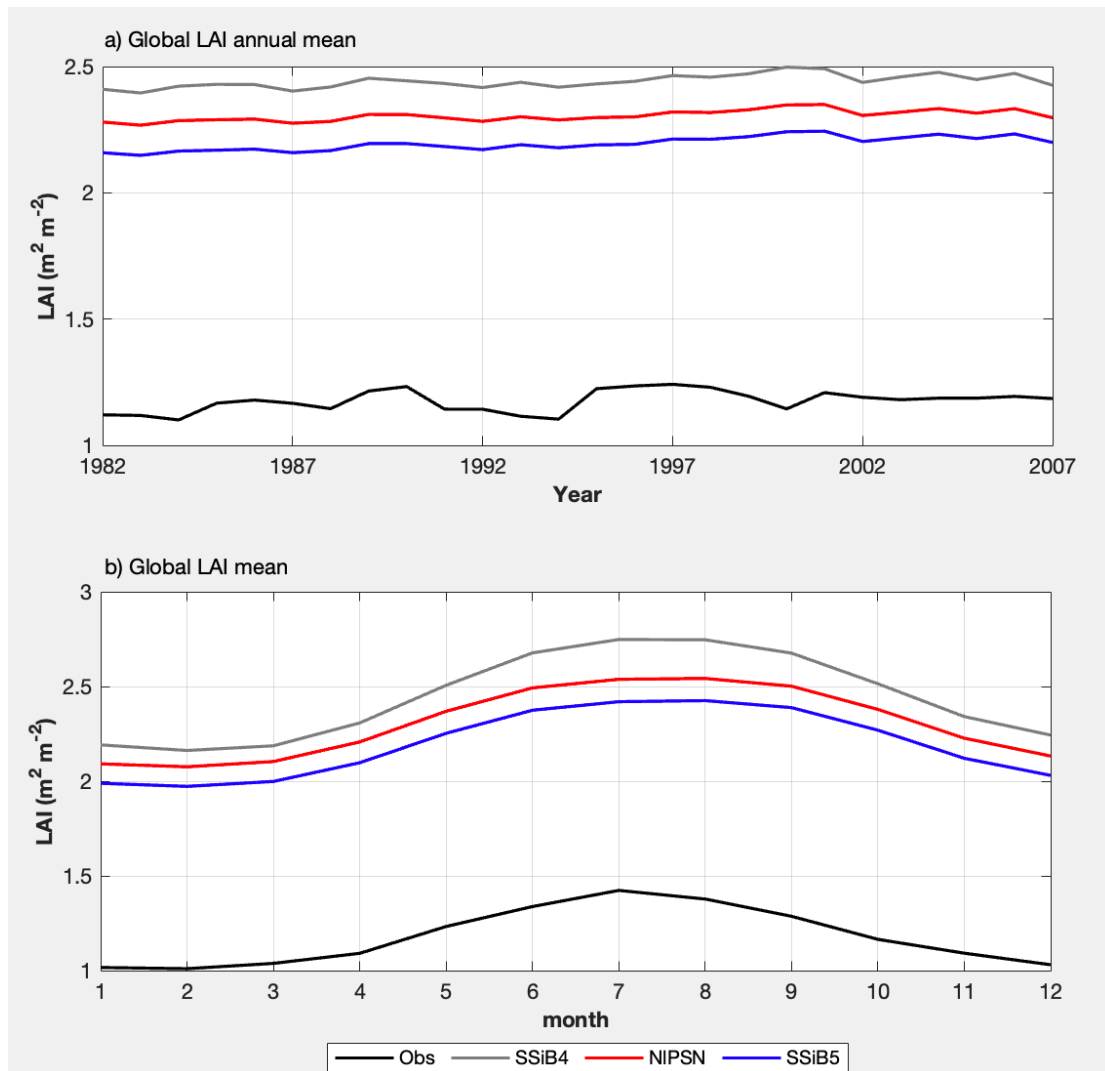
690 The improvement, however, is not homogeneous ~~over~~across the globe but displays apparent regional characteristics. The GPP biases in tropical Africa, ~~the~~ North American boreal region, ~~the~~ South American savanna, and ~~the~~ central U.S. ~~show~~showed substantial ~~reduction~~reductions (Fig. 8f), which ~~help~~helped improve the spatial distribution of SSiB5. The global spatial correlation coefficient increases from 0.88 to 0.90 (Fig. 8). ~~Meanwhile~~Moreover, the GPP simulations ~~did not improve~~ in some regions, such as in ~~the~~ temperate East Asian mixed forest-grassland regions and in some areas ~~in~~of Siberia (Fig. 8); ~~did not improve~~8). In particular, the negative GPP bias in the Amazon ~~is~~increased (Fig. 8f). This phenomenon ~~has~~also appeared in the offline test ~~in~~at the Amazon site (the BR-Sa1 ~~Site~~site, Table 54). Du et al. (2020) ~~indicate~~indicated that phosphorus (P) has ~~more~~a greater effect in tropical areas. ~~This paper mainly focuses on model development and preliminary global evaluation. More regional evaluation is necessary for further investigation, especially for the regions where the N limitation is not dominant.~~

695



700

Figure 10. Intercomparisons of global monthly/annual mean GPPs among OBS, SSiB4 (control), NIPSN (N limitation on photosynthesis only), and SSiB5 (all N processes) over the period of 1982-2007.



705

Figure 11. Same as [figure](#) [Figure 10](#), but for [the](#) LAI.

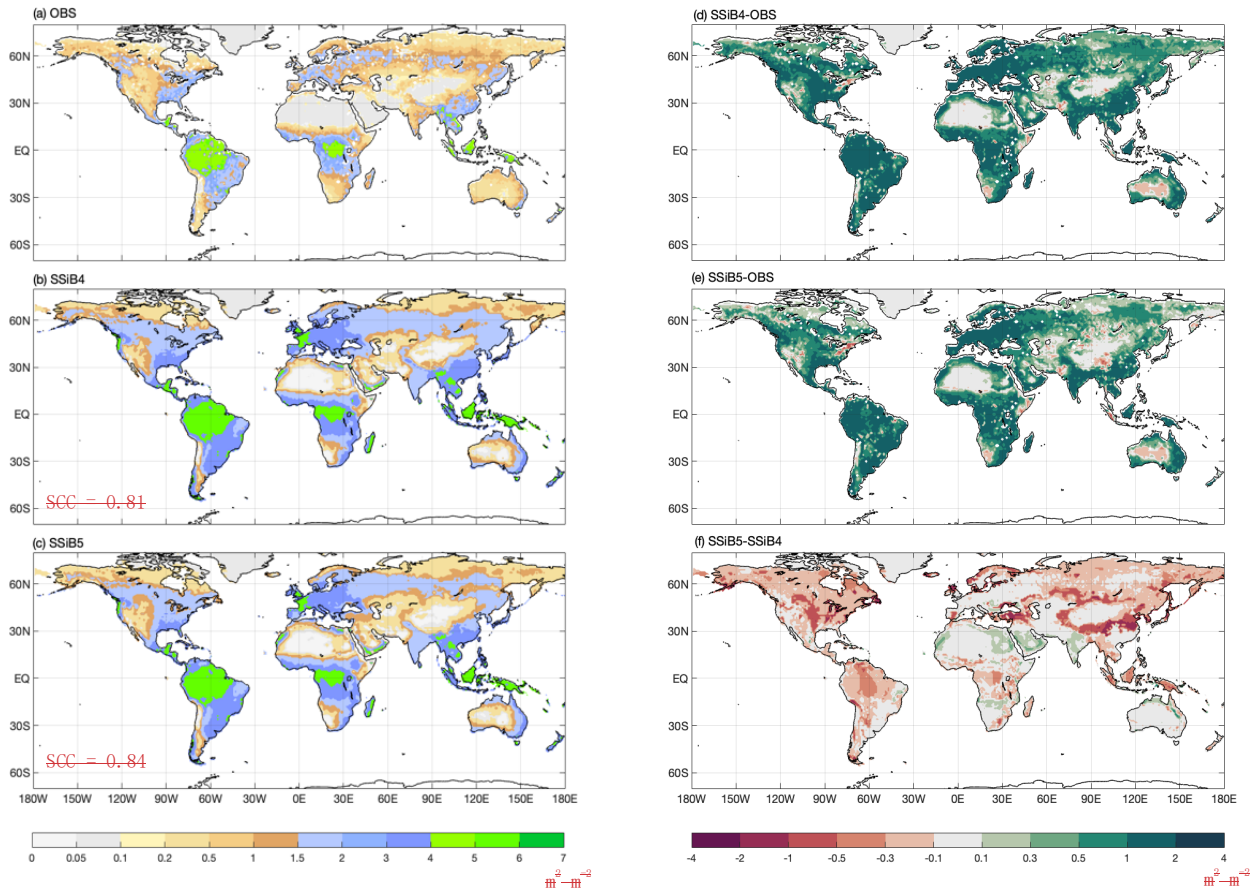
[Note:](#) Observed LAI is the GIMMS LAI.

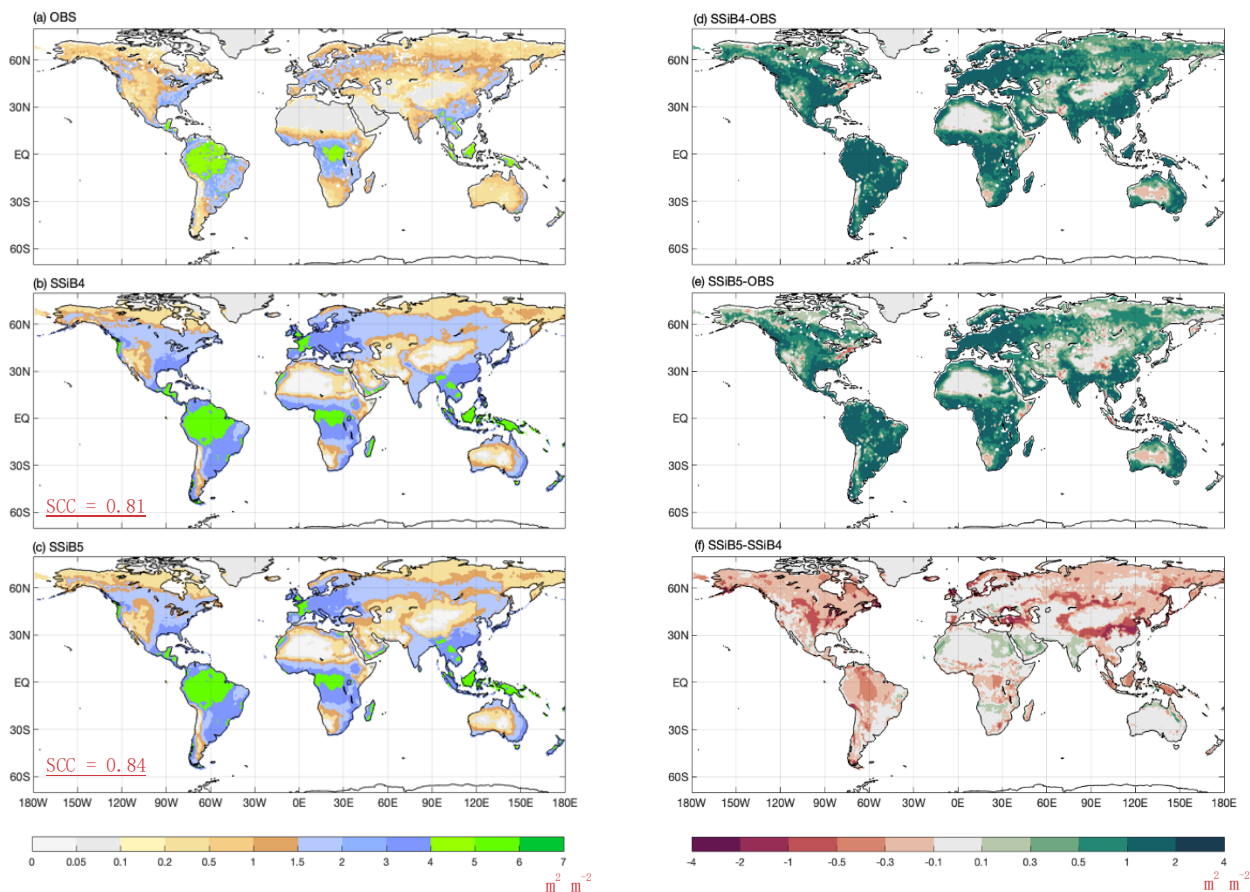
710

Furthermore, the [N-limitation](#) effect [of N limitations](#) on the LAI simulation [iswas](#) also investigated. [Both-Compared with](#) [satellite-derived products, both](#) SSiB4 and SSiB5 [produceexhibit](#) reasonable spatial [distribution-compared-with-satellite-](#) [derived-productsdistributions](#) (Figs. 12a-c). The highest LAI occurs in [the](#) tropical evergreen [forestforests](#) and decreases with latitude in both the observations and the model (Fig. 9b). [Compared with the control, Exp. SSiB5](#) also generally [reducesreduced](#) the positive bias in [the](#) simulated LAI [compared to the control](#) (Fig. 12f). The simulated LAI in Exp. SSiB4 has a global positive bias. After introducing [the](#) three N limitation processes, the positive bias [is-reduceddecreased](#) over most parts of the world (Fig. 12f). Globally, Exp. SSiB5 has an LAI bias of 0.94/1.12 for GIMMS/GLASS, respectively (Table [78](#)), which is

715

lower than the LAI bias of 1.26/1.44 for GIMMS/GLASS, respectively, in Exp. SSiB4, with a substantial 31.1% reduction in the bias (compared to GIMMS, Table 78). However, ~~thea substantial~~ positive bias still exists ~~substantially over~~across the globe (Fig. 12e). ~~In a land model intercomparison, the positive LAI prevailed in almost every dynamic vegetation model (Murray-Tortarolo et al., 2013).~~ Our study ~~showsshowed~~ that imposing N limitation is an adequate step to overcome ~~the~~ dynamic vegetation models' systematic LAI positive bias, but ~~thethis~~ issue ~~ishas~~ still not ~~solvedbeen resolved~~ and requires ~~morefurther~~ investigation. ~~In~~ addition, the correlation coefficients between ~~the~~ observed and simulated monthly/annual average LAIs ~~are~~ improved from 0.49/0.97 (Exp. SSiB4) to 0.51/0.98 (Exp. SSiB5) (Fig. 11).





725

Figure 12. Same as Figure 8, but for the LAI.

Note: SCC indicates the spatial correlation coefficient between the model simulation and the GIMMS LAI (OBS).

730

It is interesting to note that despite the global general LAI reduction, the SSiB5 slightly increased the LAI estimation in North Africa and India (Fig. 12). The N impacts of N on phenology and respiration cause a slight shift in the vegetation from shrubs (N. Africa) or C4 grasses (India) to C3 grasses in these areas, which contributes to the increases in GPP and LAI increase (Fig. 13). Furthermore, in areas such as the Amazon, and East Asian mixed forest-grassland regions, SSiB5 improved only improves the LAI simulation, and not the GPP simulation. We will further identify the effect of N limitation on the photosynthesis process and other processes on simulated GPP and LAI. More observational data are necessary to gain more understanding.

735

Table 78. Regional and Global LAI for (a) GIMMS LAI (observation), (b) GLASS LAI (second observation), (c) SSiB4 (control), (d) NIPSN (N limitation on photosynthesis only) and (e) SSiB5 (N limitation on photosynthesis, autotrophic respiration, and phenology). The bias is relative to the GIMMS LAI.

Regions	Sub-regions	LAI Mean ($\text{m}^2 \text{m}^{-2}$)									
		GIMMS		GLASS		SSiB4		NIPSN		SSiB5	
		mean	bias	mean	bias	mean	bias	mean	bias	mean	bias
Arid and Semi-Arid Areas	West Africa	1.08		1.01	-0.07(-6.5%)	2.04	0.96(88.9%)	1.89	0.81(75.0%)	1.73	0.65(60.2%)
	West NA	0.62		0.49	-0.13(-21.0%)	1.38	0.76(122.6%)	1.18	0.56(90.3%)	1.09	0.47(75.8%)
	SA Savanna	1.99		1.91	-0.18(-4.0%)	3.34	1.35(67.8%)	3.23	1.24(62.3%)	2.97	0.98(49.2%)
	East Africa	1.59		1.55	-0.04(-2.5%)	3.02	1.43(89.9%)	2.89	1.30(81.8%)	2.66	1.07(67.3%)
	East Asian semi-arid	1.60		1.36	-0.24(-15.0%)	3.35	1.75(109.4%)	2.84	1.24(77.5%)	2.61	1.01(63.1%)
NH High-Mid Latitude Areas	NA High-Mid Latitude	0.84		0.49	-0.35(-41.7%)	1.91	1.07(127.4%)	1.66	0.82(97.6%)	1.53	0.69(82.1%)
	Eurasian High-Mid	1.14		0.57	-0.57(-50.0%)	2.29	1.15(100.9%)	2.08	0.94(82.5%)	1.91	0.77(67.5%)
Equator	Amazon Basin	4.19		4.08	-0.11(-2.6%)	6.01	1.82(43.4%)	5.98	1.79(42.7%)	5.50	1.31(31.3%)
	Southeast Asia	3.93		3.88	-0.05(-1.3%)	4.68	0.75(19.1%)	4.68	0.75(19.1%)	4.31	0.38(9.7%)
	Equator Africa	3.83		3.76	-0.07(-1.8%)	5.74	1.91(49.9%)	5.72	1.89(49.3%)	5.27	1.44(37.6%)
Subarctic Areas and Tibet	NA Subarctic	0.32		0.14	-0.18(-56.3%)	0.71	0.39(121.9%)	0.51	0.19(59.4%)	0.47	0.15(46.9%)
	Eurasian Subarctic	0.33		0.12	-0.21(-63.6%)	0.87	0.54(163.6%)	0.65	0.32(97.0%)	0.60	0.27(81.8%)
	Tibet	0.64		0.54	-0.10(-15.6%)	1.36	0.72(112.5%)	0.81	0.17(26.6%)	0.75	0.11(17.2%)
Global		1.18		1.00	-0.18(-15.3%)	2.44	1.26(110.8%)	2.31	1.13(95.8%)	2.12	0.94(79.7%)

Note: the numbers in parentheses are relative biases

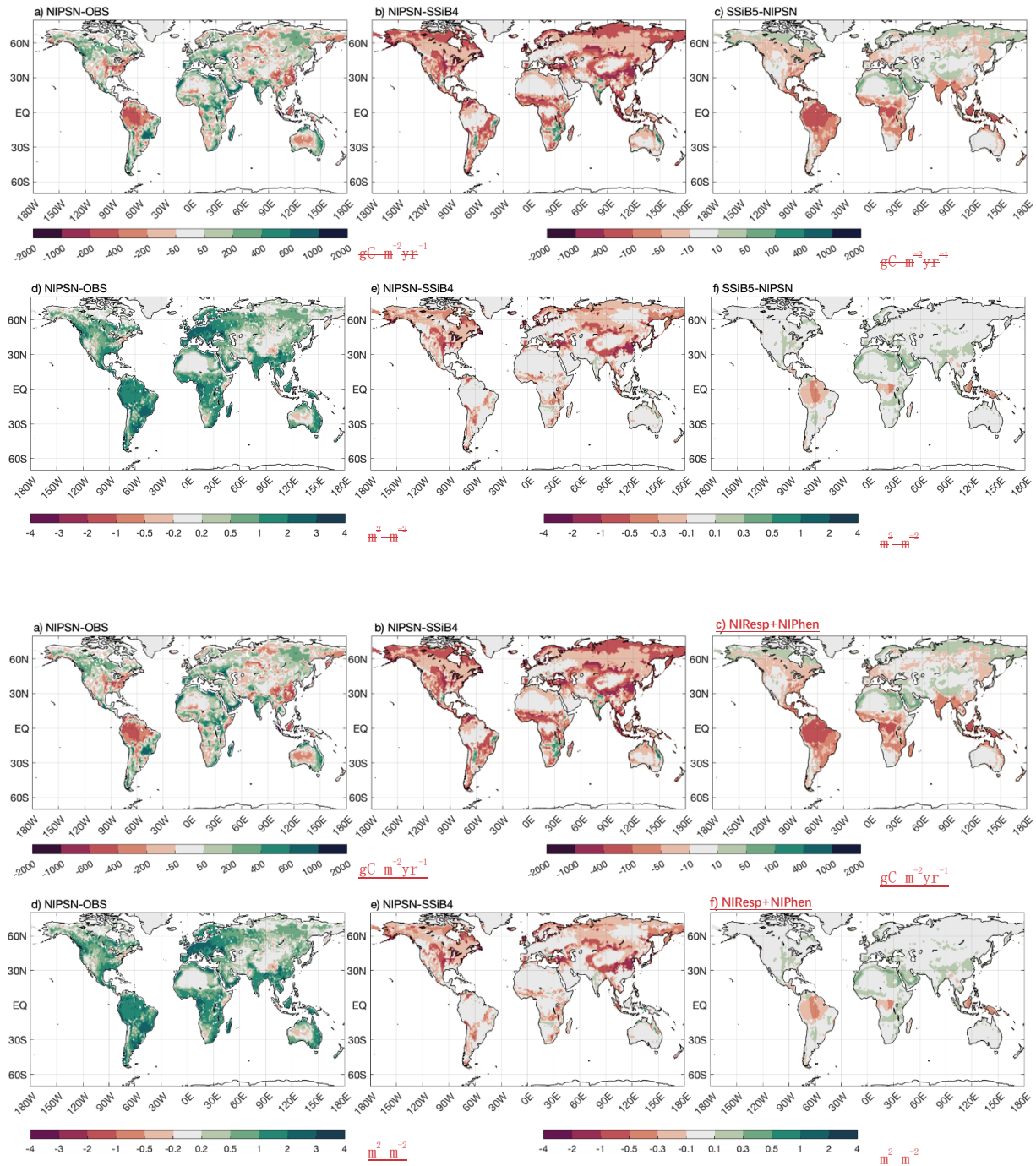


Figure 13. The 1982-2007 average gross primary production difference (a) NIPSN-OBS, (b) NIPSN-SSiB4, (c) ~~SSiB5-NIPSN~~
~~NIPSN~~NIResp+NIPhen, and leaf area index difference (d) NIPSN-OBS, (e) NIPSN-SSiB4, (f) ~~SSiB5-NIPSN~~
~~NIPSN~~NIResp+NIPhen

Note: NIPSN is N limitation on photosynthesis ($V_{c, \max}$) only.

750 We imposed N limitation on several processes. Among them, Exp. NIPSN ~~shows~~has the largest and most significant impact. ~~The~~This paper mainly discusses the results from Exp. NIPSN, which ~~apply~~applies Eq. (6) to scale down the $V_{c, \max}$, ~~are~~
755 ~~discussed here. Please note, the differences between Exp. SSiB5 and Exp. NIPSN show the effects due to another two N~~
~~limitation processes (Eqs. 10 and 13).~~ ~~Exp.~~Exp. NIPSN has a lower global GPP bias ($128.52 \text{ g C m}^{-2} \text{ yr}^{-1}$) ~~compared to~~
~~FLUXNET MTE estimates~~ than does Exp. SSiB4 ~~does~~ ($219.50 \text{ g C m}^{-2} \text{ yr}^{-1}$) (Fig. 13, Table ~~67~~), but it is larger than that of
760 Exp. SSiB5, in which the bias is $79 \text{ g C m}^{-2} \text{ yr}^{-1}$ (Table ~~67~~). In addition, Exp. NIPSN has a global LAI bias of 1.13 (Fig. 13,
Table ~~78~~), which is also lower than the LAI bias in Exp. SSiB4 (1.26~~;~~) but higher than that in Exp. SSiB5 (0.94). The largest
reductions in the magnitude of the LAI bias are in North America, the Eurasian ~~continents~~continent, and tropical
~~Savannas~~savanna regions in South America and Africa (Figs. 13b and 13e). That said, ~~the~~ N limitation ~~on~~of photosynthesis
plays a dominant role, contributing to ~~about~~approximately 65%/41% of the improvement ~~for~~in the GPP/LAI simulations in
765 Exp. SSiB5, respectively. Adjusting $V_{c, \max}$ is the most direct and process-based approach based on physiology and ~~yield~~s
~~has~~the largestgreatest impact. ~~But~~However, the effects of N limitation on the other two processes ~~is~~are still substantial. The N
limitations on respiration and phenology have the ~~most~~greatest impact in tropical forest and savanna regions (Figs. 13c and
13f). ~~For~~The GPP, ~~they~~ also ~~reduce~~reduced the positive bias over boreal regions and the negative bias ~~in the~~over polar regions.
The results from Exp. NIResp or Exp. NIphen individually did not show a statistically significant impact. However, the sum
770 of these two N limitations still has substantial impacts on many parts of the world, as displayed in Fig. 13b, mainly in tropical
rainforests and some midlatitude regions. In addition, the differences between Exp. SSiB5, which includes three limitations,
and Exp. NIPSN, as displayed in Figs. 10 and 11, also delineate the characteristics of the global impacts of these two effects
at seasonal and interannual scales.

770 5 Discussion and Conclusions

This study presents improvements in ~~modelling~~modeling the C cycle by introducing plant N processes into ~~the~~
SSiB5/TRIFFID/DayCent-SOM, using DayCent-SOM to obtain the amount of N available to plants and plant soil N uptake.
The approach presented in this study can also be applied to other models with similar physical and biological principles. The
new C-N coupling framework allows us to use the dynamic ~~C/N ratios~~CNR to represent plant resistance and ~~self-~~
775 ~~adjustment~~response, which ~~allow~~allows adaptations in the stoichiometry of C and N. Since these processes can increase
nutrient use efficiency and reduce the impact of N limitation through N remobilization and resorption, ~~N-limit~~the N limitation
effect ~~would~~does not linearly ~~nor~~or instantaneously respond to the available N content. A linear relationship between the N
limitation factor and available N is valid only when N availability is not sufficient for the minimum N demand for new growth.
This is an advantage of our approach. ~~That said, with~~With the new model structure, ~~N~~the impacts of N on GPP are predicted

780 directly but not linearly with leaf N content, which is affected by the state of plant growth, autotrophic respiration, and plant phenology.

By comparing site-level results from SSiB4 and SSiB5 to FLUXNET GPP and surface heat fluxes from ~~twelve~~thirteen sites with representative biome types and climate zones, we gained confidence in the ability of the new N processes to enhance global model performance. We also evaluated the model performance against global satellite product ~~data-sets~~datasets for GPP and LAI. In general, with the new plant C-N coupling framework, SSiB5/TRIFFID/DayCent-SOM ~~produces~~produced significantly less absolute bias for GPP and LAI than ~~did~~ the baseline version of SSiB4/TRIFFID (without N processes), with a global decrease ~~of~~in the bias in GPP and LAI ~~by~~of 16.3% and 27.1%, respectively. The main improvements are found in tropical Africa and the boreal forest. The more realistic representation of ~~the~~ dynamic ~~C/N-ratios~~CNR and plant C-N framework leads to general improvements in ~~SSiB5/TRIFFID/DayCent-SOM's~~the global C cycling simulations of ~~SSiB5/TRIFFID/DayCent-SOM~~. From the perspective of plant physiology (Högberg et al., 2017), the downregulation of the canopy photosynthetic rate based on the available mineral N for ~~the~~ growth of plant tissues is more reasonable than the simple and direct downregulation of GPP or NPP. In fact, we ~~have~~ conducted a test to directly downscale GPP and NPP, and our simulation results (not shown) support this viewpoint. This coupled model can better reproduce observed state variables and their emergent properties (such as GPP, NPP, LAI, and respiration).

795 Despite the general improvement globally, the GPP simulation in temperate East Asian mixed forest-grassland regions seems to be worse with SSiB5 than with SSiB4. In some regions, such as the Amazon, while SSiB4 produced lower GPP than did the observations, the imposed N limitation in SSiB5 further increased the bias in these regions. ~~This mismatch is a common issue reported in a number of publications (Anav et al., 2015; Liu et al., 2019; Piao et al., 2013). Further investigations are necessary.~~ Recently, the important influence of phosphorus availability on terrestrial ecosystem carbon uptake has been increasingly recognized (Du et al., 2020). Recently, initiated ecosystem-scale manipulation experiments in phosphorus-poor environments (Fleischer et al., 2019) call for the need for new phosphorus-enabled LSMs to track these actions (Goll et al., 2017; Reed et al., 2015). We plan to incorporate other plant processes, such as plant/soil phosphorus processes, to further improve the performance of the model in the future. More evaluations for regions where N limitation is not dominant are necessary.

800 Although the global GPP of SSiB5 was similar to that of the satellite-derived GPP, the positive bias for the LAI was still very large (Table 7). Recent review papers seem to confirm that overestimation of LAI is a common issue in current dynamic vegetation models. Murray-Tortarolo et al. (2013) and Anav et al. (2013) evaluated the performance of dynamic vegetation models in simulating LAI from a CMIP model intercomparison. The simulated LAI for almost every dynamic vegetation model is twice as large as the satellite-derived LAI. More recent studies (Zaehle et al., 2015; Mueller et al., 2019; Gristina et al., 2020; Oliveira et al., 2021; Heikkinen et al., 2021) have confirmed this shortcoming in current dynamic vegetation models. Further investigations are necessary.

810 Anthropogenic N input is one of the major factors affecting C–N coupling and N limitation. The anthropogenic N inputs to terrestrial ecosystems have been much greater than the vegetation N fixation in recent decades in some areas, such as eastern

815 China and the central USA, which can relieve N limitations (Tian et al., 2022). Due to the scope of this paper, this issue is not
addressed in this paper but is an important subject for further investigation to comprehensively understand the N limitation
effect. Finally, this is an offline experiment in which the atmospheric forcing (such as downward radiation) is fixed. With a
fixed atmospheric demand, the heat flux response due to the N limitation effect is also limited, as shown in section 4.1. A
comprehensive assessment of the effect of N limitation on heat fluxes and atmospheric circulation needs to be conducted in a
fully coupled atmosphere–land model.

820

Data availability. The evaluation/reference data sets from model data discussed in this paper are archived at <https://doi.org/10.5281/zenodo.7196869>

825 **Code availability.** The source code of biophysical-ecosystem-biogeochemical model, SSiB version5/TRIFFID/DayCent-SOM
is archived at <https://doi.org/10.5281/zenodo.7297108>

Author contributions. ZX, YX, MH, and YL designed the coupling strategy between SSiB4/TRIFFID and DayCent-SOM.
ZX conducted the simulation with suggestions from YX, WG, and WP. ZX, YX, and MH drafted the text and ZX made the
830 figures. All authors (ZX, YX, WG, MH, YL and WP) have contributed to the analysis and the text.

Competing interests. The authors declare that they have no conflict of interest.

Acknowledgments. This study is supported by the National Science Foundation, Division of Atmospheric and Geospace
835 Sciences (Grant No. AGS-1419526, AGS-1849654), and the Fundamental Research Funds for the Central Universities (Grant
No. 14380172). The authors acknowledge the use of the Cheyenne supercomputer (<https://doi.org/10.5065/D6RX99HX>,
Computational and Information Systems Laboratory, 2019), provided by NCAR CISL, for providing HPC resources. We also
appreciate very comprehensive and constructive reviews by two anonymous reviewers, which greatly enhance this paper.

840 References

- Aber, J. D., Goodale, C. L., Ollinger, S. V., Smith, M.-L., Magill, A. H., Martin, M. E., Hallett, R. A., and Stoddard, J. L.: Is nitrogen deposition altering the nitrogen status of northeastern forests?, *Bioscience*, 53, 375–389, [https://doi.org/10.1641/0006-3568\(2003\)053\[0375:INDATN\]2.0.CO;2](https://doi.org/10.1641/0006-3568(2003)053[0375:INDATN]2.0.CO;2), 2003.
- Aerts, R.: Nutrient Resorption from Senescing Leaves of Perennials: Are there General Patterns?, *J. Ecol.*, 84, 597, <https://doi.org/10.2307/2261481>, 1996.
- ~~Aerts, R. and Berendse, F.: The effect of increased nutrient availability on vegetation dynamics in wet heathlands, *Vegetatio*, 76, 63–69, <https://doi.org/10.1007/BF00047389>, 1988.~~
- Ali, A. A., Xu, C., Rogers, A., McDowell, N. G., Medlyn, B. E., Fisher, R. A., Wullschlegel, S. D., Reich, P. B., Vrugt, J. A., Bauerle, W. L., Santiago, L. S., and Wilson, C. J.: Global-scale environmental control of plant photosynthetic capacity, *Ecol. Appl.*, 25, 2349–2365, <https://doi.org/10.1890/14-2111.1>, 2015.
- Anav, A., Friedlingstein, P., Beer, C., Ciais, P., Harper, A., Jones, C., Murray-Tortarolo, G., Papale, D., Parazoo, N. C., Peylin, P., Wiltshire, A., and Zhao, M.: Spatiotemporal patterns of terrestrial gross primary production: A review, *Rev. Geophys.*, 53, 785–818, <https://doi.org/10.1002/2015RG000483>, 2015.
- Arora, V. K., Katavouta, A., Williams, R. G., Jones, C. D., Brovkin, V., Friedlingstein, P., Schwinger, J., Bopp, L., Boucher, O., Cadule, P., and Chamberlain, M. A.: Carbon – concentration and carbon – climate feedbacks in CMIP6 models and their comparison to CMIP5 models, 4173–4222, 2020.
- Asaadi, A., Arora, V. K., and Arora, V. K.: Implementation of nitrogen cycle in the CLASSIC land model, *Biogeosciences*, 18, <https://doi.org/10.5194/bg-18-669-2021>, 2021.
- ~~Bai, X., Dippold, M. A., An, S., Wang, B., Zhang, H., and Loeppmann, S.: Extracellular enzyme activity and stoichiometry: The effect of soil microbial element limitation during leaf litter decomposition, *Ecol. Indic.*, 121, <https://doi.org/10.1016/j.ecolind.2020.107200>, 2021.~~
- Beer, C., Reichstein, M., Tomelleri, E., Ciais, P., Jung, M., Carvalhais, N., Rodenbeck, C., Arain, M. A., Baldocchi, D., Bonan, G. B., Bondeau, A., Cescatti, A., Lasslop, G., Lindroth, A., Lomas, M., Luyssaert, S., Margolis, H., Oleson, K. W., Rouspard, O., Veenendaal, E., Viovy, N., Williams, C., Woodward, F. I., and Papale, D.: Terrestrial Gross Carbon Dioxide Uptake: Global Distribution and Covariation with Climate, *Science (80-.)*, 329, 834–838, <https://doi.org/10.1126/science.1184984>, 2010.
- ~~Best, M. J., Pryor, M., Clark, D. B., Rooney, G. G., Essery, R. L. H., Ménard, C. B., Edwards, J. M., Hendry, M. A., Porson, A., Gedney, N., Mercado, L. M., Sitch, S., Blyth, E., Boucher, O., Cox, P. M., Grimmond, C. S. B., and Harding, R. J.: The Joint UK Land Environment Simulator (JULES), model description – Part 1: Energy and water fluxes, *Geosci. Model Dev.*, 4, 677–699, <https://doi.org/10.5194/gmd-4-677-2011>, 2011.~~
- Bonan, G. B.: Forests and Climate Change : Climate Benefits of Forests, *Science (80-.)*, 320, 1444–1449, 2008.

- Bonan, G. B., Hartman, M. D., Parton, W. J., and Wieder, W. R.: Evaluating litter decomposition in earth system models with long-term litterbag experiments: An example using the Community Land Model version 4 (CLM4), *Glob. Chang. Biol.*, 19, 957–974, <https://doi.org/10.1111/gcb.12031>, 2013.
- 875 ~~Chang, Y., Zhong, Q., Yang, H., Xu, C., Hua, W., and Li, B.: Patterns and driving factors of leaf C, N, and P stoichiometry in two forest types with different stand ages in a mid-subtropical zone, *For. Ecosyst.*, 9, <https://doi.org/10.1016/j.fees.2022.100005>, 2022.~~
- Chen, X. and Chen, H. Y. H.: Plant mixture balances terrestrial ecosystem C:N:P stoichiometry, *Nat. Commun.*, 12, <https://doi.org/10.1038/s41467-021-24889-w>, 2021.
- 880 ~~Clark, D. B., Mercado, L. M., Sitch, S., Jones, C. D., Gedney, N., Best, M. J., Pryor, M., Rooney, G. G., Essery, R. L. H., Blyth, E., Boucher, O., Harding, R. J., Huntingford, C., and Cox, P. M.: The Joint UK Land Environment Simulator (JULES), model description Part 2: Carbon fluxes and vegetation dynamics, *Geosci. Model Dev.*, 4, 701–722, <https://doi.org/10.5194/gmd-4-701-2011>, 2011.~~
- Clarkson, D. T. and Hanson, J. B.: The Mineral Nutrition of Higher Plants, *Annu. Rev. Plant Physiol.*, 31, 239–298, <https://doi.org/10.1146/annurev.pp.31.060180.001323>, 1980.
- 885 Collatz, G. J., Ball, J. T., Grivet, C., and Berry, J. A.: Physiological and environmental regulation of stomatal conductance, photosynthesis and transpiration: a model that includes a laminar boundary layer, *Agric. For. Meteorol.*, 54, 107–136, [https://doi.org/10.1016/0168-1923\(91\)90002-8](https://doi.org/10.1016/0168-1923(91)90002-8), 1991.
- Cox, P. M.: Description of the “TRIFFID” Dynamic Global Vegetation Model, Hadley Cent. Tech. Note-24, 2001.
- 890 Dan, L., Yang, X., Yang, F., Peng, J., Li, Y., Gao, D., Ji, J., ~~Andand~~ Huang, M.: Integration of nitrogen dynamics into the land surface model AVIM. Part 2: baseline data and variation of carbon and nitrogen fluxes in China, *Atmos. Ocean. Sci. Lett.*, 13, <https://doi.org/10.1080/16742834.2020.1819145>, 2020.
- Davies-Barnard, T., Meyerholt, J., Zaehle, S., Friedlingstein, P., Brovkin, V., Fan, Y., Fisher, R. A., Jones, C. D., Lee, H., Peano, D., Smith, B., Wärlind, D., and Wiltshire, A. J.: Nitrogen cycling in CMIP6 land surface models: Progress and
895 limitations, *Biogeosciences*, 17, 5129–5148, <https://doi.org/10.5194/bg-17-5129-2020>, 2020.
- ~~Ding, D., Arif, M., Liu, M., LiDelpierre, N., Vitasse, Y., Chuine, I., Guillemot, J., Hu, X., Geng, Q., Yin, F, Bazot, S., Rutishauser, T., and LiRathgeber, C.: Plant-soil interactions, B. K.: Temperate and C:N:P stoichiometric homeostasis of plant organs in riparian plantation, *Front. Plant Sci.*, 13, <https://doi.org/10.3389/fpls.2022.979023>, 20221007/s13595-015-0477-6, 2016.~~
- 900 Dorman, J. L. and Sellers, P. J.: A global climatology of albedo, roughness length and stomatal resistance for atmospheric general circulation models as represented by the Simple Biosphere Model (SiB), *J. Appl. Meteorol.*, 28, 833–855, [https://doi.org/10.1175/1520-0450\(1989\)028<0833:AGCOAR>2.0.CO;2](https://doi.org/10.1175/1520-0450(1989)028<0833:AGCOAR>2.0.CO;2), 1989.
- Drewniak, B. and Gonzalez-Meler, M.: Earth System Model Needs for Including the Interactive Representation of Nitrogen Deposition and Drought Effects on Forested Ecosystems, *Forests*, 8, 267, <https://doi.org/10.3390/f8080267>, 2017.

- 905 Du, E., Terrer, C., Pellegrini, A. F. A., Ahlström, A., van Lissa, C. J., Zhao, X., Xia, N., Wu, X., and Jackson, R. B.: Global patterns of terrestrial nitrogen and phosphorus limitation, *Nat. Geosci.*, 13, 221–226, <https://doi.org/10.1038/s41561-019-0530-4>, 2020.
- ~~Evans, J. R.: Photosynthesis and nitrogen relationships in leaves of C_3 plants, *Oecologia*, 78, 9–19, <https://doi.org/10.1007/BF00377192>, 1989.~~
- 910 [Enquist, B., J. Brown, and G. West: Allometric scaling of plant energetics and population density. *Nature*, 395, 163–166, 1998.](https://doi.org/10.1038/395163a)
- Eyring, V., Bony, S., Meehl, G. A., Senior, C. A., Stevens, B., Stouffer, R. J., and Taylor, K. E.: Overview of the Coupled Model Intercomparison Project Phase 6 (CMIP6) experimental design and organization, *Geosci. Model Dev.*, 9, 1937–1958, <https://doi.org/10.5194/gmd-9-1937-2016>, 2016.
- Farquhar, G. D., von Caemmerer, S., and Berry, J. A.: A biochemical model of photosynthetic CO₂ assimilation in leaves of
- 915 *C₃* species, *Planta*, 149, 78–90, <https://doi.org/10.1007/BF00386231>, 1980.
- Fisher, J. B., Sitch, S., Malhi, Y., Fisher, R. A., Huntingford, C., and Tan, S.-Y.: Carbon cost of plant nitrogen acquisition: A mechanistic, globally applicable model of plant nitrogen uptake, retranslocation, and fixation, *Global Biogeochem. Cycles*, 24, n/a–n/a, <https://doi.org/10.1029/2009gb003621>, [20102010a](https://doi.org/10.1029/2009gb003621).
- [Fisher, R., McDowell, N., Purves, D., Moorcroft, P., Sitch, S., Cox, P., Huntingford, C., Meir, P., and Ian Woodward, F.:](https://doi.org/10.1111/j.1469-8137.2010.03340.x)
- 920 [Assessing uncertainties in a second-generation dynamic vegetation model caused by ecological scale limitations, *New Phytol.*, 187, 666–681, <https://doi.org/10.1111/j.1469-8137.2010.03340.x>, 2010b.](https://doi.org/10.1111/j.1469-8137.2010.03340.x)
- Fleischer, K., Rammig, A., De Kauwe, M. G., Walker, A. P., Domingues, T. F., Fuchslueger, L., Garcia, S., Goll, D. S., Grandis, A., Jiang, M., Haverd, V., Hofhansl, F., Holm, J. A., Kruijt, B., Leung, F., Medlyn, B. E., Mercado, L. M., Norby, R. J., Pak, B., von Randow, C., Quesada, C. A., Schaap, K. J., Valverde-Barrantes, O. J., Wang, Y. P., Yang, X., Zaehle, S., Zhu,
- 925 Q., and Lapola, D. M.: Amazon forest response to CO₂ fertilization dependent on plant phosphorus acquisition, *Nat. Geosci.*, 12, <https://doi.org/10.1038/s41561-019-0404-9>, 2019.
- Foley, J. A., Levis, S., Prentice, I. C., Pollard, D., and Thompson, S. L.: Coupling dynamic models of climate and vegetation, *Glob. Chang. Biol.*, 4, 561–579, <https://doi.org/10.1046/j.1365-2486.1998.t01-1-00168.x>, 1998.
- Friedlingstein, P., Cox, P., Betts, R., Bopp, L., von Bloh, W., Brovkin, V., Cadule, P., Doney, S., Eby, M., Fung, I., Bala, G.,
- 930 John, J., Jones, C., Joos, F., Kato, T., Kawamiya, M., Knorr, W., Lindsay, K., Matthews, H. D., Raddatz, T., Rayner, P., Reick, C., Roeckner, E., Schnitzler, K.-G., Schnur, R., Strassmann, K., Weaver, A. J., Yoshikawa, C., and Zeng, N.: Climate–Carbon Cycle Feedback Analysis: Results from the C₄ MIP Model Intercomparison, *J. Clim.*, 19, 3337–3353, <https://doi.org/10.1175/JCLI3800.1>, 2006.
- [Fu, Y. H., Piao, S., Delpierre, N., Hao, F., Hänninen, H., Geng, X., Peñuelas, J., Zhang, X., Janssens, I. A., and Campioli, M.:](https://doi.org/10.1093/treephys/tpz041)
- 935 [Nutrient availability alters the correlation between spring leaf-out and autumn leaf senescence dates, *Tree Physiol.*, 39, <https://doi.org/10.1093/treephys/tpz041>, 2019.](https://doi.org/10.1093/treephys/tpz041)
- Gerber, S., Hedin, L. O., Oppenheimer, M., Pacala, S. W., and Shevliakova, E.: Nitrogen cycling and feedbacks in a global dynamic land model, *Global Biogeochem. Cycles*, 24, 1–15, <https://doi.org/10.1029/2008GB003336>, 2010.

- Ghimire, B., Riley, W. J., Koven, C. D., Mu, M., and Randerson, J. T.: Representing leaf and root physiological traits in CLM
940 improves global carbon and nitrogen cycling predictions, *J. Adv. Model. Earth Syst.*, 8, 598–613,
<https://doi.org/10.1002/2015MS000538>, 2016.
- Goll, D. S., Winkler, A. J., Raddatz, T., Dong, N., Colin Prentice, I., Ciais, P., and Brovkin, V.: Carbon-nitrogen interactions
in idealized simulations with JSBACH (version 3.10), *Geosci. Model Dev.*, 10, 2009–2030, <https://doi.org/10.5194/gmd-10-2009-2017>, 2017.
- 945 Gregory, J. M., Jones, C. D., Cadule, P., and Friedlingstein, P.: Quantifying carbon cycle feedbacks, *J. Clim.*, 22, 5232–5250,
<https://doi.org/10.1175/2009JCLI2949.1>, 2009.
- Gristina, L., Scalenghe, R., García-Díaz, A., Matranga, M. G., Ferraro, V., Guaitoli, F., and Novara, A.: Soil organic carbon
stocks under recommended management practices in different soils of semiarid vineyards, *L. Degrad. Dev.*, 31,
<https://doi.org/10.1002/ldr.3339>, 2020.
- 950 Del Grosso, S. J., Parton, W. J., Mosier, A. R., Ojima, D. S., Kulmala, A. E., and Phongpan, S.: General model for N₂O and
N₂ gas emissions from soils due to denitrification, *Global Biogeochem. Cycles*, 14, 1045–1060,
<https://doi.org/10.1029/1999GB001225>, 2000.
- Harper, A. B., Cox, P. M., Friedlingstein, P., Wiltshire, A. J., Jones, C. D., Sitch, S., Mercado, L. M., Groenendijk, M.,
Robertson, E., Kattge, J., Bönisch, G., Atkin, O. K., Bahn, M., Cornelissen, J., Niinemets, Ü., Onipchenko, V., Peñuelas, J.,
955 Poorter, L., Reich, P. B., Soudzilovskaia, N. A., and Van Bodegom, P.: Improved representation of plant functional types and
physiology in the Joint UK Land Environment Simulator (JULES v4.2) using plant trait information, *Geosci. Model Dev.*, 9,
2415–2440, <https://doi.org/10.5194/gmd-9-2415-2016>, 2016.
- Heikkinen, J., Keskinen, R., Regina, K., Honkanen, H., and Nuutinen, V.: Estimation of carbon stocks in boreal cropland soils
- methodological considerations, *Eur. J. Soil Sci.*, 72, <https://doi.org/10.1111/ejss.13033>, 2021.
- 960 Herbert, D. A. and Fownes, J. H.: Phosphorus limitation of forest leaf area and net primary production on a highly weathered
soil, *Ecosystems*, 29, 242–25, <https://doi.org/10.1007/BF02186049>, 1999.
- Högberg, P., Näsholm, T., Franklin, O., and Högberg, M. N.: Tamm Review: On the nature of the nitrogen limitation to plant
growth in Fennoscandian boreal forests, <https://doi.org/10.1016/j.foreco.2017.04.045>, 1 November 2017.
- Hu, S., Chapin, F. S., Firestone, M. K., Field, C. B., and Chiariello, N. R.: Nitrogen limitation of microbial decomposition in
965 a grassland under elevated CO₂, *Nature*, 409, 188–191, <https://doi.org/10.1038/35051576>, 2001.
- Huang, H., Xue, Y., Li, F., and Liu, Y.: Modeling long-term fire impact on ecosystem characteristics and surface energy using
a process-based vegetation-fire model SSiB4/TRIFFID-Fire v1.0, *Geosci. Model Dev. Discuss.*, 1–41,
<https://doi.org/10.5194/gmd-2020-122>, 2020.
- 970 ~~Jiang, L., Lu, L., Jiang, L., Qi, Y., and Yang, A.: Impact of a detailed urban parameterization on modeling the urban heat island
in beijing using TEB RAMS, *Adv. Meteorol.*, 2014, <https://doi.org/10.1155/2014/602528>, 2014.~~

- Jung, M., Reichstein, M., and Bondeau, A.: Towards global empirical upscaling of FLUXNET eddy covariance observations: Validation of a model tree ensemble approach using a biosphere model, *Biogeosciences*, 6, 2001–2013, <https://doi.org/10.5194/bg-6-2001-2009>, 2009.
- Jung, M., Reichstein, M., Margolis, H. A., Cescatti, A., Richardson, A. D., Arain, M. A., Arneeth, A., Bernhofer, C., Bonal, D.,
975 Chen, J., Gianelle, D., Gobron, N., Kiely, G., Kutsch, W., Lasslop, G., Law, B. E., Lindroth, A., Merbold, L., Montagnani, L.,
Moors, E. J., Papale, D., Sottocornola, M., Vaccari, F., and Williams, C.: Global patterns of land-atmosphere fluxes of carbon
dioxide, latent heat, and sensible heat derived from eddy covariance, satellite, and meteorological observations, *J. Geophys.
Res. Biogeosciences*, 116, <https://doi.org/10.1029/2010JG001566>, 2011.
- ~~Kaiser, C., Franklin, O., Dieckmann, U., and Richter, A.: Microbial community dynamics alleviate stoichiometric constraints
980 during litter decay, *Ecol. Lett.*, 17, <https://doi.org/10.1111/ele.12269>, 2014.~~
- Kattge, J., Knorr, W., Raddatz, T., and Wirth, C.: Quantifying photosynthetic capacity and its relationship to leaf nitrogen
content for global-scale terrestrial biosphere models, *Glob. Chang. Biol.*, 15, 976–991, [https://doi.org/10.1111/j.1365-
2486.2008.01744.x](https://doi.org/10.1111/j.1365-
2486.2008.01744.x), 2009.
- Kolb, K. J. and Evans, R. D.: Implications of leaf nitrogen recycling on the nitrogen isotope composition of deciduous plant
985 tissues, *New Phytol.*, 156, 57–64, <https://doi.org/10.1046/j.1469-8137.2002.00490.x>, 2002.
- ~~Krinner, G., Viovy, N., de Noblet-Ducoudré, N., Ogée, J., Polcher, J., Friedlingstein, P., Ciais, P., Sitch, S., and Prentice, I.
C.: A dynamic global vegetation model for studies of the coupled atmosphere-biosphere system, *Global Biogeochem. Cycles*,
19, 1–33, <https://doi.org/10.1029/2003GB002199>, 2005.~~
- ~~Kou-Giesbrecht, S., Arora, V. K., Seiler, C., Arneeth, A., Falk, S., Jain, A. K., Joos, F., Kennedy, D., Knauer, J., Sitch, S.,
990 O'sullivan, M., Pan, N., Sun, Q., Tian, H., Vuichard, N., and Zaehle, S.: Evaluating nitrogen cycling in terrestrial biosphere
models: a disconnect between the carbon and nitrogen cycles, *Earth Syst. Dyn.*, 14, <https://doi.org/10.5194/esd-14-767-2023>,
2023.~~
- Lawrence, D. M., Fisher, R. A., Koven, C. D., Oleson, K. W., Swenson, S. C., Bonan, G., Collier, N., Ghimire, B., van
Kampenhout, L., Kennedy, D., Kluzek, E., Lawrence, P. J., Li, F., Li, H., Lombardozzi, D., Riley, W. J., Sacks, W. J., Shi, M.,
995 Vertenstein, M., Wieder, W. R., Xu, C., Ali, A. A., Badger, A. M., Bisht, G., van den Broeke, M., Brunke, M. A., Burns, S.
P., Buzan, J., Clark, M., Craig, A., Dahlin, K., Drewniak, B., Fisher, J. B., Flanner, M., Fox, A. M., Gentine, P., Hoffman, F.,
Keppel-Aleks, G., Knox, R., Kumar, S., Lenaerts, J., Leung, L. R., Lipscomb, W. H., Lu, Y., Pandey, A., Pelletier, J. D., Perket,
J., Randerson, J. T., Ricciuto, D. M., Sanderson, B. M., Slater, A., Subin, Z. M., Tang, J., Thomas, R. Q., Val Martin, M., and
Zeng, X.: The Community Land Model Version 5: Description of New Features, Benchmarking, and Impact of Forcing
1000 Uncertainty, *J. Adv. Model. Earth Syst.*, 11, 4245–4287, <https://doi.org/10.1029/2018MS001583>, 2019.
- LeBauer, D. S. and Treseder, K. K.: ~~NITROGEN LIMITATION OF NET PRIMARY PRODUCTIVITY IN TERRESTRIAL
ECOSYSTEMS IS GLOBALLY DISTRIBUTED: Nitrogen Limitation of Net Primary Productivity In Terrestrial Ecosystems
Is Globally Distributed~~, *Ecology*, 89, 371–379, <https://doi.org/10.1890/06-2057.1>, 2008.

- 1005 ~~Lin, Y., Lai, Y., Tang, S., Qin, Z., Liu, J., Kang, F., and Kuang, Y.: Climatic and edaphic variables determine leaf C, N, P stoichiometry of deciduous Quercus species, Plant Soil, 474, <https://doi.org/10.1007/s11104-022-05342-3>, 2022.~~
- Liu, Y., Xue, Y., Macdonald, G., Cox, P., and Zhang, Z.: Global vegetation variability and its response to elevated CO₂, global warming, and climate variability - A study using the offline SSiB4/TRIFFID model and satellite data, Earth Syst. Dyn., 10, 9–29, <https://doi.org/10.5194/esd-10-9-2019>, 2019.
- Liu, Y., Xue, Y., Li, Q., Lettenmaier, D., and Zhao, P.: Investigation of the Variability of Near-Surface Temperature Anomaly and Its Causes Over the Tibetan Plateau, J. Geophys. Res. Atmos., 125, <https://doi.org/10.1029/2020JD032800>, 2020.
- ~~Luke McCormack, M., Adams, T. S., Smithwick, E. A. H., and Eissenstat, D. M.: Variability in root production, phenology, and turnover rate among 12 temperate tree species. Ecology, 95, <https://doi.org/10.1890/13-1942.1>, 2014.~~
- ~~Lund, M., Falk, J. M., Friborg, T., Mbufong, H. N., Sigsgaard, C., Soegaard, H., and Tamstorf, M. P.: Trends in CO₂ exchange in a high Arctic tundra heath, 2000-2010, J. Geophys. Res. Biogeosciences, 117, <https://doi.org/10.1029/2011JG001901>, 2012.~~
- 1015 Ma, H.-Y., Mechoso, C. R., Xue, Y., Xiao, H., Neelin, J. D., and Ji, X.: On the connection between continental-scale land surface processes and the tropical climate in a coupled ocean-atmosphere-land system, J. Clim., 26, 9006–9025, <https://doi.org/10.1175/JCLI-D-12-00819.1>, 2013.
- MacDonald, J. A., Dise, N. B., Matzner, E., Armbruster, M., Gundersen, P., and Forsius, M.: Nitrogen input together with ecosystem nitrogen enrichment predict nitrate leaching from European forests, Glob. Chang. Biol., 8, 1028–1033, <https://doi.org/10.1046/j.1365-2486.2002.00532.x>, 2002.
- 1020 Makino, A. and Osmond, B.: Effects of Nitrogen Nutrition on Nitrogen Partitioning between Chloroplasts and Mitochondria in Pea and Wheat, Plant Physiol., 96, 355–362, <https://doi.org/10.1104/pp.96.2.355>, 1991.
- Marmann, P., Wendler, R., Millard, P., and Heilmeyer, H.: Nitrogen storage and remobilization in ash (*Fraxinus excelsior*) under field and laboratory conditions, Trees - Struct. Funct., 11, 298–305, <https://doi.org/10.1007/s004680050088>, 1997.
- 1025 ~~Matson, P., Lohse, K. A., and Hall, S. J.: The Globalization of Nitrogen Deposition: Consequences for Terrestrial Ecosystems, AMBIO A J. Hum. Environ., 31, 113–119, <https://doi.org/10.1579/0044-7447-31.2.113>, 2002.~~
- May, J. D. and Killingbeck, K. T.: Effects of preventing nutrient resorption on plant fitness and foliar nutrient dynamics, Ecology, 73, 1868–1878, <https://doi.org/10.2307/1940038>, 1992.
- McDowell, N., Pockman, W. T., Allen, C. D., Breshears, D. D., Cobb, N., Kolb, T., Plaut, J., Sperry, J., West, A., Williams, 1030 D. G., Williams, D. G., and Yezpez, E. A.: Mechanisms of plant survival and mortality during drought: Why do some plants survive while others succumb to drought?, New Phytol., 178, 719–739, <https://doi.org/10.1111/j.1469-8137.2008.02436.x>, 2008.
- McGroddy, M. E., Daufresne, T., and Hedin, L. O.: Scaling of C:N:P stoichiometry in forests worldwide: Implications of terrestrial redfield-type ratios, <https://doi.org/10.1890/03-0351>, 2004.
- 1035 ~~Medlyn, B. E., Zaehle, S., De Kauwe, M. G., Walker, A. P., Dietze, M. C., Hanson, P. J., Hickler, T., Jain, A. K., Luo, Y., Parton, W., Oren, R., and Norby, R. J.: Using ecosystem experiments to improve vegetation models, Nat. Clim. Chang., 5, 528–534, <https://doi.org/10.1038/nclimate2621>, 2015.~~

- Meyer-Grünefeldt, M., Calvo, L., Marcos, E., Von Oheimb, G., and Härdtle, W.: Impacts of drought and nitrogen addition on Calluna heathlands differ with plant life-history stage, *J. Ecol.*, 103, 1141–1152, <https://doi.org/10.1111/1365-2745.12446>, 2015.
- ~~Meyerholt, J., Sickel, K., and Zaehle, S.: Ensemble projections elucidate effects of uncertainty in terrestrial nitrogen limitation on future carbon uptake, *Glob. Chang. Biol.*, 26, <https://doi.org/10.1111/gcb.15114>, 2020.~~
- Millard, P.: Measurement of the remobilization of nitrogen for spring leaf growth of trees under field conditions, *Tree Physiol.*, 14, 1049–1054, <https://doi.org/10.1093/treephys/14.7-8-9.1049>, 1994.
- Morgan, J. B. and Connolly, E. L.: Plant - Soil Interactions : Nutrient Uptake, *Nat. Educ. Knowl.*, 4, 2013.
- Mueller, P., Ladiges, N., Jack, A., Schmieidl, G., Kutzbach, L., Jensen, K., and Nolte, S.: Assessing the long-term carbon-sequestration potential of the semi-natural salt marshes in the European Wadden Sea, *Ecosphere*, 10, <https://doi.org/10.1002/ecs2.2556>, 2019.
- Murray-Tortarolo, G., Anav, A., Friedlingstein, P., Sitch, S., Piao, S., Zhu, Z., Poulter, B., Zaehle, S., Ahlström, A., Lomas, M., Viovy, N., and Zeng, N.: Evaluation of land surface models in reproducing satellite-derived LAI over the high-latitude northern hemisphere. Part I: Uncoupled DGVMs, *Remote Sens.*, 5, 4819–4838, <https://doi.org/10.3390/rs5104819>, 2013.
- Neilsen, D., Millard, P., Neilsen, G. H., and Hogue, E. J.: Sources of N for leaf growth in a high-density apple (*Malus domestica*) orchard irrigated with ammonium nitrate solution, *Tree Physiol.*, 17, 733–739, <https://doi.org/10.1093/treephys/17.11.733>, 1997.
- ~~Niu, G. Y., Fang, Y. H., Chang, L. L., Jin, J., Yuan, H., and Zeng, X.: Enhancing the Noah-MP Ecosystem Response to Droughts With an Explicit Representation of Plant Water Storage Supplied by Dynamic Root Water Uptake, *J. Adv. Model. Earth Syst.*, 12, <https://doi.org/10.1029/2020MS002062>, 2020.~~
- Oleson, K. W., Lawrence, D. M., Bonan, G. B., Drewniak, B., Huang, M., Charles, D., Levis, S., Li, F., Riley, W. J., Zachary, M., Swenson, S. C., Thornton, P. E., Bozbiyik, A., Fisher, R., Heald, C. L., Kluzek, E., Lamarque, F., Lawrence, P. J., Leung, L. R., Muszala, S., Ricciuto, D. M., and Sacks, W.: Technical description of version 4.5 of the Community Land Model (CLM), NCAR Technical Note NCAR/TN-503+STR, Natl. Cent. Atmos. Res. Boulder, CO, 420pp, <https://doi.org/DOI:10.5065/D6RR1W7M>, 2013.
- Oliveira, D. C. de, Oliveira, D. M. da S., Freitas, R. de C. A. de, Barreto, M. S., Almeida, R. E. M. de, Batista, R. B., and Cerri, C. E. P.: Depth assessed and up-scaling of single case studies might overestimate the role of C sequestration by pastures in the commitments of Brazil's low-carbon agriculture plan, *Carbon Manag.*, 12, <https://doi.org/10.1080/17583004.2021.1977390>, 2021.
- ~~Pan, Y., Liu, Y., Wentworth, G. R., Zhang, L., Zhao, Y., Li, Y., Liu, X., Du, E., Fang, Y., Xiao, H., Ma, H., and Wang, Y.: Letter to the editor: Critical assessments of the current state of scientific knowledge, terminology, and research needs concerning the ecological effects of elevated atmospheric nitrogen deposition in China, *Atmos. Environ.*, 153, 109–116, <https://doi.org/10.1016/j.atmosenv.2017.01.015>, 2017.~~

- Parton, W., Silver, W. L., Burke, I. C., Grassens, L., Harmon, M. E., Currie, W. S., King, J. Y., Adair, E. C., Brandt, L. A., Hart, S. C., and Fasth, B.: Global-scale similarities in nitrogen release patterns during long-term decomposition, *Science* (80-.), 315, 361–364, <https://doi.org/10.1126/science.1134853>, 2007.
- 1075 Parton, W. J., Scurlock, J. M. O., Ojima, D. S., Gilmanov, T. G., Scholes, R. J., Schimel, D. S., Kirchner, T., Menaut, J.-C., Seastedt, T., Garcia Moya, E., Kamnalrut, A., and Kinyamario, J. I.: Observations and modeling of biomass and soil organic matter dynamics for the grassland biome worldwide, *Global Biogeochem. Cycles*, 7, 785–809, <https://doi.org/10.1029/93GB02042>, 1993.
- Parton, W. J., Ojima, D. S., Cole, C. V., and Schimel, D. S.: A general model for soil organic matter dynamics: sensitivity to litter chemistry, texture and management, *Quant. Model. soil Form. Process. Proc. Symp. Minneapolis*, 1992, 1994.
- 1080 Parton, W. J., Hartman, M., Ojima, D., and Schimel, D.: DAYCENT and its land surface submodel: description and testing, *Glob. Planet. Change*, 19, 35–48, [https://doi.org/10.1016/S0921-8181\(98\)00040-X](https://doi.org/10.1016/S0921-8181(98)00040-X), 1998.
- Parton, W. J., Hanson, P. J., Swanston, C., Torn, M., Trumbore, S. E., Riley, W., and Kelly, R.: ForCent model development and testing using the Enriched Background Isotope Study experiment, *J. Geophys. Res. Biogeosciences*, 115, 1–15, <https://doi.org/10.1029/2009JG001193>, 2010.
- 1085 Pastorello, G., Trotta, C., Canfora, E., Chu, H., Christianson, D., Cheah, Y. W., Poindexter, C., Chen, J., Elbashandy, A., Humphrey, M., Isaac, P., Polidori, D., Ribeca, A., van Ingen, C., Zhang, L., Amiro, B., Ammann, C., Arain, M. A., Ardö, J., Arkebauer, T., Arndt, S. K., Arriga, N., Aubinet, M., Aurela, M., Baldocchi, D., Barr, A., Beamesderfer, E., Marchesini, L. B., Bergeron, O., Beringer, J., Bernhofer, C., Berveiller, D., Billesbach, D., Black, T. A., Blanken, P. D., Bohrer, G., Boike, J., Bolstad, P. V., Bonal, D., Bonnefond, J. M., Bowling, D. R., Bracho, R., Brodeur, J., Brümmer, C., Buchmann, N., Burban, 1090 B., Burns, S. P., Buysse, P., Cale, P., Cavagna, M., Cellier, P., Chen, S., Chini, I., Christensen, T. R., Cleverly, J., Collalti, A., Consalvo, C., Cook, B. D., Cook, D., Coursolle, C., Cremonese, E., Curtis, P. S., D’Andrea, E., da Rocha, H., Dai, X., Davis, K. J., De Cinti, B., de Grandcourt, A., De Ligne, A., De Oliveira, R. C., Delpierre, N., Desai, A. R., Di Bella, C. M., di Tommasi, P., Dolman, H., Domingo, F., Dong, G., Dore, S., Duce, P., Dufrêne, E., Dunn, A., Dušek, J., Eamus, D., Eichelmann, U., ElKhidir, H. A. M., Eugster, W., Ewenz, C. M., Ewers, B., Famulari, D., Fares, S., Feigenwinter, I., Feitz, A., Fensholt, 1095 R., Filippa, G., Fischer, M., Frank, J., Galvagno, M., Gharun, M., Gianelle, D., et al.: The FLUXNET2015 dataset and the ONEFlux processing pipeline for eddy covariance data, *Sci. data*, 7, <https://doi.org/10.1038/s41597-020-0534-3>, 2020.
- [Peng, J., Wang, Y. P., Houlton, B. Z., Dan, L., Pak, B., and Tang, X.: Global Carbon Sequestration Is Highly Sensitive to Model-Based Formulations of Nitrogen Fixation, *Global Biogeochem. Cycles*, 34, <https://doi.org/10.1029/2019GB006296>, 2020.](https://doi.org/10.1029/2019GB006296)
- 1100 Peñuelas, J., Poulter, B., Sardans, J., Ciais, P., Van Der Velde, M., Bopp, L., Boucher, O., Godderis, Y., Hinsinger, P., Llusia, J., Nardin, E., Vicca, S., Obersteiner, M., and Janssens, I. A.: Human-induced nitrogen-phosphorus imbalances alter natural and managed ecosystems across the globe, *Nat. Commun.*, 4, <https://doi.org/10.1038/ncomms3934>, 2013.
- Piao, S., ~~Sitch, S., Ciais, P., Friedlingstein, P., Peylin, P., Wang, X., Ahlström, Liu, Q., Chen, A., Anav, Janssens, I. A., Canadell, Fu, Y., Dai, J.-G., Cong, N., Zaehle, S., Liu, L., Lian, X., Shen, M., and Zeng, N.:~~ [Evaluation of terrestrial carbon](https://doi.org/10.1029/2019GB006296)

- 1105 [eye models for their response to](#)Zhu, X.: [Plant phenology and global climate variability and to CO₂ trends](#), *Glob. Chang. Biol.*, 19, 2117–2132, [https://doi.org/10.1111/gcb.12187](#), 2013, 14619, 2019.
- Raddatz, T. J., Reick, C. H., Knorr, W., Kattge, J., Roeckner, E., Schnur, R., Schnitzler, K. G., Wetzell, P., and Jungclaus, J.: Will the tropical land biosphere dominate the climate-carbon cycle feedback during the twenty-first century?, *Clim. Dyn.*, 29, 565–574, [https://doi.org/10.1007/s00382-007-0247-8](#), 2007.
- 1110 Reed, S. C., Yang, X., and Thornton, P. E.: Incorporating phosphorus cycling into global modeling efforts: A worthwhile, tractable endeavor, *New Phytol.*, 208, [https://doi.org/10.1111/nph.13521](#), 2015.
- Reich, P. B., Hobbie, S. E., Lee, T., Ellsworth, D. S., West, J. B., Tilman, D., Knops, J. M. H., Naeem, S., and Trost, J.: Nitrogen limitation constrains sustainability of ecosystem response to CO₂, *Nature*, 440, 922–925, [https://doi.org/10.1038/nature04486](#), 2006.
- 1115 Reich, P. B., Tjoelker, M. G., Pregitzer, K. S., Wright, I. J., Oleksyn, J., and Machado, J. L.: Scaling of respiration to nitrogen in leaves, stems and roots of higher land plants, *Ecol. Lett.*, 11, 793–801, [https://doi.org/10.1111/j.1461-0248.2008.01185.x](#), 2008.
- Richardson, A. D., Anderson, R. S., Arain, M. A., Barr, A. G., Bohrer, G., Chen, G., Chen, J. M., Ciais, P., Davis, K. J., Desai, A. R., Dietze, M. C., Dragoni, D., Garrity, S. R., Gough, C. M., Grant, R., Hollinger, D. Y., Margolis, H. A., Mccaughy, H., 1120 Migliavacca, M., Monson, R. K., Munger, J. W., Poulter, B., Raczka, B. M., Ricciuto, D. M., Sahoo, A. K., Schaefer, K., Tian, H., Vargas, R., Verbeeck, H., Xiao, J., and Xue, Y.: Terrestrial biosphere models need better representation of vegetation phenology: Results from the North American Carbon Program Site Synthesis, *Glob. Chang. Biol.*, 18, [https://doi.org/10.1111/j.1365-2486.2011.02562.x](#), 2012.
- Rogers, A.: The use and misuse of V(c,max) in Earth System Models., *Photosynth. Res.*, 119, 15–29, 1125 [https://doi.org/10.1007/s11120-013-9818-1](#), 2014.
- Sardans, J., Rivas-Ubach, A., and Peñuelas, J.: The C:N:P stoichiometry of organisms and ecosystems in a changing world: A review and perspectives, [https://doi.org/10.1016/j.ppees.2011.08.002](#), 2012.
- Sellers, P. J., Mintz, Y., Sud, Y. C., and Dalcher, A.: A Simple Biosphere Model (SIB) for Use within General Circulation Models, *J. Atmos. Sci.*, 43, 505–531, [https://doi.org/10.1175/1520-0469\(1986\)043<0505:ASBMFU>2.0.CO;2](#), 1986.
- 1130 Sheffield, J., Goteti, G., and Wood, E. F.: Development of a 50-year high-resolution global dataset of meteorological forcings for land surface modeling, *J. Clim.*, 19, 3088–3111, [https://doi.org/10.1175/JCLI3790.1](#), 2006.
- Sitch, S., Prentice, I. C., Arneth, A., Bondeau, A., Cramer, W., Kaplan, J. O., Levis, S., Lucht, W., Sykes, M. T., Thonicke, K., and Venevsky, S.: Evaluation of ecosystem dynamics, plant geography and terrestrial carbon cycling in the LPJ dynamic global vegetation model, *Glob. Chang. Biol.*, 9, 161–185, [https://doi.org/10.1046/j.1365-2486.2003.00569.x](#), 2003.
- 1135 Smith, B., Wärlind, D., Arneth, A., Hickler, T., Leadley, P., Siltberg, J., and Zaehle, S.: Implications of incorporating N cycling and N limitations on primary production in an individual-based dynamic vegetation model, *Biogeosciences*, 11, 2027–2054, [https://doi.org/10.5194/bg-11-2027-2014](#), 2014.

- Smith, S. V.: Stoichiometry of C:N:P Fluxes in Shallow-Water Marine Ecosystems, in: Comparative Analyses of Ecosystems, https://doi.org/10.1007/978-1-4612-3122-6_13, 1991.
- 1140 Stenberg, J. A. and Muola, A.: How should plant resistance to herbivores be measured?, <https://doi.org/10.3389/fpls.2017.00663>, 2017.
- Sterner, R. . and Elser, J. .: Ecological Stoichiometry: The Biology of Elements from Molecules to the Biosphere: Robert W. Sterner, James J. Elser, Peter Vitousek, 2002.
- Sun, S. and Xue, Y.: Implementing a New Snow Scheme in Simplified Simple Biosphere Model, *Adv. Atmos. Sci.*, 18, 1145 <https://doi.org/10.1007/bf02919314>, 2001.
- Talhelm, A. F., Pregitzer, K. S., and Burton, A. J.: No evidence that chronic nitrogen additions increase photosynthesis in mature sugar maple forests, *Ecol. Appl.*, 21, 2413–2424, <https://doi.org/10.1890/10-2076.1>, 2011.
- Talmy, D., Blackford, J., Hardman-Mountford, N. J., Polimene, L., Follows, M. J., and Geider, R. J.: Flexible C : N ratio enhances metabolism of large phytoplankton when resource supply is intermittent, *Biogeosciences*, 11, 1150 <https://doi.org/10.5194/bg-11-4881-2014>, 2014.
- Thomas, R. Q., Brookshire, E. N. J., and Gerber, S.: Nitrogen limitation on land: How can it occur in Earth system models?, *Glob. Chang. Biol.*, 21, 1777–1793, <https://doi.org/10.1111/gcb.12813>, 2015.
- ~~Thornely, J. H. M. and Johnson, I. R.: *Plant Growth Modelling: A Mathematical approach to Plant and Crop Physiology*, 1990.~~
- Thum, T., Caldararu, S., Engel, J., Kern, M., Pallandt, M., Schnur, R., Yu, L., and Zaehle, S.: A new model of the coupled carbon, nitrogen, and phosphorus cycles in the terrestrial biosphere (QUINCY v1.0; revision 1996), *Geosci. Model Dev.*, 12, 1155 <https://doi.org/10.5194/gmd-12-4781-2019>, 2019.
- ~~Tian, H., Bian, Z., Shi, H., Qin, X., Pan, N., Lu, C., Pan, S., Tubiello, F. N., Chang, J., Conchedda, G., Liu, J., Mueller, N., Nishina, K., Xu, R., Yang, J., You, L., and Zhang, B.: History of anthropogenic Nitrogen inputs (HaNi) to the terrestrial biosphere: A 5arcmin resolution annual dataset from 1860 to 2019, *Earth Syst. Sci. Data*, 14, <https://doi.org/10.5194/essd-14-4551-2022>, 2022.~~
- 160 Vicca, S., Luysaert, S., Peñuelas, J., Campioli, M., Chapin, F. S., Ciais, P., Heinemeyer, A., Högberg, P., Kutsch, W. L., Law, B. E., Malhi, Y., Papale, D., Piao, S. L., Reichstein, M., Schulze, E. D., and Janssens, I. A.: Fertile forests produce biomass more efficiently, *Ecol. Lett.*, 15, 520–526, <https://doi.org/10.1111/j.1461-0248.2012.01775.x>, 2012.
- ~~Vitasse, Y., Ursenbacher, S., Klein, G., Bohnenstengel, T., Chittaro, Y., Delestrade, A., Monnerat, C., Rebetez, M., Rixen, C., Strebel, N., Schmidt, B. R., Wipf, S., Wohlgemuth, T., Yoccoz, N. G., and Lenoir, J.: Phenological and elevational shifts of plants, animals and fungi under climate change in the European Alps, *Biol. Rev.*, 96, <https://doi.org/10.1111/brv.12727>, 2021.~~
- 165 Vitousek, P.: Nutrient Cycling and Nutrient Use Efficiency Author (s): Peter Vitousek Source : The American Naturalist , Vol . 119 , No . 4 (Apr ., 1982), pp . 553-572 Published by : The University of Chicago Press for The American Society of Naturalists Stable URL, 119, 553–572, 1982.
- 1170 Vitousek, P. and Howarth, R.: Nitrogen limitation on land and in the sea: How can it occur?, *Biogeochemistry*, 13, 3646–3653, <https://doi.org/10.1007/BF00002772>, 1991.

- Walker, A. P., Beckerman, A. P., Gu, L., Kattge, J., Cernusak, L. A., Domingues, T. F., Scales, J. C., Wohlfahrt, G., Wullschlegel, S. D., and Woodward, F. I.: The relationship of leaf photosynthetic traits - V_{max} and J_{max} - to leaf nitrogen, leaf phosphorus, and specific leaf area: A meta-analysis and modeling study, *Ecol. Evol.*, 4, <https://doi.org/10.1002/ece3.1173>, 2014.
- 1175 Wang, C. and Tang, Y.: Responses of plant phenology to nitrogen addition: a meta-analysis, *Oikos*, 128, <https://doi.org/10.1111/oik.06099>, 2019.
- Wang M, Liu Y, Hao Z, Wang Y. Respiration rate of broadleaved Korean pine forest ecosystem in Changbai Mountains.. - *Chin. J. Appl. Ecol.* 2006,17(10) : 1789 ~ 1795.
- 1180 Wang, Y. P., Law, R. M., and Pak, B.: A global model of carbon, nitrogen and phosphorus cycles for the terrestrial biosphere, *Biogeosciences*, 7, 2261–2282, <https://doi.org/10.5194/bg-7-2261-2010>, 2010.
- Wiltshire, A., Burke, E., Chadburn, S., Jones, C., Cox, P., Davies-Barnard, T., Friedlingstein, P., Harper, A., Liddicoat, S., Sitch, S., and Zaehle, S.: JULES-CN: a coupled terrestrial Carbon-Nitrogen Scheme (JULES vn5.1), *Geosci. Model Dev. Discuss.*, 1–40, <https://doi.org/10.5194/gmd-2020-205>, 2020.
- 1185 Wingler, A., Purdy, S., MacLean, J. A., and Pourtau, N.: The role of sugars in integrating environmental signals during the regulation of leaf senescence, in: *Journal of Experimental Botany*, <https://doi.org/10.1093/jxb/eri279>, 2006.
- Xiao, Z., Liang, S., Wang, J., Chen, P., Yin, X., Zhang, L., and Song, J.: Use of general regression neural networks for generating the GLASS leaf area index product from time-series MODIS surface reflectance, *IEEE Trans. Geosci. Remote Sens.*, 52, 209–223, <https://doi.org/10.1109/TGRS.2013.2237780>, 2014.
- 1190 Xue, Y., Sellers, P. J., Kinter, J. L., and Shukla, J.: A Simplified biosphere model for global climate studies, *J. Clim.*, 4, 345–364, [https://doi.org/10.1175/1520-0442\(1991\)004<0345:ASBMFG>2.0.CO;2](https://doi.org/10.1175/1520-0442(1991)004<0345:ASBMFG>2.0.CO;2), 1991.
- Xue, Y., Zeng, F. J., and Schlosser, C. A.: SSiB and its sensitivity to soil properties-A case study using HAPEX-Mobilhy data, *Glob. Planet. Change*, 13, [https://doi.org/10.1016/0921-8181\(95\)00045-3](https://doi.org/10.1016/0921-8181(95)00045-3), 1996.
- Xue, Y., Sellers, P. J., Zeng, F. J., and Schlosser, C. A.: Comments on “Use of midlatitude soil moisture and meteorological observations to validate soil moisture simulations with biosphere and bucket models,” *J. Clim.*, 10, [https://doi.org/10.1175/1520-0442\(1997\)010<0374:COUOMS>2.0.CO;2](https://doi.org/10.1175/1520-0442(1997)010<0374:COUOMS>2.0.CO;2), 1997.
- 1195 Xue, Y., Juang, H.-M. H., Li, W.-P., Prince, S., DeFries, R., Jiao, Y., and Vasic, R.: Role of land surface processes in monsoon development: East Asia and West Africa, *J. Geophys. Res. Atmos.*, 109, n/a-n/a, <https://doi.org/10.1029/2003jd003556>, 2004.
- Xue, Y., De Sales, F., Vasic, R., Mechoso, C. R., Arakawa, A., and Prince, S.: Global and seasonal assessment of interactions between climate and vegetation biophysical processes: A GCM study with different land-vegetation representations, *J. Clim.*, 23, 1411–1433, <https://doi.org/10.1175/2009JCLI3054.1>, 2010.
- 1200 Xue, Y., Diallo, I., Boone, A. A., Yao, T., Zhang, Y., Zeng, X., Neelin, J. D., Lau, W. K. M., Pan, Y., Liu, Y., Pan, X., Tang, Q., Oevelen, P. J. van, Sato, T., Koo, M.-S., Materia, S., Shi, C., Yang, J., Ardilouze, C., Lin, Z., Qi, X., Nakamura, T., Saha, S. K., Senan, R., Takaya, Y., Wang, H., Zhang, H., Zhao, M., Nayak, H. P., Chen, Q., Feng, J., Brunke, M. A., Fan, T., Hong, S., Nobre, P., Peano, D., Qin, Y., Vitart, F., Xie, S., Zhan, Y., Klocke, D., Leung, R., Li, X., Ek, M., Guo, W., Balsamo, G.,
- 1205

- Bao, Q., Chou, S. C., Rosnay, P. de, Lin, Y., Zhu, Y., Qian, Y., Zhao, P., Tang, J., Liang, X.-Z., Hong, J., Ji, D., Ji, Z., Qiu, Y., Sugimoto, S., Wang, W., Yang, K., and Yu, M.: Spring Land Temperature in Tibetan Plateau and Global-Scale Summer Precipitation: Initialization and Improved Prediction, *Bull. Am. Meteorol. Soc.*, 103, <https://doi.org/10.1175/bams-d-21-0270.1>, 2022.
- 1210 Xue, Y., Diallo, I., Boone, A. A., Zhang, Y., Zeng, X., Lau, W. K. M., Neelin, J. D., Yao, T., Tang, Q., Sato, T., Koo, M. S., Vitart, F., Ardilouze, C., Saha, S. K., Materia, S., Lin, Z., Takaya, Y., Yang, J., Nakamura, T., Qi, X., Qin, Y., Nobre, P., Senan, R., Wang, H., Zhang, H., Zhao, M., Nayak, H. P., Pan, Y., Pan, X., Feng, J., Shi, C., Xie, S., Brunke, M. A., Bao, Q., Bottino, M. J., Fan, T., Hong, S., Lin, Y., Peano, D., Zhan, Y., Mechoso, C. R., Ren, X., Balsamo, G., Chou, S. C., de Rosnay, P., van Oevelen, P. J., Klocke, D., Ek, M., Li, X., Guo, W., Zhu, Y., Tang, J., Liang, X. Z., Qian, Y., and Zhao, P.: Remote
- 1215 effects of Tibetan Plateau spring land temperature on global subseasonal to seasonal precipitation prediction and comparison with effects of sea surface temperature: the GEWEX/LS4P Phase I experiment, *Clim. Dyn.*, <https://doi.org/10.1007/s00382-023-06905-5>, 2023.
- Yang, S., Shi, Z., Zhang, M., Li, Y., Gao, J., Wang, X.N., Zavišić, A., Pena, R., and Liu, D.: ~~Stoichiometry of Carbon, Nitrogen~~Polle, A.: Phenology, photosynthesis, and Phosphorus~~in Shrub Organs Linked Closely With Mycorrhizal~~
1220 Strategy~~European beech (*Fagus sylvatica* L.) in Northern China, Front, two forest soils with contrasting P contents, J. Plant Nutr. Soil Sci.~~, 12179, <https://doi.org/10.3389/fpls.2021.687347>, 20211002/jpln.201500539, 2016.
- Yang, X., Dan, L., Yang, S., Wen S., Lin J and Yin Z. Respiration of non-photosynthetic organs of Korean pine in spring. - Chin.J. Appl. Ecol, 1992,3(4):386—388.
- Yin, T. F., Peng, J., Li, Y., Gao, D., Ji, J., And Huang,Zheng, L. L., Cao, G. M.: The integration of, Song, M. H., and Yu, F.
1225 H.: Species-specific phenological responses to long-term nitrogen dynamics into a land surface model. Part 1: model description and site scale validation, Atmos. Ocean. Sci. Lett., 12fertilization in an alpine meadow, J. Plant Ecol., 10, <https://doi.org/10.1080/16742834.2019.1548246>, 20191093/jpe/rtw026, 2017.
- Yu, L., Ahrens, B., Wutzler, T., Zaehle, S., and Schrupf, M.: Modeling Soil Responses to Nitrogen and Phosphorus Fertilization Along a Soil Phosphorus Stock Gradient, *Front. For. Glob. Chang.*, 3, <https://doi.org/10.3389/ffgc.2020.543112>,
- 1230 2020.
- Zaehle, S., Jones, C. D., Houlton, B., Lamarque, J. F., and Robertson, E.: Nitrogen availability reduces CMIP5 projections of twenty-first-century land carbon uptake, *J. Clim.*, 28, 2494–2511, <https://doi.org/10.1175/JCLI-D-13-00776.1>, 2015.
- Zhan, X., Xue, Y., and Collatz, G. J.: An analytical approach for estimating CO₂ and heat fluxes over the Amazonian region, *Ecol. Modell.*, 162, 97–117, [https://doi.org/10.1016/S0304-3800\(02\)00405-2](https://doi.org/10.1016/S0304-3800(02)00405-2), 2003.
- 1235 Zhang, C., Zeng, F., Zeng, Z., Du, H., Zhang, L., Su, L., Lu, M., and Zhang, H.: Carbon, Nitrogen and Phosphorus Stoichiometry and Its Influencing Factors in Karst Primary Forest, Forests, 13, <https://doi.org/10.3390/f13121990>, 2022.
- Zhang, G., Han, X., and Elser, J. J.: Rapid top-down regulation of plant C:N:P stoichiometry by grasshoppers in an Inner Mongolia grassland ecosystem, Oecologia, 166, <https://doi.org/10.1007/s00442-011-1904-5>, 2011.

- 1240 [Zhang, Z., Xue, Y., MacDonald, G., Cox, P. M., and Collatz, G. J.:](#) Investigation of North American vegetation variability under recent climate: A study using the SSiB4/TRIFFID biophysical/dynamic vegetation model, *J. Geophys. Res.*, 120, 1300–1321, <https://doi.org/10.1002/2014JD021963>, 2015.
- [Zhou, L., Zhou, W., Chen, J., Xu, X., Wang, Y., Zhuang, J., and Chi, Y.:](#) [Land surface phenology detections from multi-source remote sensing indices capturing canopy photosynthesis phenology across major land cover types in the Northern Hemisphere, *Ecol. Indic.*, 135, <https://doi.org/10.1016/j.ecolind.2022.108579>, 2022.](#)
- 1245 Zhu, Q., Riley, W. J., Tang, J., Collier, N., Hoffman, F. M., Yang, X., and Bisht, G.: Representing Nitrogen, Phosphorus, and Carbon Interactions in the E3SM Land Model: Development and Global Benchmarking, *J. Adv. Model. Earth Syst.*, 11, <https://doi.org/10.1029/2018MS001571>, 2019.
- Zhu, Z., Bi, J., Pan, Y., Ganguly, S., Anav, A., Xu, L., Samanta, A., Piao, S., Nemani, R. R., and Myneni, R. B.: Global data sets of vegetation leaf area index (LAI)_{3g} and fraction of photosynthetically active radiation (FPAR)_{3g} derived from global inventory modeling and mapping studies (GIMMS) normalized difference vegetation index (NDVI_{3G}) for the period 1981 to 1250 2, *Remote Sens.*, 5, 927–948, <https://doi.org/10.3390/rs5020927>, 2013.